6. INTERPRETATION OF RESULTS

6.1 Identification of mineralogically and chemically different types of UG2 chromitite

The distribution of selected mineralogical and chemical characteristics of the fourteen feed samples are graphically compared in Figure 88. There are pronounced differences between the fourteen samples in terms of these parameters. The amount of non-sulphide PGE mineral, the median chromite grain diameter, the pentlandite/(pentlandite+millerite) ratio, and the amount of PGE mineral locked in gangue, were selected as being the most diagnostic characteristics of mineralogically different types of UG2 chromitite. Based on these four mineralogical parameters, four groups of samples with different mineralogical characteristics were identified using cluster analysis.[+] The members of the four groups are listed in Table 6.1, together with descriptive statistics for the mineralogical, chemical and flotation characteristics of each group.

- ***Cluster number 1 – Relatively unaltered UG2 chromitite***

  Samples A1, A2, A3, B1, B2 and B3 belong to the first group. The mineralogical characteristics of the members of this group are essentially that of normal UG2 chromitite as summarised in section 2.3.1 – the amount of non-sulphide PGE mineral is low, ranging between 5 and 23 volume per cent, the degree of sintering of chromite grains is low, with median chromite diameters of 164 to 191 µm, the amount of PGE mineral associated with gangue is low, 4 to 20 per cent, and pentlandite is the major nickel-bearing sulphide, with millerite absent or present in very low amounts.

- ***Cluster number 2 – Sintered UG2 chromitite***

  The next group has two members, A4 and B4, which are characterised by a large amount of non-sulphide PGE mineral, 58 and 53 volume per cent respectively,

---

[+] *k-means cluster analysis* using the Statistica package. The program starts with *k* random clusters and then allocates objects between those clusters with the goal to (1) minimize variability within clusters and (2) maximize variability between those clusters.

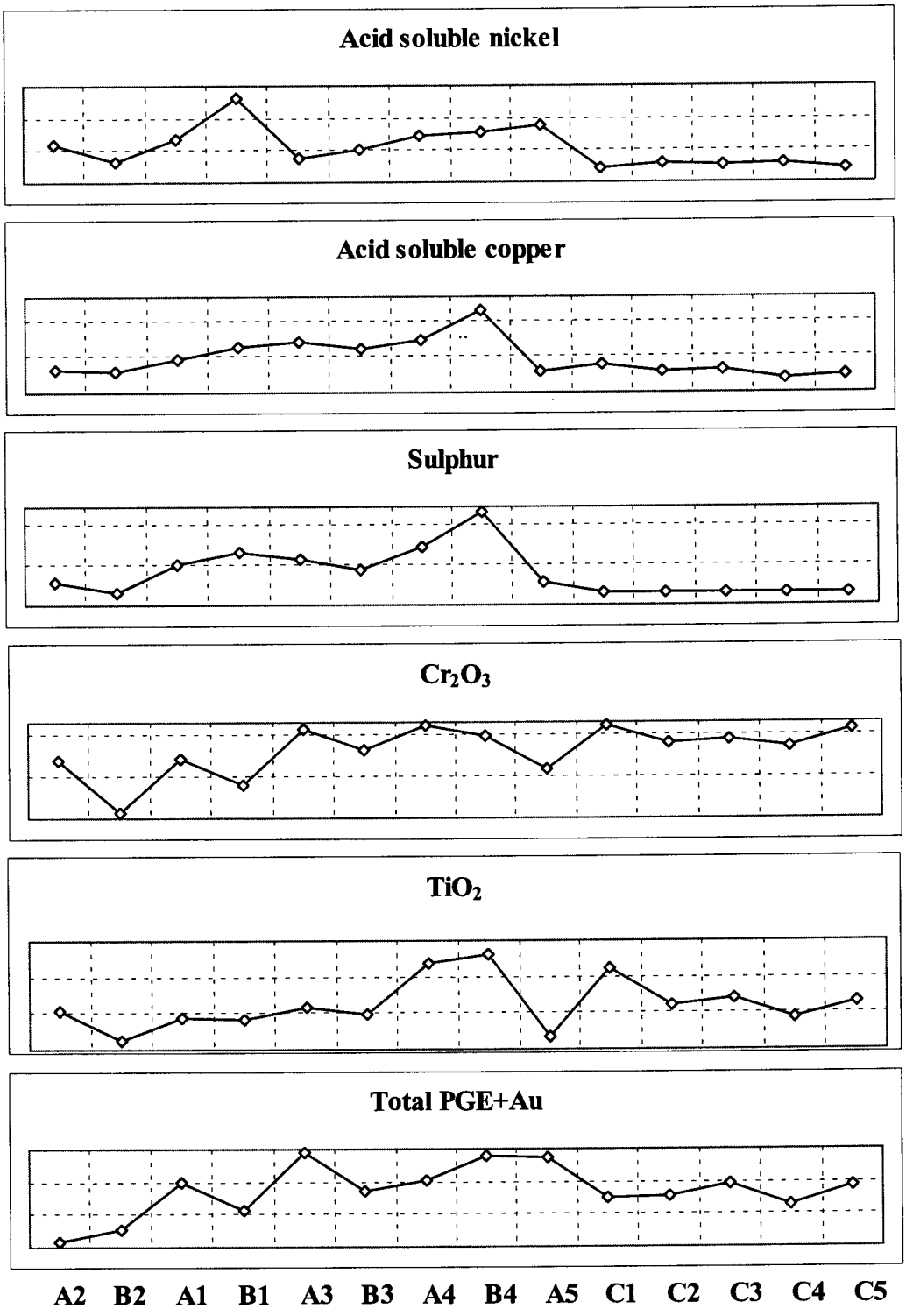

p.t.o.

Figure 88 *The distribution of selected chemical and mineralogical parameters between fourteen samples of UG2 chromitite.*

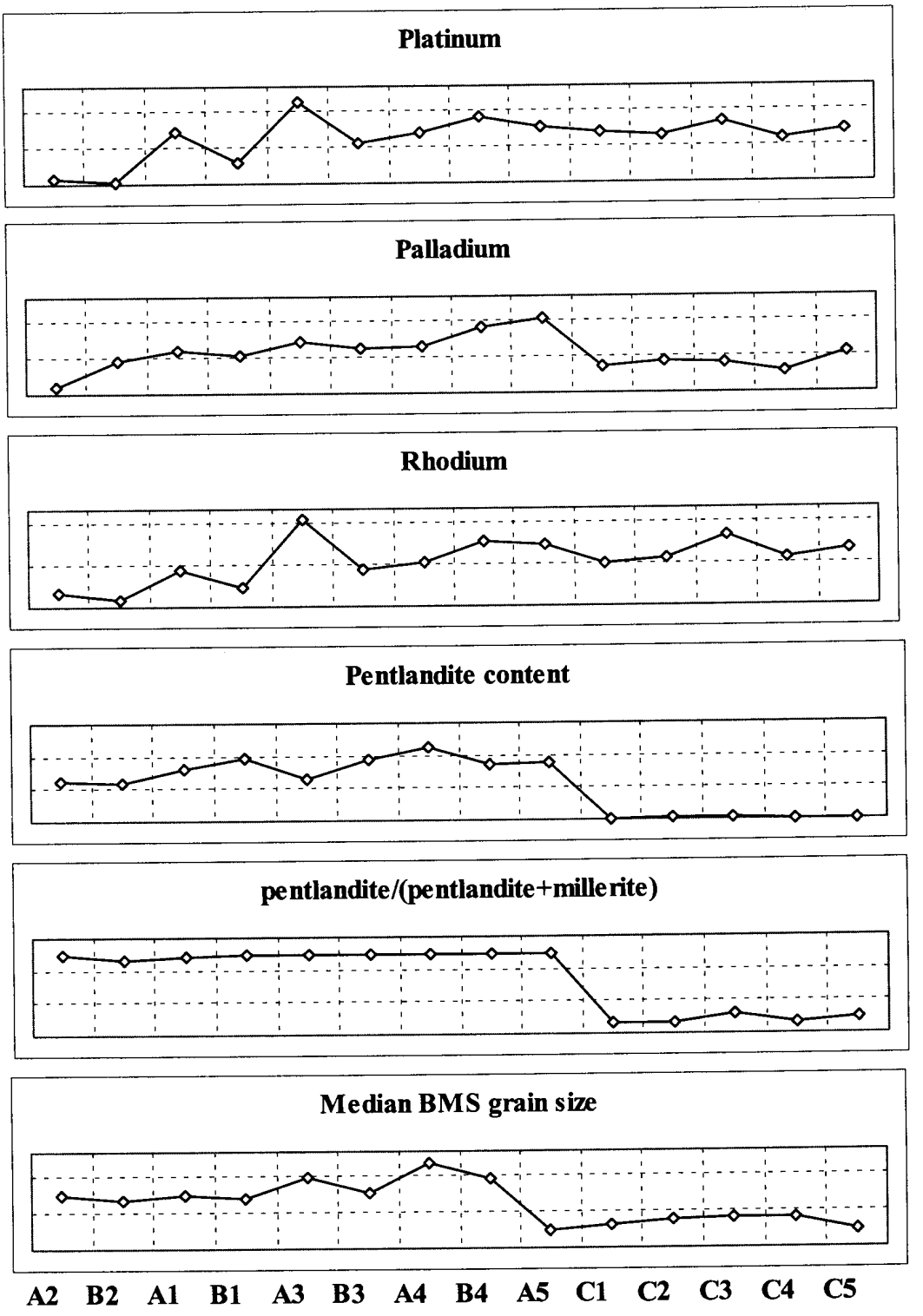

p.t.o.

Figure 88 continued *The distribution of selected chemical and mineralogical parameters between fourteen samples of UG2 chromitite.*

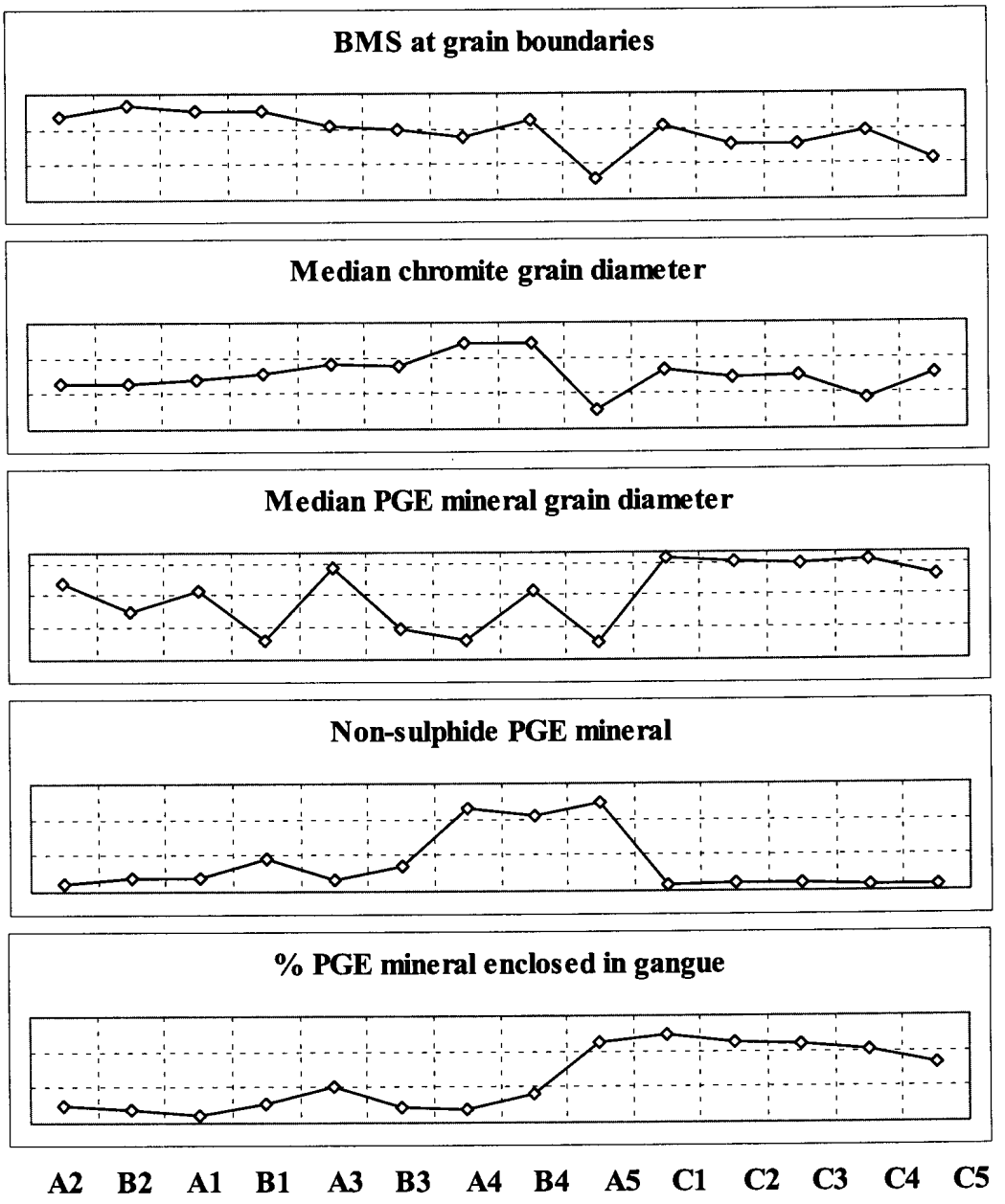

Figure 88 continued *The distribution of selected chemical and mineralogical parameters between fourteen samples of UG2 chromitite.*

Table 6.1 *Members and descriptive statistics for the mineralogical, chemical and flotation characteristics of each cluster.*

Members of Cluster Number 1						
	A1	***A2***	***A3***	***B1***	***B2***	***B3***
Distance from cluster center	4.9	7.4	9.7	8.0	6.5	7.4
Descriptive statistics (n=6)						
Mineralogical and chemical characteristics						
	Mean		*Range*		*Std. Deviation*	
% non-sulphide PGEM	12		5-23		7	
Median chromite grain diameter (µm)	175		164-191		12	
pentlandite/(pentlandite+millerite)	1.0		0.9-1.0		0.0	
% PGEM associated with gangue	10		4-20		5	
Acid soluble nickel (ppm)	252		126-525		144	
Acid soluble copper (ppm)	75		42-107		27	
Sulphur (%)	0.03		0.01-0.05		0.01	
Cr_2O_3 (%)	28.2		20.9-33.8		4.5	
TiO_2 (%)	0.7		0.6-0.7		0.1	
Total PGE+Au (ppm)	4.4		3.2-5.9		1.0	
Platinum (ppm)	2.7		2.0-3.7		0.6	
Palladium (ppm)	1.3		0.7-1.6		0.3	
Rhodium (ppm)	0.4		0.3-0.6		0.1	
Pentlandite content (%)	0.06		0.05-0.08		0.01	
Median BMS grain size (µm)	32		30-39		3	
% BMS at grain boundaries	84		74-92		7	
Median PGEM grain diameter (µm)	2.2		1.8-2.8		0.4	
Flotation characteristics						
	Mean		*Range*		*Std. Deviation*	
R_f (%)	75		63-80		6	
R_s (%)	19		15-26		4	
100-U (%)	6		4-11		3	
k_f (min^{-1})	2.3		2.1-2.9		0.3	
k_s (min^{-1})	0.22		0.18-0.25		0.03	

p.t.o.

Table 6.1 continued *Members and descriptive statistics for the mineralogical, chemical and flotation characteristics of each cluster.*

Members of Cluster Number 2			
	A4	***B4***	
Distance from cluster center	2.5	2.5	
Descriptive statistics (n=2)			
Mineralogical and chemical characteristics			
	Mean	*Range*	*Std. Deviation*
% non-sulphide PGEM	55	53-58	4
Median chromite grain diameter (µm)	221	-	-
pentlandite/(pentlandite+millerite)	1.0	-	-
% PGEM associated with gangue	12	8-16	5
Acid soluble nickel (ppm)	305	295-316	15
Acid soluble copper (ppm)	140	109-170	43
Sulphur (%)	0.07	0.05-0.08	0.02
Cr_2O_3 (%)	33.7	32.9-34.5	1.1
TiO_2 (%)	1.0	-	-
Total PGE+Au (ppm)	5.4	5.0-5.8	0.6
Platinum (ppm)	3.2	3.1-3.3	0.2
Palladium (ppm)	1.7	1.5-1.9	0.3
Rhodium (ppm)	0.5	-	-
Pentlandite content (%)	0.08	0.07-0.09	0.02
Median BMS grain size (µm)	42	38-45	5
% BMS at grain boundaries	76	70-82	8
Median PGEM grain diameter (µm)	2.1	1.8-2.5	0.5
Flotation characteristics			
	Mean	*Range*	*Std. Deviation*
R_f (%)	58	57-60	2
R_s (%)	36	34-38	3
100-U (%)	6	-	0
k_f (min^{-1})	1.9	1.6-2.2	0.4
k_s (min^{-1})	0.23	0.22-0.24	0.01

p.t.o.

Table 6.1 continued *Members and descriptive statistics for the mineralogical, chemical and flotation characteristics of each cluster.*

Members of Cluster Number 3						
	C1	***C2***	***C3***	***C4***	***C5***	
Distance from cluster center	7.8	2.0	2.7	14.0	5.8	
Descriptive statistics (n=5)						
Mineralogical and chemical characteristics						
	Mean		*Range*		*Std. Deviation*	
% non-sulphide PGEM	4		4-6		1	
Median chromite grain diameter (µm)	170		142-184		16	
pentlandite/(pentlandite+millerite)	0.1		0.0-0.2		0.1	
% PGEM associated with gangue	43		33-50		6	
Acid soluble nickel (ppm)	101		82-114		15	
Acid soluble copper (ppm)	43		30-57		11	
Sulphur (%)	<0.01		-		-	
Cr_2O_3 (%)	32.7		31.2-34.6		1.4	
TiO_2 (%)	0.8		0.7-1.0		0.1	
Total PGE+Au (ppm)	4.6		4.3-4.9		0.3	
Platinum (ppm)	3.0		2.9-3.2		0.1	
Palladium (ppm)	1.1		0.9-1.3		0.1	
Rhodium (ppm)	0.5		-		-	
Pentlandite content (%)	0.00		-		-	
Median BMS grain size (µm)	20		17-23		2	
% BMS at grain boundaries	66		53-77		9	
Median PGEM grain diameter (µm)	2.8		2.7-2.9		0.1	
Flotation characteristics						
	Mean		*Range*		*Std. Deviation*	
R_f(%)	71		66-75		4	
R_s (%)	22		20-25		2	
100-U (%)	7		4-9		2	
k_f (min^{-1})	2.1		2.0-2.2		0.1	
k_s (min^{-1})	0.20		0.19-0.22		0.01	

p.t.o.

Table 6.1 continued *Members and descriptive statistics for the mineralogical, chemical and flotation characteristics of each cluster.*

Members of Cluster Number 4			
	A5		
Distance from cluster center	0.0		
Descriptive statistics (n=1)			
Mineralogical and chemical characteristics			
	Mean	*Range*	*Std. Deviation*
% non-sulphide PGEM	81	-	-
Median chromite grain diameter (μm)	127	-	-
pentlandite/(pentlandite+millerite)	1.0	-	-
% PGEM associated with gangue	45	-	-
Acid soluble nickel (ppm)	356	-	-
Acid soluble copper (ppm)	44	-	-
Sulphur (%)	0.02	-	-
Cr_2O_3 (%)	27.70	-	-
TiO_2 (%)	0.57	-	-
Total PGE+Au (ppm)	5.74	-	-
Platinum (ppm)	3.13	-	-
Palladium (ppm)	2.05	-	-
Rhodium (ppm)	0.52	-	-
Pentlandite content (%)	0.07	-	-
Median BMS grain size (μm)	17	-	-
% BMS at grain boundaries	40	-	-
Median PGEM grain diameter (μm)	1.8	-	-
Flotation characteristics			
	Mean	*Range*	*Std. Deviation*
R_f (%)	40	-	-
R_s (%)	29	-	-
100-U (%)	32	-	-
$k_f (min^{-1})$	1.6	-	-
$k_s (min^{-1})$	0.15	-	-

and enlargement of chromite grains (median chromite diameter = 220 µm in both samples). Pentlandite is the dominant nickel-bearing base-metal sulphide, and the amount of PGE mineral associated with gangue (8 to 16 per cent) is similar to that of the relatively unaltered UG2 chromitite. These two samples are characterised by elevated TiO_2 contents (>0.9 per cent). A strong positive linear relationship (Pearson correlation coefficient r=0.80) exists between TiO_2 content and median chromite grain diameter for the fourteen samples (Figure 89, Table 6.2).

- ***Cluster number 3 – Millerite-bearing UG2 chromitite***

Cluster number 3 includes all the samples from area C. Millerite, instead of pentlandite, is the major nickel-bearing sulphide in these samples, and a large proportion of the PGE minerals in these samples is associated with gangue (33 to 50 per cent). Chromite diameters (142 to 184 µm) are similar to that of relatively unaltered UG2, and the amount of non-sulphide PGE mineral is low (<6 volume per cent). These samples are also characterised by smaller base-metal sulphide grain diameters, and a relatively small proportion of the base-metal sulphide grains located at grain boundaries. Note the relatively low sulphur, acid soluble nickel, copper and palladium values. Platinum and rhodium don't seem to follow the same trend. A parameter not quantified, and therefore not taken into account during the statistical analysis, is the degree of silicate alteration, which is relatively high for this group of samples.

- ***Cluster number 4 – Cataclastic UG2 chromitite***

This group, which comprises only sample A5, is characterised by a small chromite grain size (median chromite diameter =127 µm), as a result of fracturing of chromite grains, a large amount of PGE mineral associated with gangue (45 per cent), and a high proportion of non-sulphide PGE mineral (81 per cent). The median grain diameter of base-metal sulphide in this sample is small, and most of the base-metal sulphide grains are enclosed in silicate. The degree of silicate alteration is relatively high in cataclastic UG2 chromitite.

Table 6.2 *Pearson correlation matrix for selected mineralogical and chemical parameters in fourteen samples of UG2 chromitite. Marked correlations (boldface) are significant at p<0.05.*

	Ni_{as}	Cu_{as}	S	Cr_2O_3	TiO_2	PGE	Pt	Pd	Rh	pn	pn:mil	BMSS	BMSM	ChrS	NSul	PSN	PBMS	PSil
Ni_{as}	1.00	0.48	**0.64**	-0.36	-0.07	0.11	-0.16	0.44	-0.22	**0.78**	**0.69**	0.37	0.15	0.08	**0.63**	**-0.75**	0.52	-0.46
Cu_{as}	0.48	1.00	**0.96**	0.24	0.59	0.50	0.36	0.54	0.25	**0.62**	0.56	**0.76**	0.33	**0.79**	0.55	-0.29	0.39	-0.48
S	**0.64**	**0.96**	1.00	0.15	0.49	0.47	0.29	**0.57**	0.18	**0.71**	**0.64**	**0.76**	0.32	**0.68**	**0.64**	-0.39	0.45	-0.55
Cr_2O_3	-0.36	0.24	0.15	1.00	0.74	0.51	**0.75**	0.06	**0.68**	-0.31	-0.41	0.05	-0.35	0.48	0.02	0.46	-0.54	0.37
TiO_2	-0.07	**0.59**	0.49	**0.74**	1.00	0.33	0.45	0.09	0.33	-0.03	-0.16	0.33	0.04	0.80	0.28	0.22	-0.15	0.08
PGE	0.11	0.50	0.47	0.51	0.33	1.00	**0.92**	**0.84**	**0.87**	0.18	0.11	0.12	-0.46	0.28	0.51	-0.04	-0.30	0.21
Pt	-0.16	0.36	0.29	**0.75**	0.45	**0.92**	1.00	0.55	**0.95**	-0.12	-0.18	0.04	-0.43	0.30	0.22	0.30	-0.50	0.38
Pd	0.44	0.54	**0.57**	0.06	0.09	**0.84**	0.55	1.00	0.50	0.54	0.47	0.20	-0.36	0.18	**0.77**	-0.50	0.07	-0.07
Rh	-0.22	0.25	0.18	**0.68**	0.33	**0.87**	**0.95**	0.50	1.00	-0.21	-0.23	-0.06	-0.54	0.18	0.18	0.34	-0.63	0.48
pn	**0.78**	**0.62**	**0.71**	-0.31	-0.03	0.18	-0.12	0.54	-0.21	1.00	**0.95**	**0.72**	0.27	0.29	**0.69**	**-0.84**	**0.78**	**-0.76**
pn:mil	**0.69**	0.56	**0.64**	-0.41	-0.16	0.11	-0.18	0.47	-0.23	**0.95**	1.00	**0.71**	0.36	0.20	0.54	**-0.72**	**0.78**	**-0.80**
BMSS	0.37	**0.76**	**0.76**	0.05	0.33	0.12	0.04	0.20	-0.06	**0.72**	**0.71**	1.00	0.56	**0.70**	0.35	-0.36	**0.72**	**-0.80**
BMSM	0.15	0.33	0.32	-0.35	0.04	-0.46	-0.43	-0.36	-0.54	0.27	0.36	0.56	1.00	0.32	-0.30	0.03	**0.68**	**-0.67**
ChrS	0.08	**0.79**	**0.68**	0.48	0.80	0.28	0.30	0.18	0.18	0.29	0.20	**0.70**	0.32	1.00	0.25	-0.05	0.29	-0.40
NSul	**0.63**	0.55	**0.64**	0.02	0.28	0.51	0.22	**0.77**	0.18	**0.69**	0.54	0.35	-0.30	0.25	1.00	**-0.70**	0.23	-0.16
PSN	**-0.75**	-0.29	-0.39	0.46	0.22	-0.04	0.30	-0.50	0.34	**-0.84**	**-0.72**	-0.36	0.03	-0.05	-0.70	1.00	**-0.65**	0.51
PBMS	0.52	0.39	0.45	-0.54	-0.15	-0.30	-0.50	0.07	**-0.63**	**0.78**	**0.78**	**0.72**	**0.68**	0.29	0.23	**-0.65**	1.00	**-0.91**
PSil	-0.46	-0.48	-0.55	0.37	0.08	0.21	0.38	-0.07	0.48	**-0.76**	**-0.80**	**-0.80**	**-0.67**	-0.40	-0.16	0.51	**-0.91**	1.00

Nias, Cuas = acid soluble nickel and copper contents *S – sulphur content* *CR_2O_3 = Cr_2O_3 content* *TiO_2 = TiO_2 content*

PGE = (Pt,Pd,Rh,Au) *Pt = platinum content* *Pd = palladium content* *Rh= rhodium content*

pn = pentlandite content *pn:mil = pentlandite/(pentlandite+millerite) ratio* *BMSS = base-metal sulphide median grain diameter*

BMSM = % base-metal sulphide located at grain boundaries *ChrS = chromite median grain diameter* *NSul = % non-sulphide PGE mineral*

PSN = PGE mineral median grain diameter i.t.o. number of grains *PBMS = % PGE mineral associated with base-metal sulphide* *PSil = % PGE mineral enclosed in gangue*

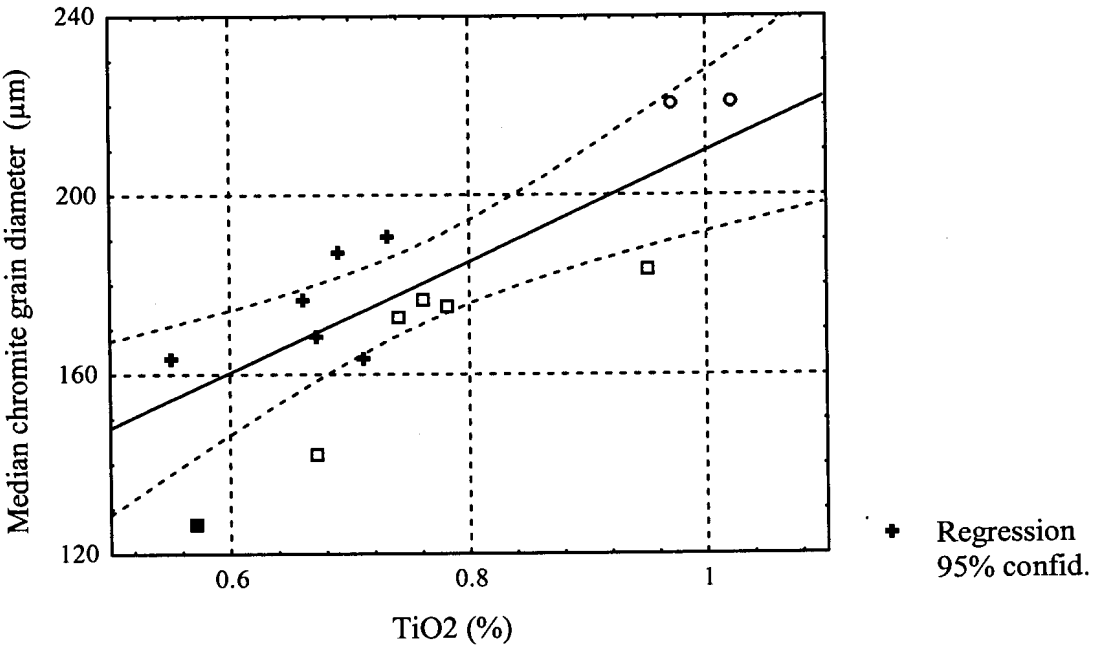

Figure 89 *Relationship between median chromite grain diameter (µm) and TiO_2 content for fourteen samples of UG2 chromitite. Pearson correlation coefficient for all fourteen samples, r=0.80. + = samples A1, A2, A3, B1, B2, and B3. □= samples C1, C2, C3, C4 and C5. o = samples A4 and B4. ■ = sample A5.*

In terms of most of the other mineralogical and chemical parameters compared in Figure 88, the differences between the four groups of samples are less clear, and often overlap. There is a positive linear relationship between median chromite and base-metal sulphide diameter, with a Pearson correlation coefficient r=0.7 (Table 6.2). This relationship does not appear to hold for the samples from area C (Figure 90), presumably because the processes causing corrosion of sulphide grains in these samples did not affect chromite grain size. If sample A5, in which chromite grain size was determined by cataclasis, and the samples from area C are excluded from the calculation, the relationship becomes even stronger (r=0.86). There does not appear to be any systematic relationship between chromite or base-metal sulphide grain size, and that of the PGE minerals (Table 6.2), indicating that an increase in base-metal sulphide grain size is not necessarily associated with an increase in PGE mineral grain size.

Total PGE+Au, platinum, rhodium and Cr_2O_3 do not appear to vary in a systematic manner in terms of the mineralogically different types of UG2 chromitite. Some

interesting trends do, however, emerge from a closer look at the relationships between the different chemical components of the UG2 chromitite (Table 6.2).

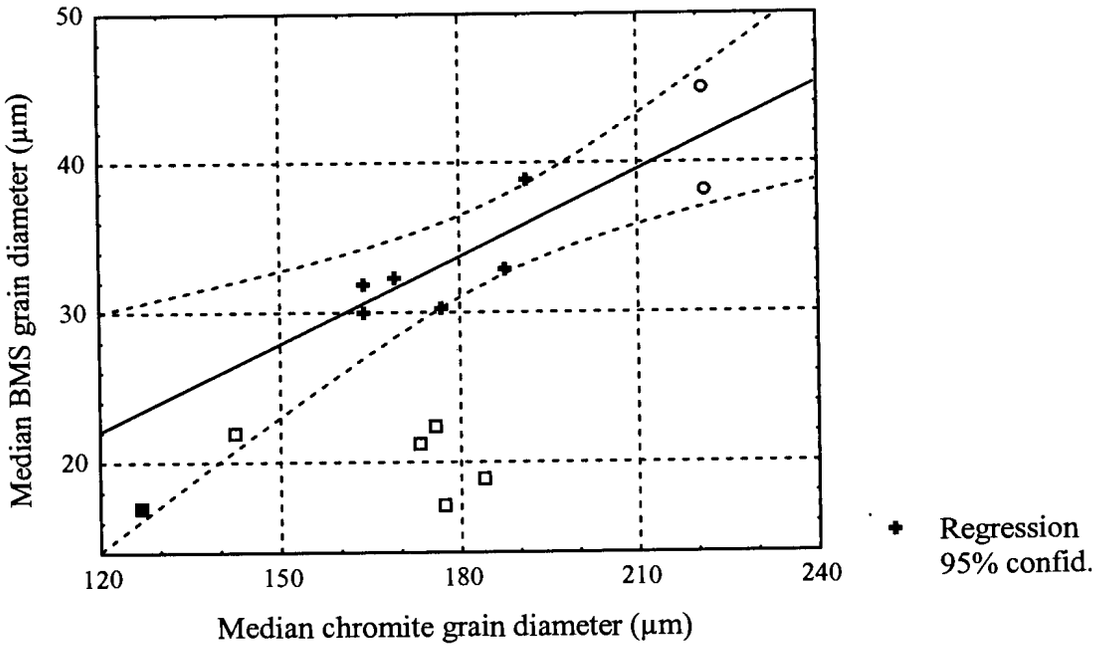

Figure 90 *Relationship between median chromite and base-metal sulphide (BMS) grain diameter. Pearson correlation coefficient r=0.86 for all samples excluding sample A5 and samples from area C. + = samples A1, A2, A3, B1, B2, and B3. □= samples C1, C2, C3, C4 and C5. o = samples A4 and B4. ■ = sample A5.*

A strong linear relationship exists between copper and sulphur (Pearson correlation coefficient r=0.96) (Figure 91). There is also a positive correlation between nickel and sulphur, albeit much weaker (r=0.64) (Figure 92).

A weak positive correlation (r=0.57) (Table 6.2) exists between palladium and sulphur. If two apparent outliers (A2 and A5), are excluded from the analysis, the correlation becomes much stronger (r=0.89) (Figure 93). If the same two outliers are excluded there is also a strong positive correlation between palladium and copper (r=0.90) (Figure 94). It is not clear why samples A2 and A5 do not follow the same trend as the remainder of the samples. After exclusion of two apparent outliers, A2 and B1, there also appear to be a positive correlation between palladium and nickel (r=0.86) (Figure 95). Considering the observation that copper, nickel, sulphur and palladium values for samples from area C are low compared to that in relatively unaltered UG2, these relationships are no surprise.

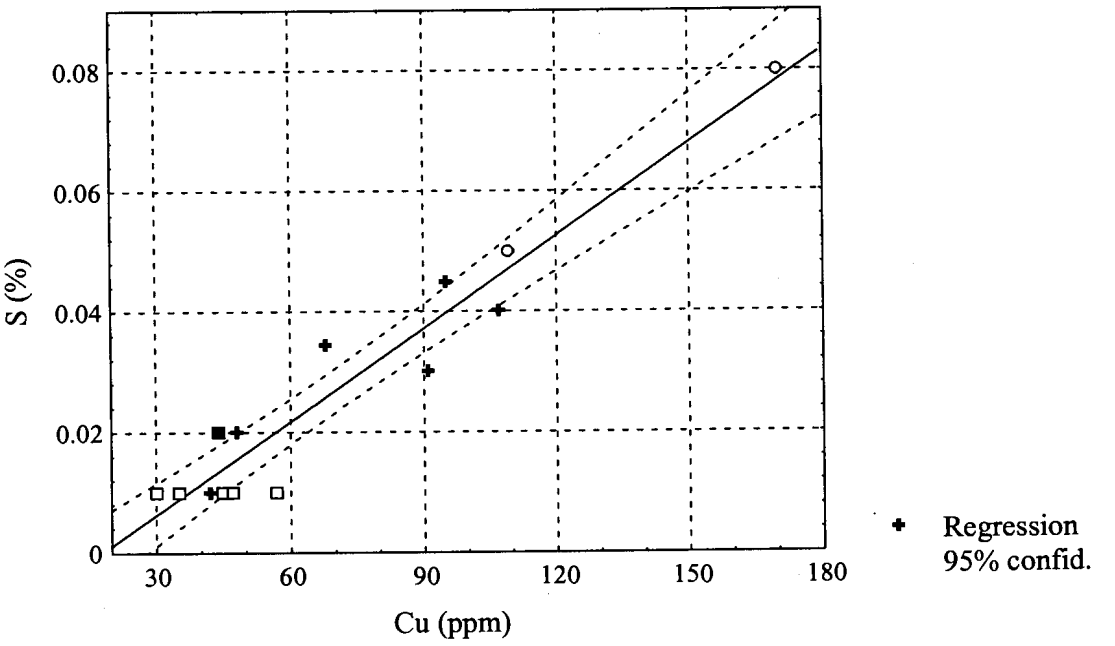

Figure 91 *Relationship between acid soluble copper and sulphur for fourteen samples of UG2 chromitite. Pearson correlation coefficient for all fourteen samples, r=0.96. + = samples A1, A2, A3, B1, B2, and B3. □ = samples C1, C2, C3, C4 and C5. o = samples A4 and B4. ■ = sample A5.*

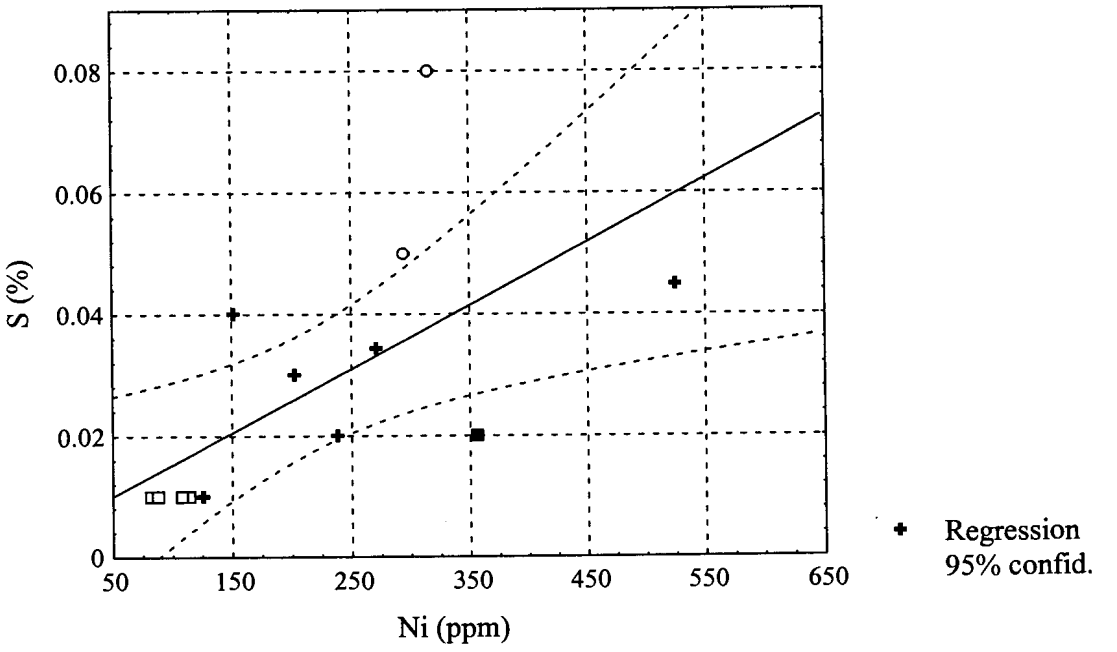

Figure 92 *Relationship between nickel and sulphur for fourteen samples of UG2 chromitite. Pearson correlation coefficient r=0.64. + = samples A1, A2, A3, B1, B2, and B3. □ = samples C1, C2, C3, C4 and C5. o = samples A4 and B4. ■ = sample A5.*

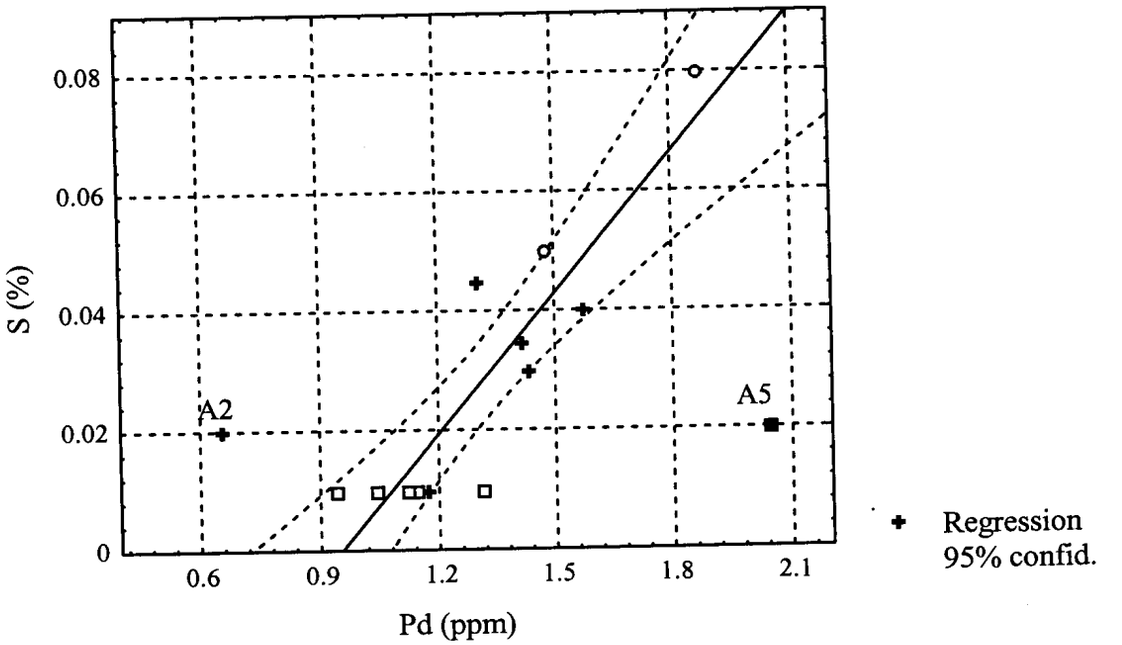

Figure 93 *Relationship between palladium and sulphur for fourteen samples of UG2 chromitite. Pearson correlation coefficient r=0.89 if A2 and A5 are excluded during the calculation of the regression line. + = samples A1, A2, A3, B1, B2, and B3. □ = samples C1, C2, C3, C4 and C5. o = samples A4 and B4. ■ = sample A5.*

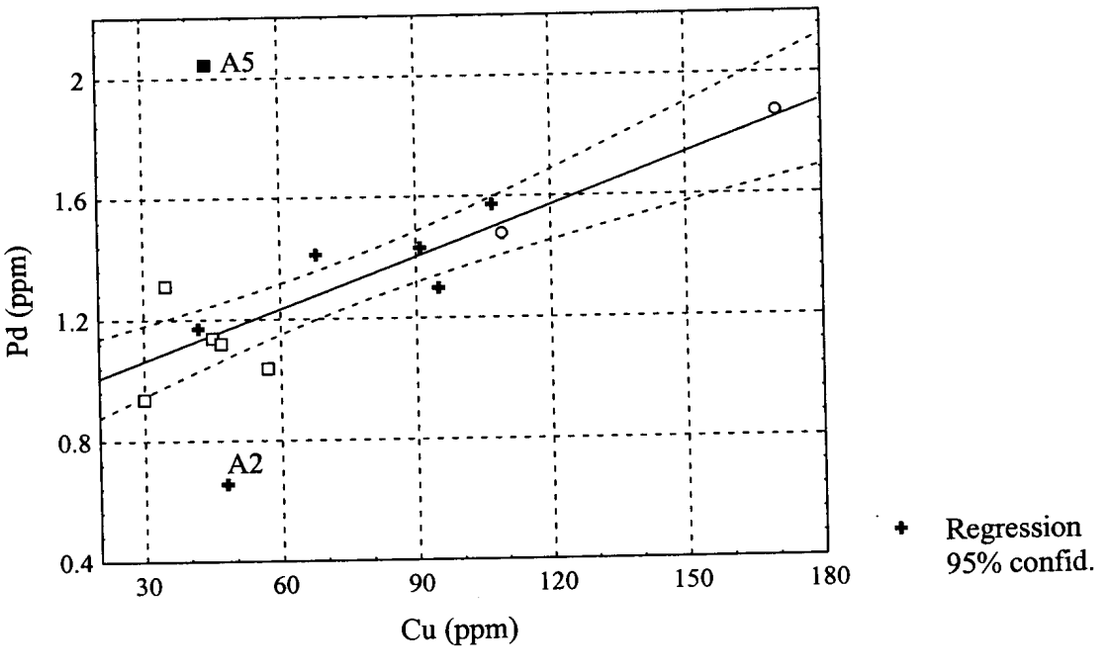

Figure 94 *Relationship between palladium and copper for fourteen samples of UG2 chromitite. Pearson correlation coefficient = 0.90 with outliers A2 and A5 excluded during the calculation of the regression line. + = samples A1, A2, A3, B1, B2, and B3. □ = samples C1, C2, C3, C4 and C5. o = samples A4 and B4. ■ = sample A5.*

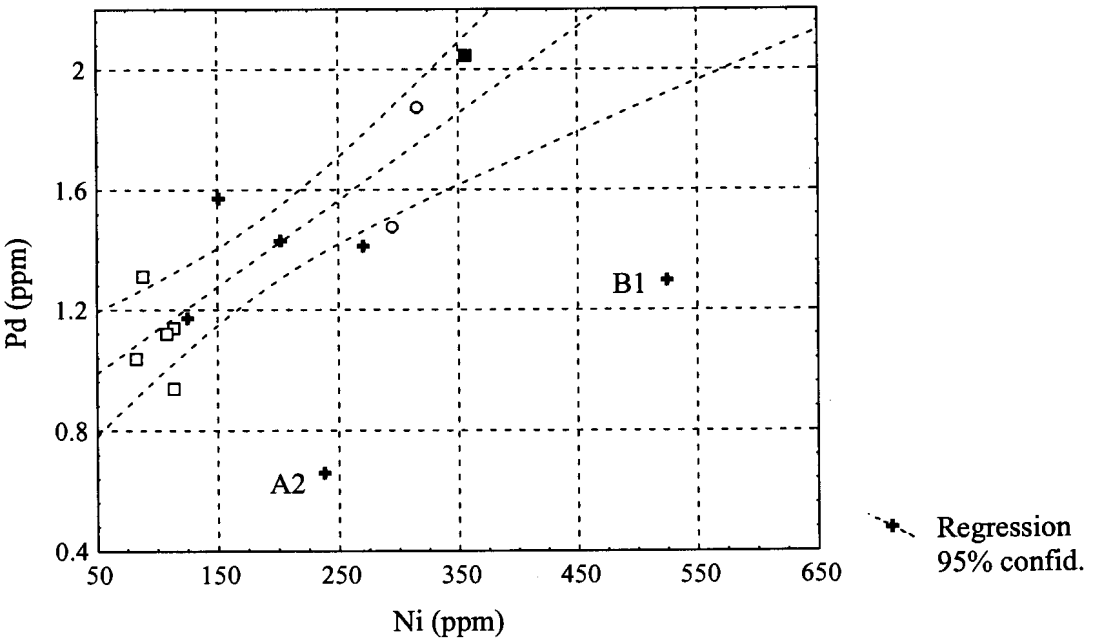

Figure 95 *Relationship between palladium and nickel for fourteen samples of UG2 chromitite. Pearson correlation coefficient = 0.86 with outliers A2 and B1 excluded during calculation of regression line. + = samples A1, A2, A3, B1, B2, and B3. □ = samples C1, C2, C3, C4 and C5. o = samples A4 and B4. ■ = sample A5.*

Platinum and rhodium do not seem to follow the same trend, explaining the weak correlation between platinum and palladium (r=0.55) (Figure 96), and between rhodium and palladium (r=50) (Figure 97). No significant correlation could be found between sulphur and platinum, or sulphur and rhodium. Similarly platinum and rhodium shows no correlation with copper or nickel values.

Platinum and rhodium contents are, however, strongly correlated (r=0.95) (Figure 98). The data also indicate a positive correlation between Cr_2O_3 and platinum (Figure 99) (r=0.75), and between Cr_2O_3 and rhodium (Figure 100) (r=0.68), but no correlation between palladium and Cr_2O_3 (Figure 101) (r=0.06). These relationships could possibly be an indication of the relative immobility of platinum and rhodium, compared to palladium and the base metals, under the conditions prevailing during the formation of the UG2 chromitite.

Note also the positive correlation between TiO_2 and Cr_2O_3 (r=0.74 for all samples). Samples A4, B4 and C1 deviates strongly from the regression line with a much higher TiO_2 content than expected (Figure 102).

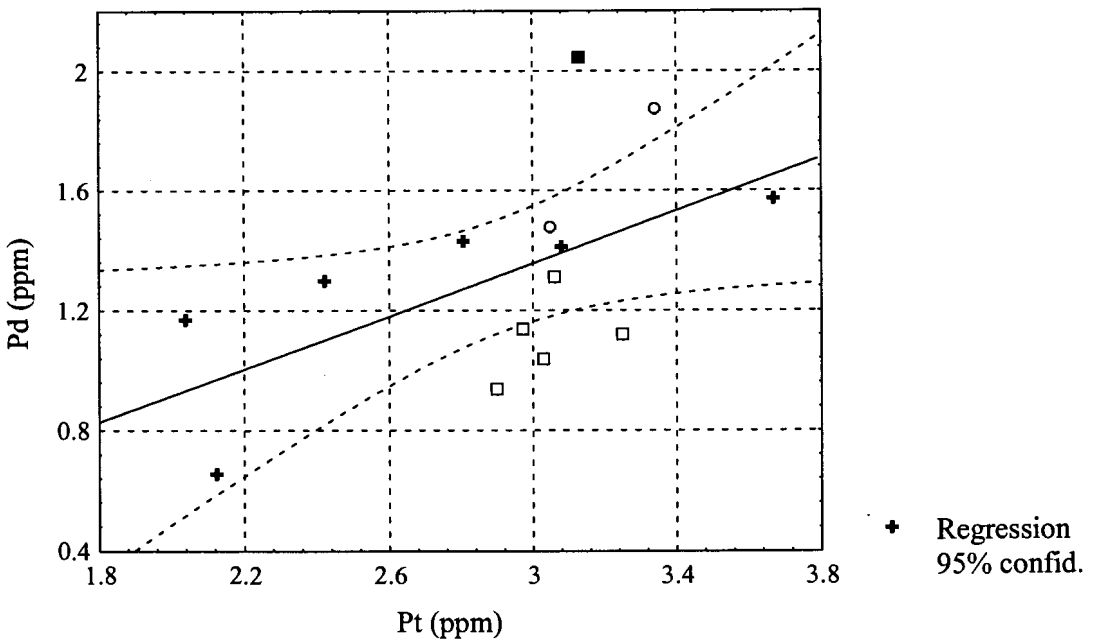

Figure 96 *Relationship between palladium and platinum for fourteen samples of UG2 chromitite. Pearson correlation coefficient r=0.55. + = samples A1, A2, A3, B1, B2, and B3. □ = samples C1, C2, C3, C4 and C5. o = samples A4 and B4. ■ = sample A5.*

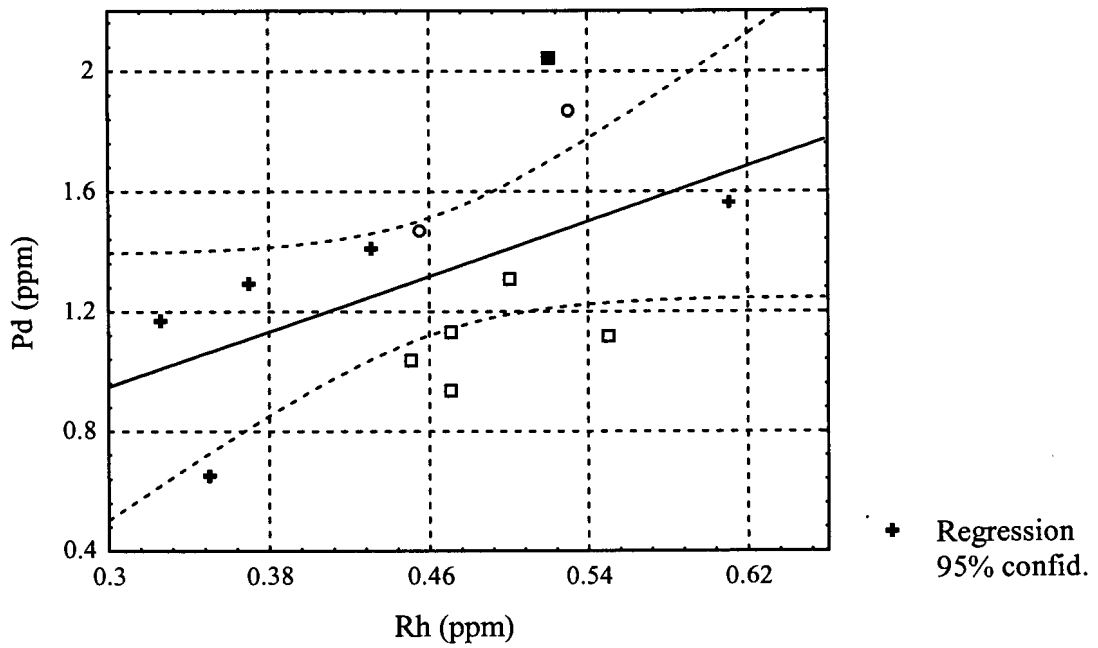

Figure 97 *Relationship between rhodium and palladium for fourteen samples of UG2 chromitite. Pearson correlation coefficient r=0.50. + = samples A1, A2, A3, B1, B2, and B3. □ = samples C1, C2, C3, C4 and C5. o = samples A4 and B4. ■ = sample A5.*

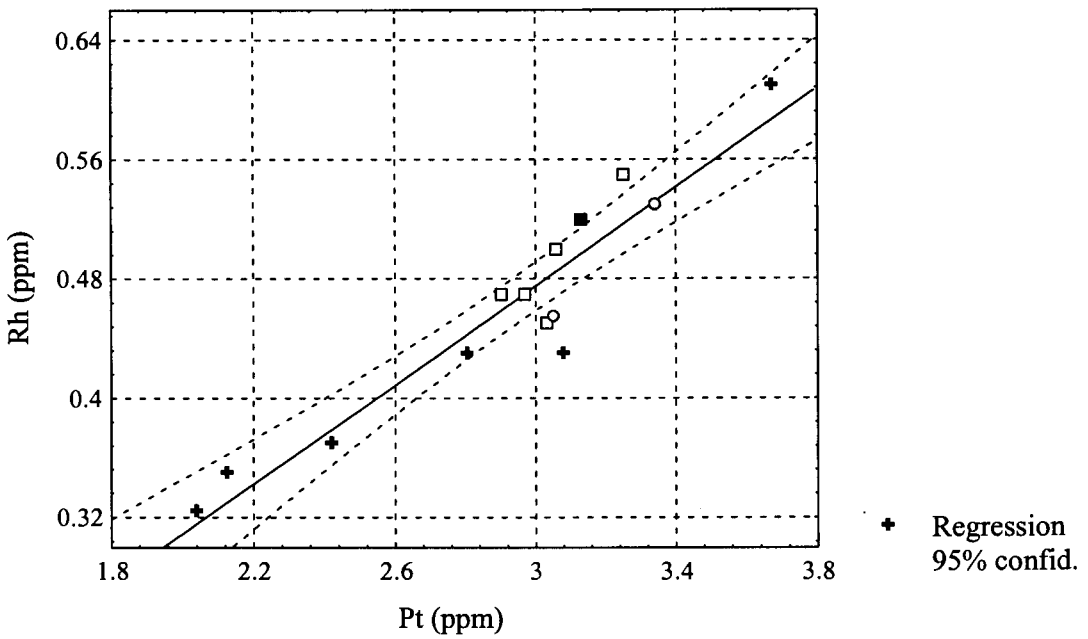

Figure 98 *Relationship between rhodium and platinum for fourteen samples of UG2 chromitite. Pearson correlation coefficient for all fourteen samples, r=0.95. + = samples A1, A2, A3, B1, B2, and B3. □ = samples C1, C2, C3, C4 and C5. o = samples A4 and B4. ■ = sample A5.*

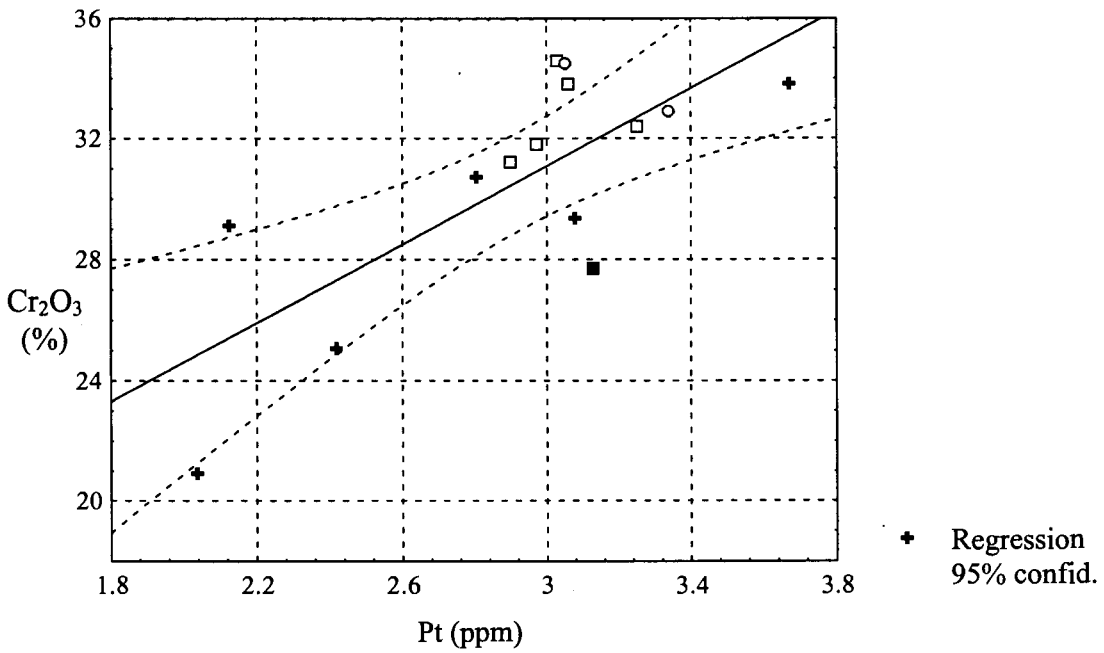

Figure 99 *Relationship between platinum and Cr_2O_3 for fourteen samples of UG2 chromitite. Pearson correlation coefficient r=0.75. + = samples A1, A2, A3, B1, B2, and B3. □ = samples C1, C2, C3, C4 and C5. o = samples A4 and B4. ■ = sample A5.*

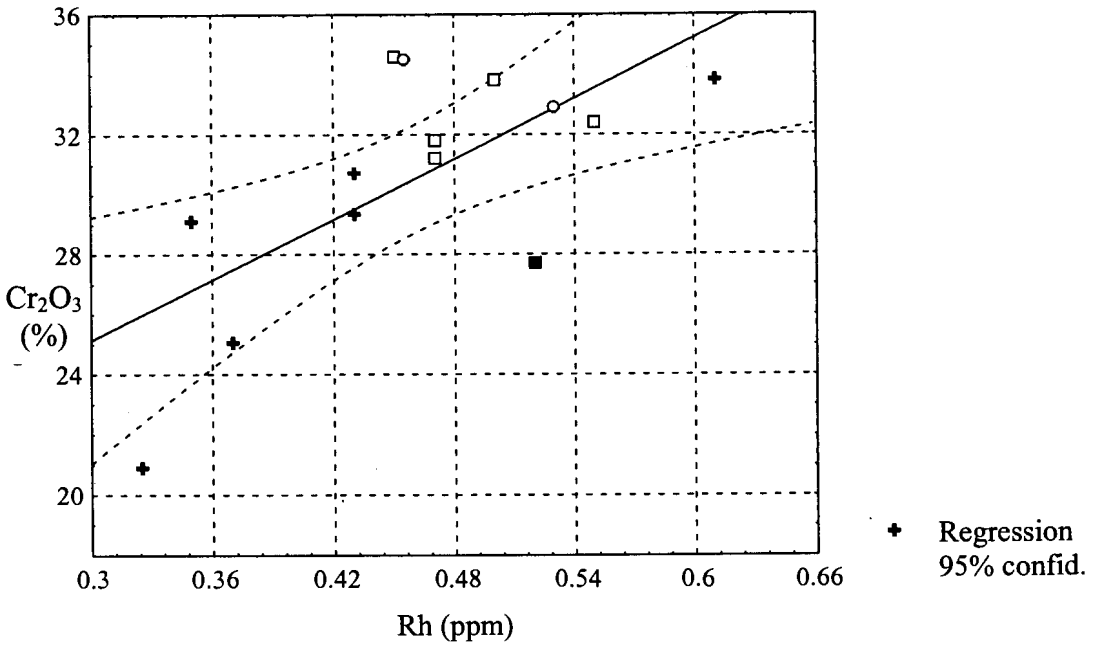

Figure 100 *Relationship between rhodium and Cr_2O_3 for fourteen samples of UG2 chromitite. Pearson correlation coefficient r=0.68. + = samples A1, A2, A3, B1, B2, and B3. □ = samples C1, C2, C3, C4 and C5. o = samples A4 and B4. ■=sample A5.*

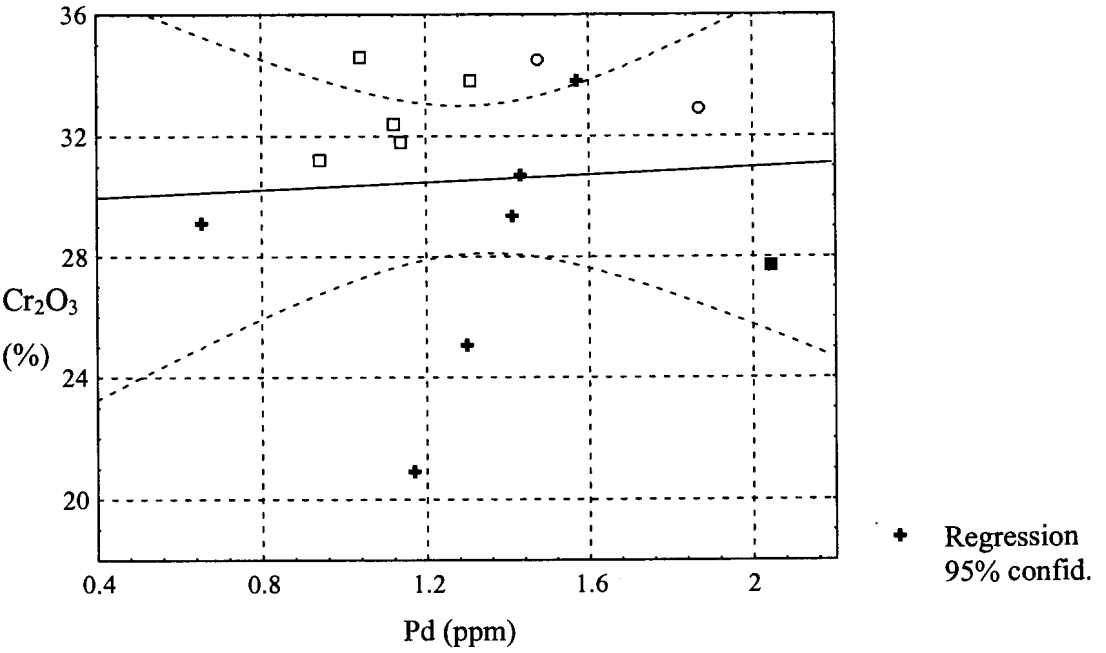

Figure 101 *Relationship between palladium and Cr_2O_3 for fourteen samples of UG2 chromitite. Pearson correlation coefficient r=0.06. + = samples A1, A2, A3, B1, B2, and B3. □ = samples C1, C2, C3, C4 and C5. o = samples A4 and B4. ■=sample A5.*

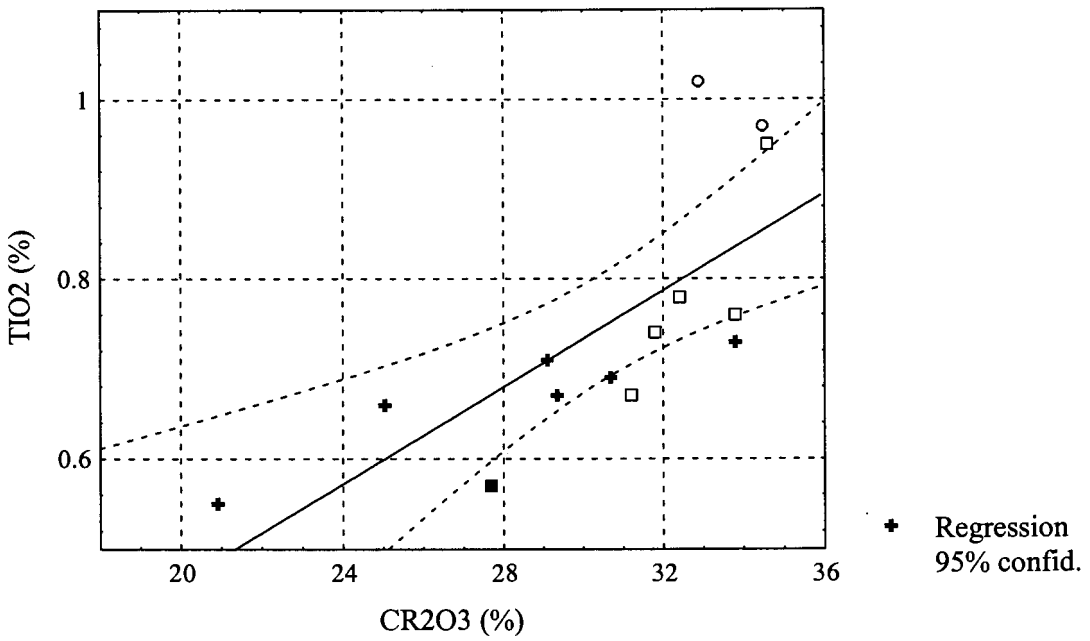

Figure 102 *Relationship between TiO_2 and Cr_2O_3 for fourteen samples of UG2 chromitite. Pearson correlation coefficient r=0.74 for all samples. + = samples A1, A2, A3, B1, B2, and B3. □ = samples C1, C2, C3, C4 and C5. o = samples A4 and B4. ■=sample A5.*

6.2 PGE mass balance calculations

The amounts of platinum, palladium, ruthenium and rhodium represented by the discrete PGE mineral phases found in sample A1 were calculated and are compared with the analytical values in Table 6.3.° Good agreement was found between the calculated and analytical values for platinum. The calculated palladium, rhodium and, to a lesser extent ruthenium values, are significantly lower than the analytical values, implying the presence of these elements in sub-microscopic form in other phases. This is in good agreement with the electron-microprobe analysis results, which indicated that significant amounts of palladium and rhodium are present in base-metal sulphide, particularly pentlandite, while platinum concentration levels are generally below the detection limit of the analysis technique.

° Such a large number of samples need to be searched for an accurate value that this was done only for sample A1.

If it is assumed that all of the acid soluble nickel occurs in pentlandite with the composition $Fe_{4.58}Ni_{4.32}Co_{0.06}S_{8.00}$, a pentlandite content of 0.08 mass per cent is indicated (compared to 0.06 mass per cent indicated by image analysis). If it is further assumed that all of the palladium and rhodium that do not occur in discrete PGE minerals, is present sub-microscopically in pentlandite, then the average palladium and rhodium content of pentlandite would be 755 ±350 ppm and 320 ±150 ppm respectively.* Unfortunately, in the absence of accurate trace element analyses of the base-metal sulphides, there is no way of testing the accuracy of these values.

Paktunc *et al.* (1990) published proton-microprobe and electron-microprobe analyses of pentlandite, chalcopyrite and pyrrhotite from two samples of UG2 chromitite. No PGEs were detected in chalcopyrite or pyrrhotite. In pentlandite, palladium values of 292±8 ppm (proton microprobe) and 342±110 ppm (electron-microprobe) were detected in the one sample, and 56±6 ppm in the other. No rhodium or platinum was recorded. These values are significantly lower than those suggested by the current study, but in the case of palladium at least, do show the same trend.

Electron-, ion- and proton-microprobe analyses of sulphide minerals from many ore deposits indicate that palladium can occur in appreciable amounts (several hundred ppm, and even up to a few per cent) in pentlandite (Genkin *et al.*, 1974; Cabri & LaFlamme, 1979; 1981; Kinloch, 1982; Peyerl, 1983; Cabri *et al.*, 1984; Paktunc *et al.*, 1990; Prendergast, 1990; Cabri, 1992; Czamanske *et al.*, 1992; Ripley & Chryssoulis, 1994; Ballhaus & Ryan, 1995; Weiser *et al.*, 1998). Traces of palladium have also been found in chalcopyrite, pyrrhotite and pyrite (Cabri *et al.*, 1984; Paktunc *et al.*, 1990; Cabri, 1992; Czamanske *et al.*, 1992; Oberthür *et al.*, 1997).

Up to a few hundred ppm rhodium have been measured in pentlandite (Genkin *et al.*, 1974; Peyerl, 1983; Cabri, 1992; Ballhaus & Ryan, 1995; Oberthür *et al.*, 1997; Garuti *et al.*, 1999). All the rhodium in the Merensky Reef is believed to occur as

---

* 90% confidence limits calculated taking into account both the precision associated with the PGE mineral modal analysis and the chemical assay.

solid solution in pentlandite (Kinloch, 1982). Traces of rhodium have been detected in pyrrhotite and pyrite (Oberthür *et al.*, 1997).

Table 6.3 *A comparison of the PGE values in sample A1 calculated from the modal analysis with chemical assay values. These values are based on data collected on 1642 PGE mineral grains found in eighty polished sections.*

Element	***Calculated value (ppm)***	***Absolute error (ppm)***	***Analytical value (ppm)***	***Absolute error (ppm)***
Platinum	3.02	±0.42	3.08	±0.70
Palladium	0.78	±0.19	1.41	±0.30
Rhodium	0.17	±0.06	0.43	±0.06
Ruthenium	0.79	±0.15	1.08	-
Σ(Pt,Pd,Rh)	3.97	±0.55	5.05	±0.23

The only reported occurrence of significant amounts of platinum in sulphides is that by Oberthür and co-workers (1997) who found up to 244 ppm platinum in pyrite. They also found traces of platinum in pyrrhotite and pentlandite.

Experimental work by Makovicky and co-workers (1985) indicated that ruthenium, rhodium and palladium can fully occupy the octahedral position in pentlandites with Fe:Ni ≈ 1:1, with complete solid solution towards PGE-free pentlandite.

In summary, it can be said that results of the current study indicated that rhodium and palladium occur in appreciable amounts in sub-microscopic form in pentlandite. Most of the platinum seems to be present as discrete PGE minerals. Electron-microprobe analysis rarely indicated the presence of sub-microscopic PGEs in chalcopyrite, pyrrhotite, millerite and pyrite. Rare grains of siegenite from area C contain significant amounts of sub-microscopic platinum and rhodium. In general terms, these observations are in agreement with findings by other workers of PGE-bearing ores from the Bushveld Complex and elsewhere.

The likelihood that trace amounts of PGE may also occur sub-microscopically in chromite and silicates was suggested by Peyerl (1983). Experiments by Capobianco and co-workers (1990; 1994) showed large crystal-chemical compatibility for ruthenium and rhodium in spinel. Unfortunately, these experiments were conducted at f_{O_2} levels not applicable to the UG2 chromitite. Hofmeyr (1998), based on SIMS analyses of a sample of UG2 chromitite, subsequently suggested that of the order of 4

per cent of the platinum, 6 per cent of the palladium, 0.4 per cent of the rhodium, and 19 per cent of the iridium, occur in solid solution in chromite.

6.3 The effect of postmagmatic alteration processes on the UG2 chromitite

6.3.1 Relatively unaltered UG2 chromitite

The mineralogical characteristics of samples A1, B1, B2, A2, B3 and A3 is typical of that of normal or undisturbed UG2 chromitite. These samples originated from a variety of environments: samples A2 and B2 represent UG2 chromitite with anorthosite and norite footwall, respectively; samples A1 and B1 were characterised by the presence of pegmatoid footwall, and samples A3 and B3 were collected from the edges of pothole structures. In addition, samples B1 and B3 may also have been exposed to the effects of iron-rich ultrabasic replacement pegmatoid present in the vicinity. Sample A1 appears to be the least altered of the samples. The presence of a notable amount of non-sulphide PGE mineral in sample B1, the increase in chromite grain size in samples B2 and A3, and even in B1, the presence of millerite and pyrite in sample B2, and the presence of varying amounts of secondary silicates in all of these samples, indicate that a variety of postmagmatic processes have left their mark on these samples. However, compared to the samples in the other groups, the degree of alteration is low.

Barnes and Campbell (1988) postulated that during formation of the Merensky Reef, molten sulphide liquid and the fractionated dregs of vapour saturated intercumulus silicate melt were pushed into the residual pore space. This sharing of pore space during the final stages of solidification accounts for the observed association of base-metal sulphide and PGE minerals with phlogopite and other hydrous silicates and an assortment of phases such as quartz, rutile and zircon. Based on the mineralogical evidence presented here, a similar scenario is proposed for the UG2 chromitite.

In the Merensky Reef, rimming of pyrrhotite by pentlandite and chalcopyrite have been interpreted as resulting from fractional crystallisation (Kingston, 1966, Vermaak & Hendriks, 1976; Mostert *et al.*, 1982; Ballhaus & Stumpfl, 1986). Similar textures were observed in the UG2 chromitite. During magmatic fractionation the sulphide liquid solidifies over at temperature interval, starting with monosulphide solid

solution at ~1050°C, and culminating in the solidification of copper-rich residual liquid at ~850°C (Craig & Kullerud, 1969). During cooling, the monosulphide solid solution field narrows to form pentlandite in a pyrrhotite-dominated matrix, which becomes stable at ~610 °C (Kullerud *et al.*, 1969).

The present pentlandite-rich assemblage in the UG2 does not represent the primary magmatic sulphide assemblage. Sulphide assemblages associated with the chromitite layers of the Bushveld Complex are enriched in PGEs, nickel and copper compared to typical magmatic sulphide assemblages (McLaren & de Villiers, 1982; Gain, 1985; Von Gruenewaldt *et al.*, 1986; Naldrett & Lehmann, 1987; Naldrett, 1989). Gain (1985) and Von Gruenewaldt *et al.* (1986) suggested that the original mass of these sulphides has been greatly reduced by the removal of iron and sulphur, with the consequent enrichment of other metals. Naldrett (1989) calculated that, assuming that all the original copper and nickel remain, approximately one half to two thirds of the original sulphide present has been lost.

Naldrett and Lehmann (1987) and Naldrett *et al.* (1989) demonstrated the feasibility of a process whereby iron may be lost from magmatic sulphides to fill vacancies in non-stoichiometric chromite crystallizing from basaltic magma. Release of sulphur resulting from the dissociation of magmatic pyrrhotite may lead to the formation of pyrite from pyrrhotite. Once the most sulphur-rich assemblage possible under the prevailing conditions has formed, further extraction of iron will lead to a bulk loss of sulphur (Merkle, 1992).

Most of the PGEs were probably scavenged by the sulphide melt. Experimental work (Distler *et al.*, 1977; Fleet *et al.*, 1993; Li *et al*, 1996) indicates that during cooling, rhodium and ruthenium will preferentially partition into the monosulphide solid solution, with palladium favouring the copper-rich residual melt. Platinum forms alloy phases at low f_{S2}, and follows palladium into the sulphide liquid at high f_{S2}.

At elevated temperatures the base-metal sulphides, especially pyrrhotite and pentlandite, can accommodate significant amounts of PGEs in solid solution (Distler *et al.*, 1977; Makovicky *et al.*, 1986; Ballhaus & Ulmer, 1995), most of which will be expelled on cooling to form discrete PGE minerals. Chalcopyrite appears to be barren of PGEs, even at elevated temperatures. This explains the observed association of

most of the PGE minerals with base-metal sulphides, occurring either at sulphide grain boundaries with silicates or chromite, at sulphide-sulphide grain boundaries, or as inclusions in sulphide. Ballhaus and Ryan (1995), and Ballhaus and Ulmer (1995) suggested that the association of discrete PGE minerals with base-metal sulphides reflect equilibration to temperatures below 100 °C.

The small proportion (~5 per cent) of PGE minerals that are present as inclusions in chromite, almost exclusively laurite, possibly formed during cooling, as a result of exsolution of PGEs in solid solution in chromite (Capobianco *et al.*, 1994).

6.3.2 Sintered UG2 chromitite - the effect of Fe-rich ultrabasic replacement pegmatoid

Late-stage hydrothermal fluids, rich in iron and titanium, sporadically altered the chemistry and mineral assemblage of the UG2 chromitite (Viljoen & Scoon, 1985; Grimbeek, 1995). The UG2 chromitite layer may have acted as a physical barrier resulting in sintering of chromite at the bottom of the layer, together with changes in the spinel composition, and the formation of ilmenite and magnetite.

The enlargement and change in the composition of chromite grains, the presence of elevated amounts of TiO_2, and the PGE mineral assemblages dominated by Pt-Fe alloys (often rhodium- or palladium-bearing), laurite, and to a lesser extent PGE-Bi-Te compounds, and other non-sulphide PGE minerals in sintered samples A4 and B4 are typical of UG2 chromitite associated with replacement pegmatoid (McLaren & De Villiers, 1982; Peyerl, 1982; Viljoen & Scoon, 1985; Grimbeek, 1995). Samples B1 and B3 also appear to have been affected by replacement pegmatoid, albeit to a lower degree. The formation of such PGE mineral assemblages have been attributed to higher f_{O2}, possibly as a result of increased volatile activity resulting in lower f_{S2} (Peyerl, 1982; Kinloch, 1982; McLaren & de Villiers, 1982; Evstigneeva *et al.*, 1995).

Based on reports in the literature (McLaren & de Villiers, 1982; Peyerl, 1982; Viljoen & Scoon, 1985; Gain, 1985; Viljoen *et al.*, 1986a, b; Leeb-du-Toit, 1986; Farquhar, 1986; Hofmeyr & Adair, 1993; Grimbeek, 1995; Van der Merwe *et al.*, 1998), the base-metal sulphide mineralogy of samples associated with dunite pipes and iron-rich ultrabasic replacement pegmatoid ranges from being similar to that of relatively unaltered UG2 chromitite, to more complex sulphide assemblages containing minerals

such as chalcocite, bornite, violarite, mooihoekite, haycockite, digenite, native copper, cubanite, mackinawite, heazlewoodite and millerite. These variations can be attributed to variable degrees of metasomatic effects from the replacement pegmatoid. In the samples investigated, the base-metal sulphide mineralogy is, aside from a slight increase in grain size, similar to that of relatively unaltered UG2 chromitite.

6.3.3 Millerite-bearing UG2 chromitite – the effect of low-temperature hydrothermal alteration

The UG2 chromitite from area C appears to have been subjected to a regional low-temperature hydrothermal alteration, not directly related to any small-scale geological disturbance. The samples displaying the highest degree of alteration often have abundant hydrothermal veins containing minerals such as calcite, quartz, prehnite, and chlorite.

The replacement of primary silicates by mineral assemblages containing albite, quartz, pumpellyite, epidote, chlorite, prehnite, sphene and talc is similar to that described by Schiffries and Skinner (1987) and Schiffries and Rye (1990) resulting from the interaction of hydrothermal fluids with wallrock at temperatures below about 600°C.

The sulphide assemblage found in these samples, chalcopyrite, millerite, pyrite and subsidiary siegenite, could not have exsolved from a magmatic sulphide melt (Kullerud *et al.*, 1969; Craig & Kullerud, 1969). Merkle (1992) suggested that the corrosion of base-metal sulphides by hydrothermal fluids leads, in places, to iron and sulphur loss, in addition to the losses as a result of sulphide-chromite equilibration. This could lead to the formation of such low temperature, high f_{S2} sulphide assemblages. Based on the lack of mineral textures suggesting replacement of pentlandite by millerite, and phase relations in the Ni-Fe-S and Ni-S systems (Kullerud & Yund, 1962; Vaughan & Craig, 1978), Verryn and Merkle (1994) suggested that millerite in such samples formed directly from hydrothermal fluids at temperatures below 379°C. Reduction of the volume of base-metal sulphides through such losses results in the PGE minerals (previously associated with base-metal sulphides) becoming isolated in hydrous silicates, filling the spaces previously occupied by sulphides.

PGE mineral assemblages in these areas are similar to those occurring in normal UG2, but with noticeably lower concentrations of cooperite, and a concomitant increase in malanite, braggite and vysotskite, possibly indicating lower temperature of formation under conditions of higher f_{S2} (Knacke *et al.,* 1991). The absence of Pt-Fe alloys, especially in sintered sample C1, also points to conditions of increased sulphur fugacity.

It is proposed that the relatively high modal proportions of palladium- and rhodium-bearing sulphides compared to PGE mineral assemblages from normal UG2 is a consequence of the paucity of pentlandite in these samples. Since pentlandite contains small amounts of palladium and rhodium in solid solution, a reduction in the amount of pentlandite may lead to a higher proportion of palladium- and rhodium-bearing PGE minerals.

Many researchers have reported the relative mobility of palladium during surface weathering (Fuchs & Rose, 1974; McCallum *et al.,* 1976; Prichard & Lord, 1994; Hey, 1999). Cousins and Kinloch (1976) speculated that during weathering, nickel and palladium are preferentially leached out of braggite, resulting in a phase with a chemical composition corresponding to that of cooperite, and the structure and optical properties of braggite. A similar process, operating under hydrothermal conditions, may account for zoned Pt-Pd-Ni-sulphide grains in UG2 chromitite (Merkle & Verryn, in preparation). This, together with corroded sulphide textures, may be an indication that the relatively low acid soluble nickel, copper, sulphur and palladium values characterising these samples are the result of secondary processes rather than a primary feature of the UG2 chromitite in this area. Platinum and rhodium values do not seem to have been affected by these processes indicating the relative immobility of these elements.

Further investigation into the significance of baddeleyite — Zr-Ti oxide —rutile assemblages in association with late- to post-magmatic phases, may shed some more light on the conditions prevailing during ore genesis. Similar assemblages have been reported by Merkle (1992) in Middle Group chromitite, and by Cabella and co-workers (1997) in ophiolitic chrome spinel from Italy.

6.3.4 Cataclastic UG2 chromitite – the effect of faulting

Three samples were taken from fault zones, sample A5, B5 and C1. Sample A5 is, however, the only sample displaying extensive cataclasis. The formation of massive chromitite from faulted areas have also been reported by Kupferbürger *et al.* (1937) and Worst (1986), who reported that the formation of this type of ore appears to be a very localised feature, the texture again becoming friable within centimetres.

The presence of fractures in faulted areas makes the UG2 chromitite layer more accessible to circulating fluids. Interaction of these fluids with primary silicate minerals causes the formation of hydrous silicates, quartz and calcite, cementing fractured chromite grains. The PGE mineral assemblage is characterised by the presence of significant amounts of non-sulphide minerals such as Pt-Fe alloy and PGE sulpharsenides which can also be attributed to the effects of fluids at intermediate to high temperatures.

6.3.3 Effect of pothole structures

Samples B3, A3, and C1 were all taken from the edges of pothole structures. The mineralogical properties of C1 were largely determined by the low temperature regional hydrothermal alteration affecting all the samples from area C. It is noteworthy that these three samples are all characterised by an enlargement in chromite grain size, and in the case of C1, elevated TiO_2 contents, but, in the case of sample B3, this can also be attributed to the presence of iron-rich ultrabasic replacement pegmatoid. It is concluded that although all three samples show evidence of secondary alteration, it is unclear whether this is related to their proximity to pothole structures.

6.4 Flotation behaviour of different types of UG2 chromitite

The flotation characteristics of the different samples are graphically compared in Figure 103 (see also Table 6.1) and vary depending on the type of UG2 chromitite. For relatively unaltered UG2 chromitite and samples from area C, the flotation characteristics for the PGEs appear to be very similar, with between 63 and 80 per cent fast-floating PGE, 15 to 26 per cent slow-floating PGE and less than 10 per cent non-floating PGE. Samples of sintered UG2 chromitite are characterised by slightly

less fast-floating PGE (57 to 60 per cent), a higher proportion of slow-floating PGE (34 to 38) and about 6 per cent non-floating PGE. Cataclastic UG2 displayed the poorest flotation characteristics with only 40 per cent fast-floating PGE+Au, 29 per cent slow-floating PGE+Au and 32% non-floating PGE+Au. The rate of flotation for the fast- and slow-floating PGE+Au fractions are more difficult to interpret as these values seem to be more erratic.

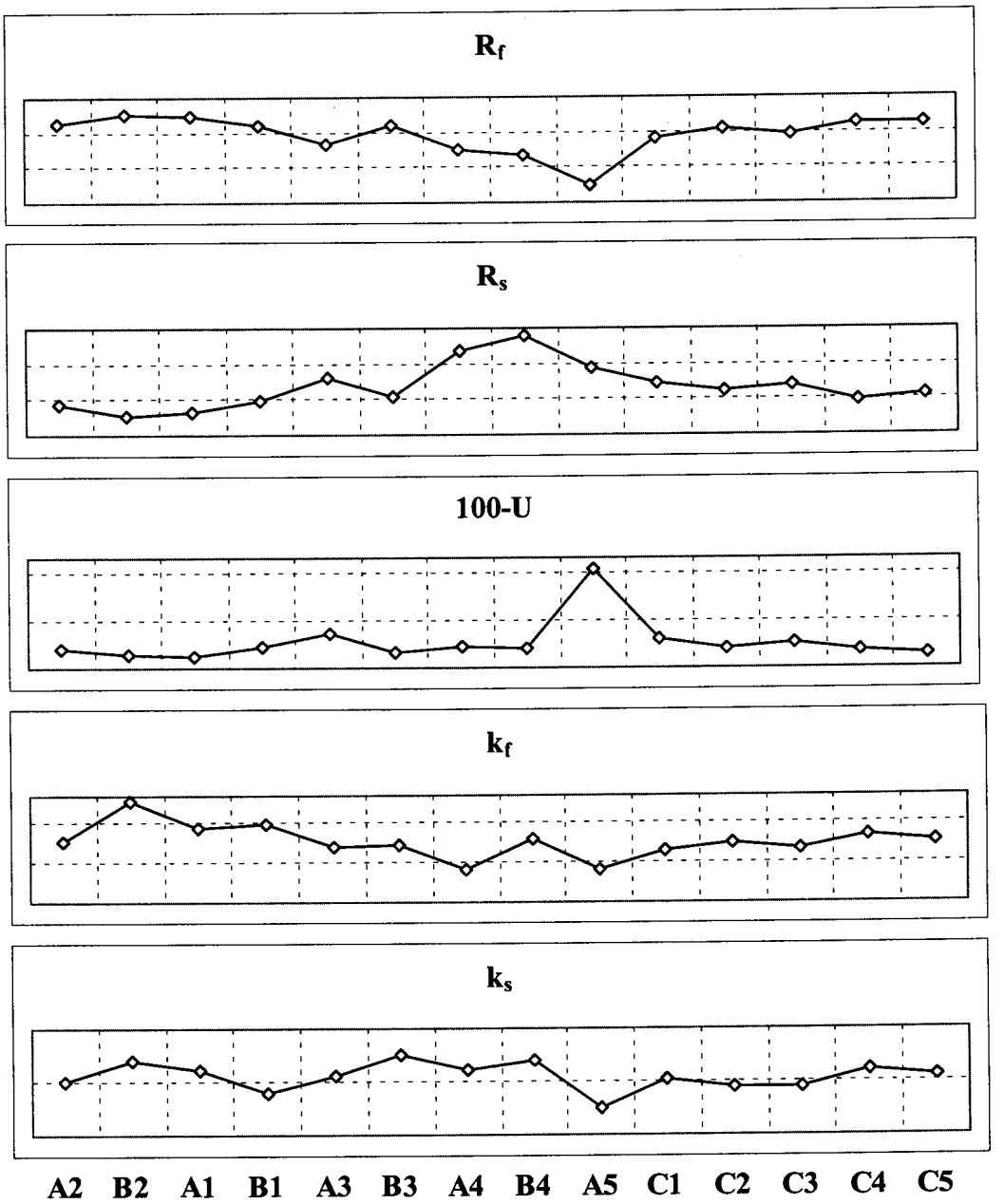

Figure 103 *Comparison of the flotation characteristics of fourteen samples of UG2 chromitite.*

6.5 Interpretation of milling and flotation results

6.5.1 Factors affecting milling time

All of the samples, except for the sample of cataclastic UG2 (A5), were relatively friable, appearing to break along grain boundaries and fractures during the initial stages of size reduction. Further milling resulted in random breakage of mineral grains.

De Waal (1972) concluded that the friability of the chromitites from the Bushveld Complex is controlled by the degree of poikilitic intergrowth of gangue with chromite, or where the gangue fraction is very small, by the degree of annealing of chromite grains. Similar factors probably also determine the response of the sample to comminution, especially during the early stages of size reduction.

Sample A5 was reduced to 80% <75µm in less than forty minutes, with the remainder of the samples requiring between sixty and one hundred and twenty minutes to achieve the same degree of size reduction. The reason for this is probably related to the fact that the chromite and primary silicate grains in this sample had already been broken during cataclasis. Some fracturing of chromite, a difficult parameter to quantify, is present in all the samples, and probably affected milling time to some extent.

Although annealing of chromite grains was observed in some of the samples (especially A4 and B4), it does not appear to have played much of a role during size reduction, possibly because the degree of sintering of chromite grains in these samples is relatively low compared to that of some samples described in the literature (*cf.* Grimbeek, 1995). No correlation was found between the time taken to reduce the samples to 80% <75µm, and chromite grain-size prior to milling, or amount of chromite in the samples (Table 6.4 and Figures 104 and 105).

What is considered more significant, is the fact that the one sample displaying virtually no alteration of plagioclase and orthopyroxene, i.e. A1, required almost twice as much milling time as samples C1 and C3, which, apart from sample A5, were characterised by the highest degree of alteration of the primary silicates. The ease of milling of these samples probably depends largely on the type and degree of silicate

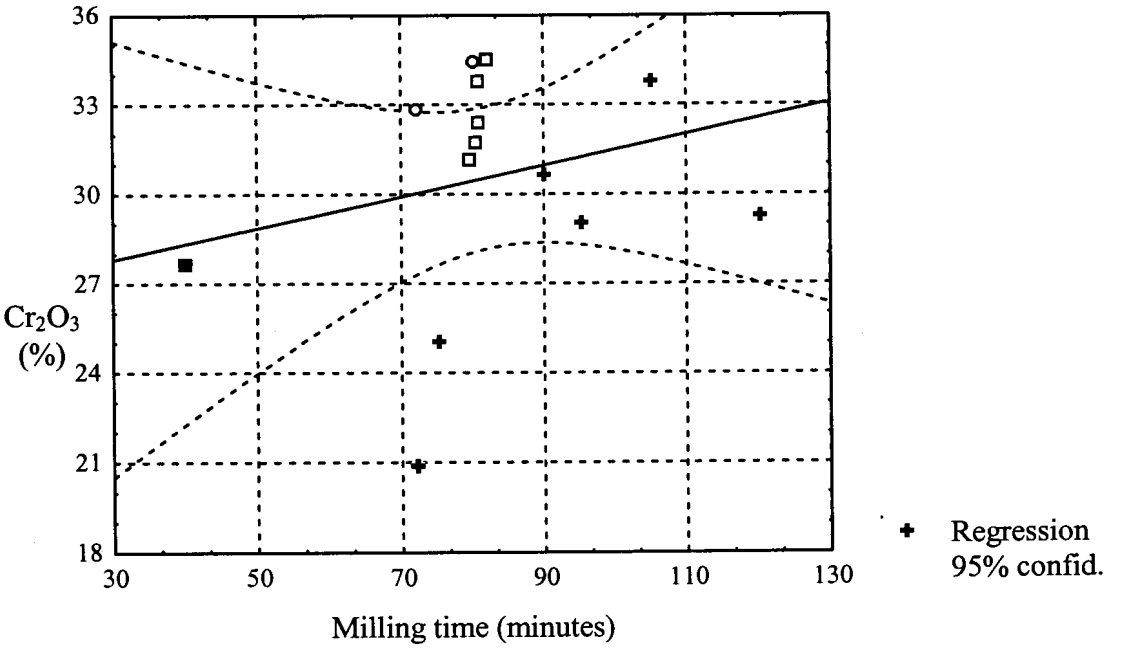

Figure 104 *Relationship between Cr_2O_3 content and time to reduce to 80%<75µm in fourteen UG2 chromitite samples. Pearson correlation coefficient for all fourteen samples, r=0.25. + = samples A1, A2, A3, B1, B2, and B3. □ = samples C1, C2, C3, C4 and C5. o = samples A4 and B4. ■ = sample A5.*

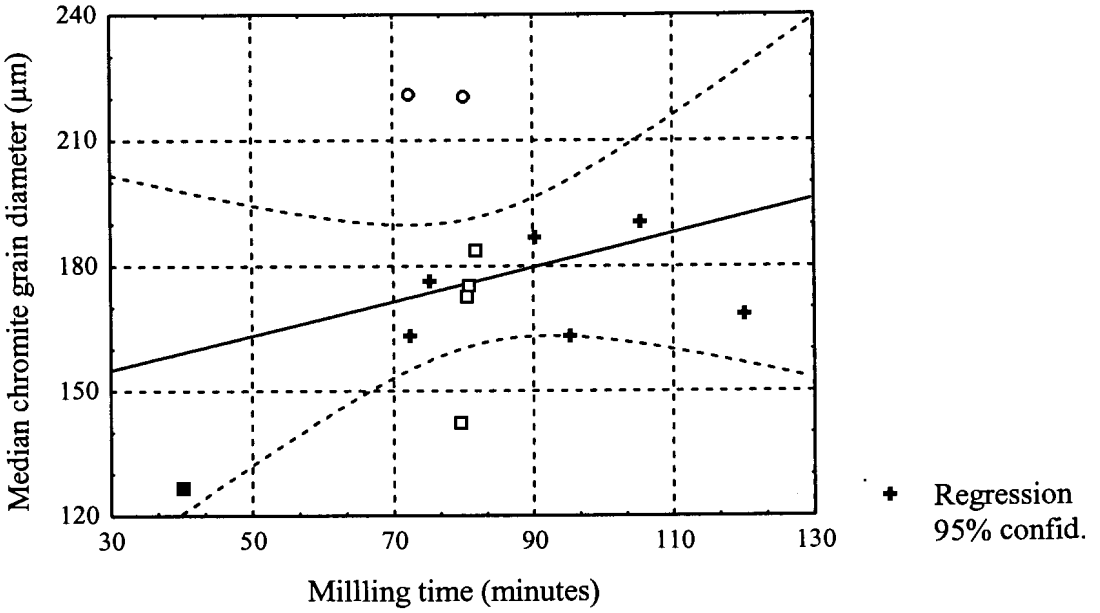

Figure 105 *Relationship between chromite grain size (median equivalent circle diameter) and time to reduce to 80%<75µm in fourteen UG2 chromitite samples. Pearson correlation coefficient, r=-0.26, for all fourteen samples. + = samples A1, A2, A3, B1, B2, and B3. □ = samples C1, C2, C3, C4 and C5. o = samples A4 and B4. ■ = sample A5.*

Table 6.4 *Pearson correlation matrix for time in minutes to mill to 80%<75µm (milltime), Cr_2O_3 content of the feed sample, chromite median grain diameter (in µm) prior to milling (chr1), chromite median grain diameter (in µm) after milling (chr2), silicate median grain diameter (in µm) after milling (sil2), % chromite recovery after 1 minute (chrrec1), % chromite recovery after 20 minutes (chrrec2), % silicate recovery after 1 minute (silrec1), % silicate recovery after 20 minutes (silrec2). Marked correlations (boldface) are significant at p<0.05.*

	Milltime	**Cr_2O_3**	**Chr1**	**Chr2**	**Sil2**	**Chrrec1**	**Chrrec2**	**Silrec1**	**Silrec2**
Milltime	1.00	0.25	-0.26	0.51	0.48	0.50	0.04	0.20	-0.20
Cr_2O_3	0.25	1.00	**0.55**	0.03	-0.18	-0.25	0.08	0.17	0.54
Chr1	-0.26	**0.55**	1.00	-0.48	**-0.60**	-0.06	0.41	-0.25	0.06
Chr2	0.51	0.03	-0.48	1.00	**0.86**	-0.21	**-0.56**	0.20	0.10
Sil2	0.48	-0.18	**-0.60**	**0.86**	1.00	-0.09	-0.48	0.08	-0.13
Chrrec1	0.50	-0.25	-0.06	-0.21	-0.09	1.00	0.49	0.10	**-0.68**
Chrrec2	0.04	0.08	0.41	-0.56	-0.48	0.49	1.00	-0.38	-0.21
Silrec1	0.20	0.17	-0.25	0.20	0.08	0.10	-0.38	1.00	0.46
Silrec1	-0.20	0.54	0.06	0.10	-0.13	**-0.68**	-0.21	0.46	1.00

alteration, with intensely altered samples (e.g. C1 and C3) being fairly friable, and requiring a relative short milling time. In comparison, sample A1 shows hardly any indication of alteration of the silicates, hence the extended milling time required.

6.5.2 Mechanisms affecting gangue recovery

The presence of gangue minerals in flotation concentrates is undesirable, as it affects both concentrate grades and recovery negatively. For the samples under investigation, the flotation concentrates were produced by rougher flotation without any cleaning stages, hence the low grades. However, it is worthwhile examining the flotation behaviour of the gangue minerals, in as far as it does shed some light on the behaviour of composite mineral particles during flotation.

Chromite recovery

Chromite grains in the flotation concentrates are fine-grained and liberated. Statistical analysis indicates a negative correlation between chromite grain size in the milled feed sample and chromite recovery after twenty minutes flotation (Table 6.4 and Figure 106). The recovery of fine-grained, liberated chromite grains, is an indication that these grains reported to the flotation concentrates as a result of entrainment rather than flotation.

True flotation occurs when hydrophobic mineral particles attach to air bubbles in an aerated, agitated pulp. The mineralised bubbles rise till they reach the top of the froth and are scraped off. This is, however, not the only mechanism responsible for the presence of mineral grains in flotation concentrates. Entrainment occurs when fine-grained material suspended in inter-bubble water is recovered with the froth. The rate of gangue mineral recovery by entrainment is dependent on the particle size of the gangue minerals, with finer gangue particles entrained more readily than coarse gangue particles (Trahar, 1981; Subrahmanyam & Forssberg, 1990; Kirjavainen, 1992; 1996).

Warren (1985) suggested that recovery due to entrainment increases linearly with water recovery. By relating water recovery to chromite recovery, Marais (1989) determined that entrainment is responsible for most of the chromite recovered during laboratory rate flotation tests of UG2 ore. It should be noted though, that recent work

by Wesseldijk and co-workers (1999), indicated that under certain conditions chromite may be activated by the reagent suite used for the flotation of UG2 ore, rendering it hydrophobic and amenable to true flotation.

Gottlieb & Adair (1991) sited rimming of chromite grains by talc as one of the reasons for chromite reporting to flotation concentrates. No evidence was found that this mechanism of chromite recovery played a role during flotation of the samples under investigation.

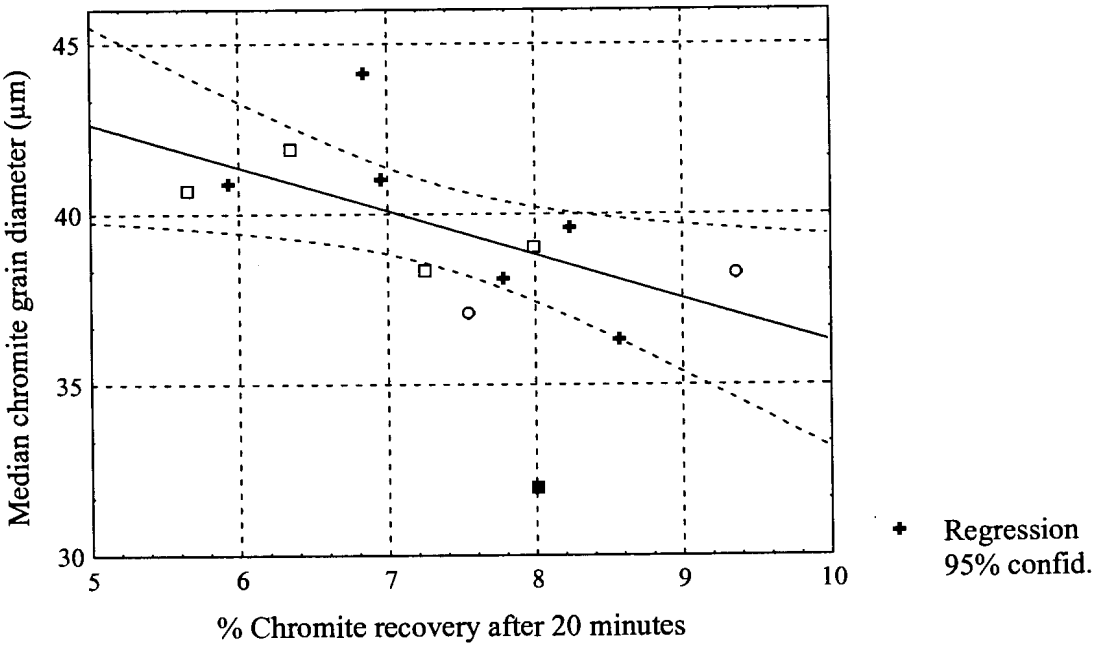

Figure 106 *% chromite recovery after 20 minutes flotation versus median chromite diameter in milled feed samples. Pearson correlation coefficient, r=-0.56 for all samples except A5. + = samples A1, A2, A3, B1, B2, and B3. □ = samples C1, C2, C3, C4 and C5. o = samples A4 and B4. ■ = sample A5.*

Silicate recovery

Entrainment probably also plays a key role in the presence of silicate minerals in flotation concentrates. Although most of the silicates in the flotation concentrates are fine-grained, no correlation was found between silicate particle size and silicate recovery (Table 6.4). This is an indication that factors other than size may affect silicate behaviour during flotation. Because of their soft platy habit, minerals belonging to the phyllosilicate group (chlorite, serpentine, talc, phlogopite, prehnite)

tend to form fines during comminution. Kirjavainen (1992; 1996) found that apart from pulp density and water recovery, which is determined by operational factors, particle mass and shape also affects the probability of entrainment of fine particles. Fine-grained, flaky minerals with low mass have the highest probability of being entrained.

Some of the liberated silicates in the flotation concentrates were, however, probably recovered by true flotation. A mineral surface will be hydrophobic if that surface was created without breakage of interatomic bonds other than residual van der Waals bonds. For that reason, talc is naturally flotable (Gaudin, 1957; Zheng & Lin, 1994). This accounts for the higher observed recovery of Fe-Mg silicates in the more altered samples and the high total silicate recoveries for samples from area C. As a result of the floatability of talc, not only talc was recovered, but also orthopyroxene attached to it. Although the flotation reagent suite included talc depressant, the dose was clearly not sufficient to effect complete depression of talc. Complete depression of talc may not be all that desirable, as it could lead to base-metal and PGE losses, due to suppression of both partly liberated sulphide and PGE mineral grains, and of liberated grains coated with talc slimes.

6.5.3 Base-metal sulphide and PGE mineral liberation

Base-metal sulphide liberation

During milling, base-metal sulphide grains occurring at chromite-silicate grain boundaries can be expected to be liberated more readily compared to those occurring as inclusions in silicate or chromite. Base-metal sulphide liberation may therefore, to a certain extent, be predicted from the amount of base-metal sulphide occurring as liberated grains and at chromite-silicate grain boundaries in the crushed feed (Table 5.1L). A comparison between this predicted liberation, and the measured amount of liberated base-metal sulphide in the milled feeds, indicates that a correlation does indeed exist ($r=0.62$, $p=0.019$) (Figure 107). The measured apparent degree of liberation is higher than predicted liberation in all but two samples, C1 and C5. Exclusion of these two outliers improves the correlation significantly ($r=0.81$, $p=0.001$).

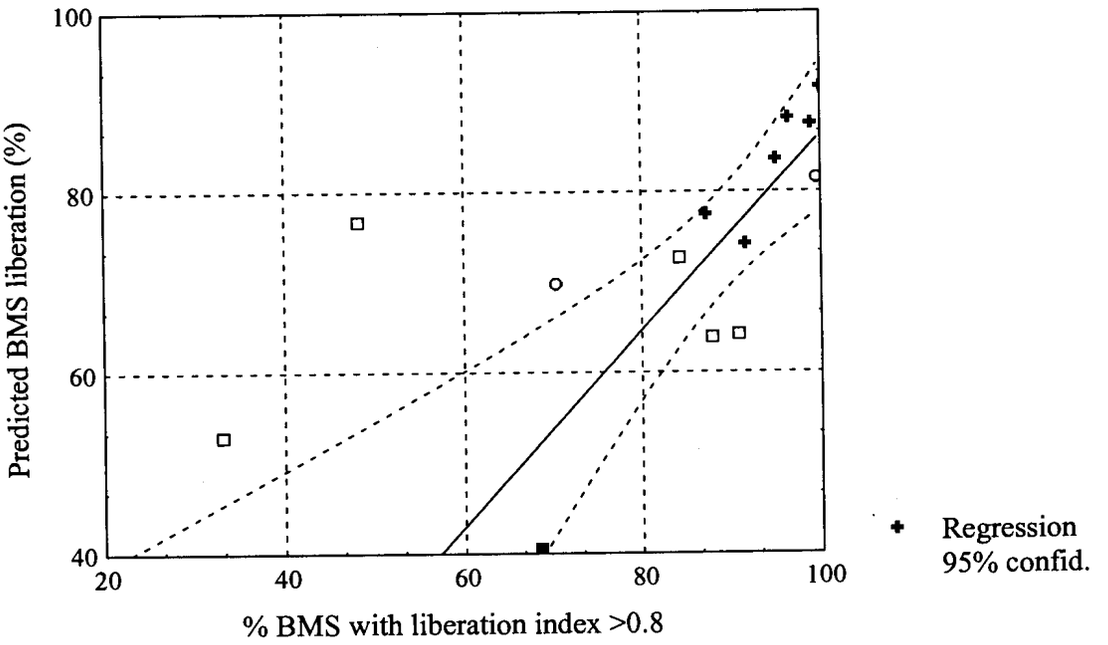

Figure 107 *Relationship between actual and predicted base-metal sulphide liberation. Pearson correlation coefficient r=0.81 for all samples except C1 and C5. + = samples A1, A2, A3, B1, B2, and B3. □ = samples C1, C2, C3, C4 and C5. o = samples A4 and B4. ■ = sample A5.*

Liberation of PGE mineral-bearing particles

Of more relevance is the degree of liberation of PGE mineral-bearing particles. A predicted combined mineral liberation index was calculated by adding together PGE minerals already liberated in the crushed feed, or located at grain boundaries (either of sulphide and gangue, or chromite and silicate), and the amount associated with sulphide multiplied by predicted sulphide liberation (Table 5.1P). There appears to be a linear relationship between this predicted combined liberation index and the percentage PGE mineral in the milled feed occurring in particles with a combined liberation index (CLI) greater than 0.8 (Pearson correlation coefficient r = 0.82) (Figure 108). Exclusion of samples C1 and C5 increases the correlation slightly to r=0.85.

As for the sulphide minerals, the actual measured liberation values are higher than the predicted values. The reason for this is twofold. Firstly, the rather simplified predicted liberation parameters calculated do not take into account base-metal sulphides and PGE minerals located at silicate-silicate grain boundaries (a difficult

parameter to quantify), nor the effect of cleavage and other planes of weakness which may affect milling response. Secondly, as discussed in section 4.6.2, the measured liberation is an overestimation of true liberation. However, these results do indicate that the liberation characteristics of base-metal sulphides and PGE minerals are not random, but depend on the texture of the samples prior to milling.

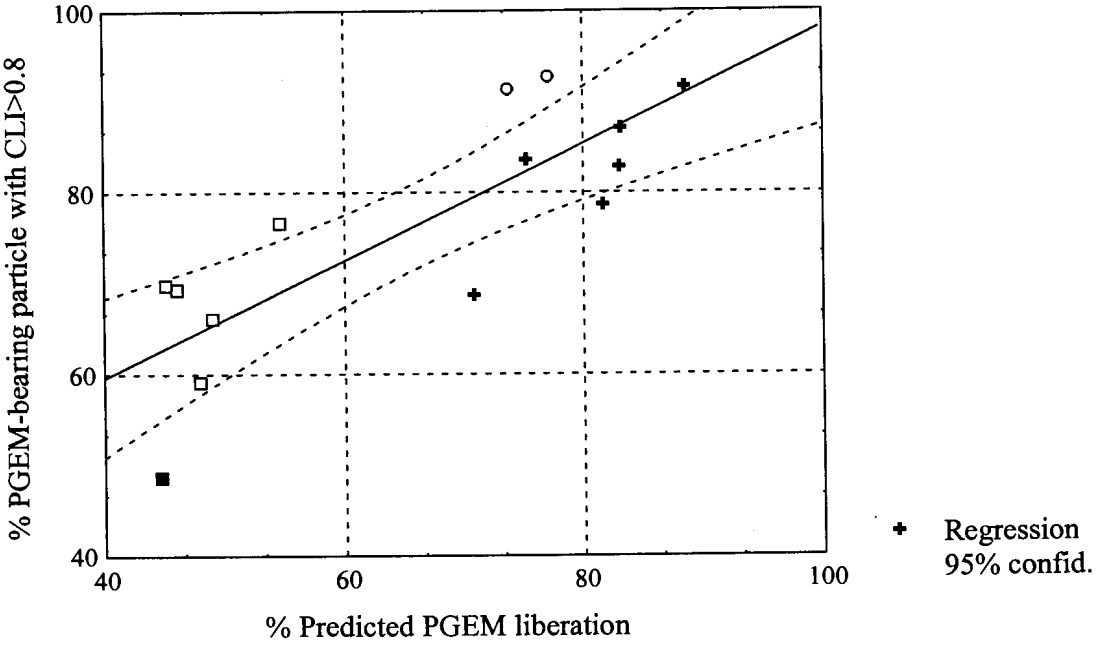

Figure 108 *Relationship between % liberated PGE mineral at 80% <75µm and the predicted PGE mineral liberation. Pearson correlation coefficient r=0.82. + = samples A1, A2, A3, B1, B2, and B3. □ = samples C1, C2, C3, C4 and C5. o = samples A4 and B4. ■ = sample A5.*

Effect of milling on PGE mineral and base-metal sulphide grain size

Both PGE mineral and base-metal sulphide grain sizes were reduced considerably during milling. There appears to be a weak positive correlation between the median equivalent circle diameter of base-metal sulphide grains before and after milling (Pearson correlation coefficient r = 0.61) (Figure 109). No correlation could be found between median equivalent circle diameter of PGE mineral before and after milling (Figure 110).

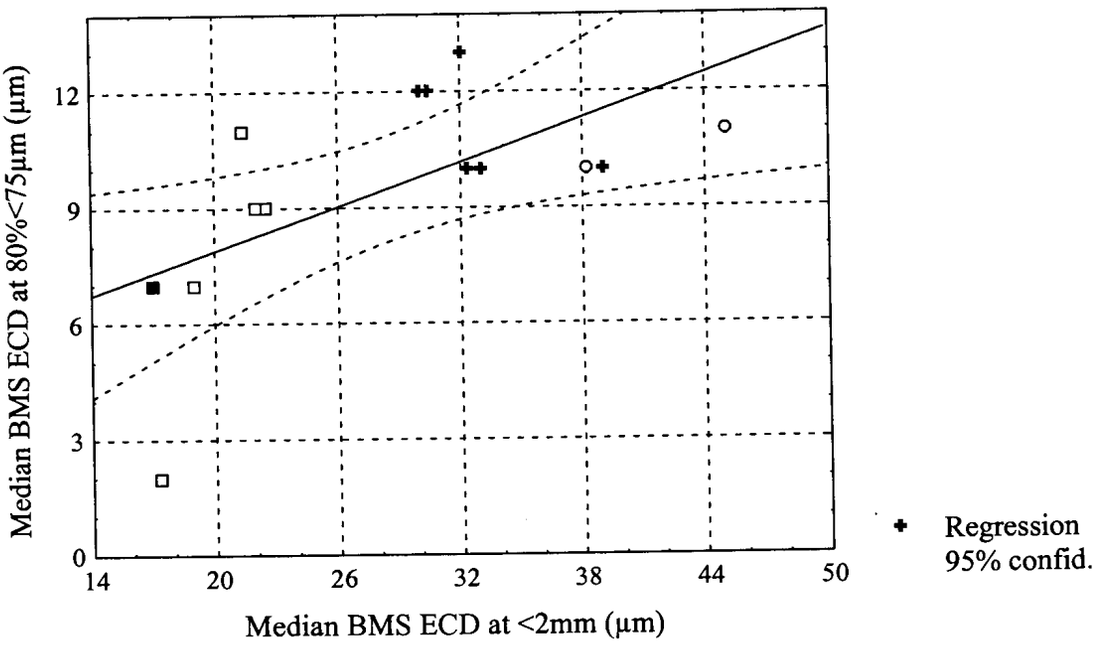

Figure 109 *Effect of milling on base-metal sulphide (BMS) mineral median equivalent circle diameter (ECD). Pearson correlation coefficient r=0.61 + = samples A1, A2, A3, B1, B2, and B3. □ = samples C1, C2, C3, C4 and C5. o = samples A4 and B4. ■ = sample A5.*

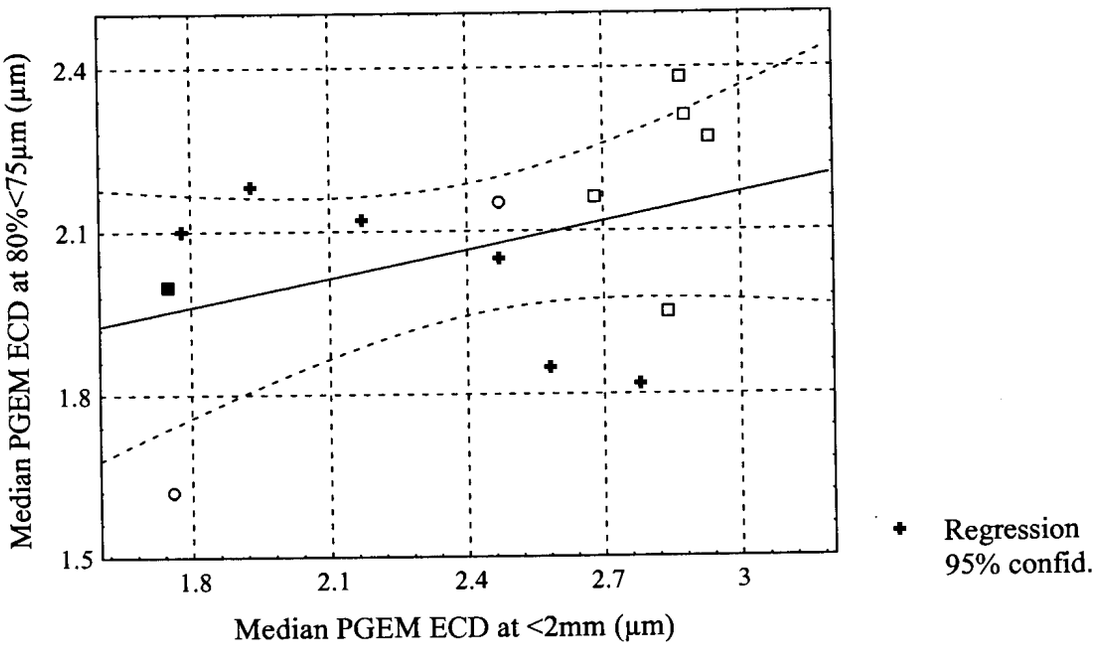

Figure 110 *Effect of milling on PGE mineral (PGEM) median equivalent circle diameter (ECD) based on % number of grains. Pearson correlation coefficient r=0.38. + = samples A1, A2, A3, B1, B2, and B3. □ = samples C1, C2, C3, C4 and C5. o = samples A4 and B4. ■ = sample A5.*

6.5.4 Flotation behaviour of base-metal sulphides

Effective recovery of the base-metal sulphides, especially pentlandite, is of the utmost importance because of their association with PGEs, both as discrete PGE minerals and in solid solution. Mineralogical examination of the flotation products indicates that most of the base-metal sulphide report to the flotation concentrates as liberated grains, with an increase in composite particles in the slower-floating concentrates. The sulphides in the tailings samples are present almost exclusively as fine-grained inclusions in coarse composite silicate particles.

Recovery of liberated base-metal sulphides

Although the flotation tailings do not contain significant concentrations of liberated base-metal sulphides, the slower-floating concentrates do. In a plant situation these slower-floating sulphides will form part of middling streams, such as tailings of cleaning circuits, which may constitute losses if they are not properly treated. In order to maximise sulphide recovery, it is important to understand the mechanisms governing the flotation rates of liberated sulphide grains.

This investigation indicated that coarse liberated base-metal sulphides are recovered at a relatively fast rate, with progressively finer grains recovered with time. Particle size is known to be a major limitation on separation efficiency, with losses in both coarse (> about 70μm) and fine fractions (below approximately 5 to 10 μm) (Trahar, 1981; Senior *et al.*, 1994; Lange *et al.*, 1997). These size ranges vary for different minerals and are also dependent on the scale of operation.

It is believed that a significant proportion of fine-grained sulphides is recovered due to entrainment rather than true flotation (Trahar, 1981). Senior *et al.* (1994) estimated from tests on synthetic mixtures of pentlandite, pyrrhotite, chalcopyrite and quartz, that less than 35 percent of 4 to 10 μm pentlandite genuinely floated, and about 15 percent of –4μm pentlandite.

However, particle size is not the only factor determining the flotation rate of liberated sulphide grains. Different sulphides float at different rates because of differences in their surface characteristics (Herrera-Urbina *et al.*, 1990). Pyrrhotite is known to be

relatively slow-floating, hence the presence of relatively coarse liberated pyrrhotite grains in the slower-floating concentrates of some of the samples.

Sulphide mineral hydrophobicity is affected by a number of variables such as reagent conditions and surface preparation conditions (e.g. pH and Eh), the presence of adsorbed hydrophylic fines e.g. gangue minerals (Edwards *et al.*, 1980; Parsonage, 1985), electrochemical interaction between minerals (Guy & Trahar, 1985; Cheng & Iwasaki, 1992, Bozkurt *et al.*, 1997) and between minerals and the grinding media (amongst others Kocabag & Smith, 1985; Pozzo *et al.*, 1990; Cheng & Iwasaki, 1992, Senior *et al.*, 1994; Yuan *et al.*, 1996). The latter is believed to be partly responsible for the slow-floating nature of pyrrhotite (Pozzo *et al.*, 1990).

The behaviour of composite particles during flotation

The behaviour of composite particles during flotation is not well documented or understood. This is partly because it is not possible to distinguish between the effects of particle composition and the effects of particle size, as composites tend to be in the slower-floating coarse sizes. It is generally assumed that locked particles float in some manner intermediate between fast-floating free particles and non-floating gangue particles. Investigations by Trahar (1991) and Sutherland (1989) indicated that a very small amount of floatable mineral is required to induce flotation of a composite particle.

In the samples under investigation, it was found that where the flotation feed was characterised by a higher proportion of the sulphide minerals occurring as part of composite particles, such as in samples from area C and sample A5, a high proportion of these composite particles reported to the flotation concentrates. The presence of talc in composite particles probably contributed to the floatability of some of these particles. The presence or absence of slow-floating pyrrhotite may also have an effect.

6.5.5 Flotation behaviour of PGE minerals

Most of the PGE minerals were recovered in the form of liberated PGE mineral grains or PGE mineral grains associated with base-metal sulphide. The rate of flotation of liberated base-metal sulphide grains is faster than that of liberated PGE minerals,

partly due to the smaller grain size of PGE mineral grains. Inherent differences in the hydrophobicity of base-metal sulphides and PGE minerals probably also play a role.

Considering the small grain size of the PGE minerals, doubt exist as to whether the liberated grains truly float, or whether their presence in flotation concentrates can be attributed to some other process such as entrainment. It would seem that at least a portion of the liberated PGE minerals were recovered by true flotation rather than entrainment, despite their small grain sizes, hence the observation that progressively finer PGE minerals are being recovered with time, in contrast to chromite and silicate of which the finest grains were recovered to the fastest-floating concentrate. The observed differences in the recoveries of the different type of PGE minerals also indicate that some selectivity is present during flotation process, although the slower rate of flotation of the non-sulphide PGE minerals may partly be related to their smaller sizes. During plant flotation some of the smaller liberated grains, especially of slow-floating types of PGE minerals may report to cleaner tailings streams and, if not properly treated, may eventually be lost. Most of the losses of PGE minerals to the tailings are in the form of incomplete liberation from silicate minerals, mostly in the coarser particle sizes.

6.6 Prediction of PGE recovery characteristics based on mineralogical and chemical parameters

The milled flotation feed samples contain a variety of different types of particles composed of a number of different minerals, occurring in different proportions, and with different grain sizes. During the mineralogical examination of the different flotation products fast-, slow- and non-floating particles were identified. Based on the type of particles present in a milled feed sample, it should therefore be possible to predict the flotation characteristics of an ore. Furthermore, as the types of particles in the milled flotation feed is determined by the mineralogical characteristics of the ore prior to milling, the flotation characteristics may also be predicted from the mineralogical characteristics of the crushed ore.

6.6.1 Relationship between flotation characteristics and selected mineralogical and chemical parameters in UG2 ore prior to milling.

The following mineralogical and chemical parameters can be used to describe the

crushed ore, and will, to a large extent, determine the types of particles generated during milling:

- mode of occurrence of PGE minerals, expressed as predicted liberation of PGE minerals
- amount of non-sulphide PGE mineral
- PGE mineral grain size, expressed as median PGE mineral grain diameter based on per cent number of grains. (As shown in Table 4.17, although the median PGE mineral grain diameter based on area per cent is a closer approximation of the true grain diameter, the median grain diameter based on per cent number of grains is a statistically more reliable parameter, allowing for comparison between samples.)
- base-metal sulphide mode of occurrence expressed as predicted liberation
- base-metal sulphide grain size expressed as median diameter
- amount of pentlandite
- pentlandite/(pentlandite+millerite) ratio
- chromite grain size expressed as median diameter
- acid copper and nickel, and PGE+Au contents.

The relationships between these parameters and the flotation characteristics of the different types of UG2 ore are reported in Table 6.5 and graphically depicted in Figure 111.

Predicted PGE mineral liberation (PGEMLib1)

For the relatively unaltered ores (A1, B1, A2, B2, A3 & B3), a positive relationship exists between the predicted degree of liberation of PGE minerals and R_f (Figure 112), with a Pearson correlation coefficient of 0.85. If extended, the regression line will intercept the y-axis at a relatively low value, suggesting that for this group of samples, the value of R_f is determined almost exclusively by the mode of occurrence of the PGE minerals.

In the case of the millerite-bearing ores (C1 to C5) the relationship is also a positive one (r=0.72), but, even though the slope of the regression line is similar to that of the relatively unaltered samples, the y-intercept value is much higher. One possible explanation for the higher than expected values of R_f for these samples, could be that the predicted degree of liberation is underestimated for these samples, partly due to

Table 6.5 *Correlation matrix of selected mineralogical and chemical parameters against R_f, R_s, 100-U, k_f and ks. Marked correlations (boldface) are significant at $p<0.05$.*

A. Samples A1, B1, A2, B2, A3 and B3 (Relatively unaltered UG2 ore)													
n=6	R_f	R_s	*100-U*	k_f	k_s	*PGEMLib1*	*NSul*	*PGEMS1*	*BMSLib1*	*BMSS1*	*pn*	*pn:mil*	*ChrS*
R_f	1.00	**-0.98**	**-0.96**	0.66	0.30	**0.85**	-0.03	-0.39	0.67	**-0.87**	0.08	-0.47	-0.79
R_s	**-0.98**	1.00	**0.88**	-0.74	-0.19	**-0.89**	0.11	0.31	-0.79	**0.87**	0.05	0.55	**0.87**
100-U	**-0.96**	**0.88**	1.00	-0.48	-0.45	-0.73	-0.09	0.48	-0.43	0.81	-0.27	0.33	0.60
k_f	0.66	-0.74	-0.48	1.00	0.12	0.59	0.04	-0.34	**0.87**	-0.67	-0.20	-0.85	-0.62
k_s	0.30	-0.19	-0.45	0.12	1.00	-0.16	-0.19	-0.07	-0.24	0.00	-0.12	-0.46	0.09
PGEMLib1	**0.85**	**-0.89**	-0.73	0.59	-0.16	1.00	-0.03	-0.22	**0.83**	-0.77	0.12	-0.22	**-0.82**
NSul	-0.03	0.11	-0.09	0.04	-0.19	-0.03	1.00	**-0.87**	-0.10	-0.29	**0.88**	0.25	0.40
PGEMS1	-0.39	0.31	0.48	-0.34	-0.07	-0.22	**-0.87**	1.00	-0.13	0.66	-0.73	0.11	-0.03
BMSLib1	0.67	-0.79	-0.43	**0.87**	-0.24	**0.83**	-0.10	-0.13	1.00	-0.68	-0.22	-0.58	-0.82
BMSS1	**-0.87**	**0.87**	0.81	-0.67	0.00	-0.77	-0.29	0.66	-0.68	1.00	-0.24	0.40	0.73
pn	0.08	0.05	-0.27	-0.20	-0.12	0.12	**0.88**	-0.73	-0.22	-0.24	1.00	0.52	0.37
pn:mil	-0.47	0.55	0.33	**-0.85**	-0.46	-0.22	0.25	0.11	-0.58	0.40	0.52	1.00	0.48
ChrS	-0.79	**0.87**	0.60	-0.62	0.09	**-0.82**	0.40	-0.03	**-0.82**	0.73	0.37	0.48	1.00
Cu_{as}	-0.76	**0.82**	0.61	-0.57	-0.22	-0.62	0.56	-0.10	-0.63	0.62	0.54	0.62	0.93
Ni_{as}	0.07	-0.08	-0.05	0.03	-0.73	0.38	0.72	-0.56	0.25	-0.40	0.71	0.45	-0.03
ΣPGE	-0.62	0.66	0.50	-0.45	0.11	-0.50	0.09	0.31	-0.51	0.80	0.19	0.40	0.79
CLI>0.8	**0.94**	**-0.89**	**-0.95**	0.58	0.31	**0.84**	0.17	-0.48	0.58	-0.78	0.34	-0.32	-0.58
CLI>0.6	**0.90**	**-0.86**	**-0.88**	0.63	0.23	**0.86**	0.21	-0.48	0.64	-0.75	0.35	-0.32	-0.55
CLI>0.4	**0.82**	-0.79	-0.81	0.67	0.22	0.79	0.35	-0.57	0.63	-0.72	0.43	-0.34	-0.43
PGEMS2	0.61	-0.50	-0.73	0.47	0.47	0.34	0.64	**-0.87**	0.19	-0.64	0.61	-0.32	-0.05
BMSLib2	**0.83**	**-0.89**	-0.68	**0.83**	-0.14	**0.85**	0.20	-0.53	**0.88**	**-0.94**	0.10	-0.51	-0.79
BMSS2	0.34	-0.41	-0.20	0.11	-0.65	0.76	-0.12	0.16	0.57	-0.32	0.10	0.31	-0.56
PGEM:BMS	**-0.86**	0.81	**0.88**	-0.47	-0.54	-0.51	0.14	0.36	-0.35	0.76	0.08	0.53	0.67

p.t.o.

Table 6.5 continued *Correlation matrix of selected mineralogical and chemical parameters against R_f, R_s, 100-U, k_f and ks. Marked correlations (boldface) are significant at $p<0.05$.*

A. Samples A1, B1, A2, B2, A3 and B3 (Relatively unaltered UG2 ore)										
n=6	*Cu $_{as}$*	*Ni $_{as}$*	*ΣPGE*	*CLI>0.8*	*CLI>0.6*	*CLI>0.4*	*PGEMS2*	*BMSLib2*	*BMSS2*	*PGEM:BMS*
R_f	-0.76	0.07	-0.62	**0.94**	**0.90**	**0.82**	0.61	**0.83**	0.34	**-0.86**
R_s	**0.82**	-0.08	0.66	**-0.89**	**-0.86**	-0.79	-0.50	**-0.89**	-0.41	0.81
100-U	0.61	-0.05	0.50	**-0.95**	**-0.88**	-0.81	-0.73	-0.68	-0.20	**0.88**
k_f	-0.57	0.03	-0.45	0.58	0.63	0.67	0.47	**0.83**	0.11	-0.47
k_s	-0.22	-0.73	0.11	0.31	0.23	0.22	0.47	-0.14	-0.65	-0.54
PGEMLib1	-0.62	0.38	-0.50	**0.84**	**0.86**	0.79	0.34	**0.85**	0.76	-0.51
NSul	0.56	0.72	0.09	0.17	0.21	0.35	0.64	0.20	-0.12	0.14
PGEMS1	-0.10	-0.56	0.31	-0.48	-0.48	-0.57	**-0.87**	-0.53	0.16	0.36
BMSLib1	-0.63	0.25	-0.51	0.58	0.64	0.63	0.19	**0.88**	0.57	-0.35
BMSS1	0.62	-0.40	0.80	-0.78	-0.75	-0.72	-0.64	**-0.94**	-0.32	0.76
pn	0.54	0.71	0.19	0.34	0.35	0.43	0.61	0.10	0.10	0.08
pn:mil	0.62	0.45	0.40	-0.32	-0.32	-0.34	-0.32	-0.51	0.31	0.53
ChrS	**0.93**	-0.03	0.79	-0.58	-0.55	-0.43	-0.05	-0.79	-0.56	0.67
Cu_{as}	1.00	0.30	0.78	-0.50	-0.43	-0.30	-0.06	-0.63	-0.25	0.80
Ni_{as}	0.30	1.00	-0.15	0.19	0.26	0.32	0.23	0.42	0.56	0.23
ΣPGE	0.78	-0.15	1.00	-0.35	-0.28	-0.19	-0.17	-0.72	-0.21	0.73
CLI>0.8	-0.50	0.19	-0.35	1.00	0.99	**0.95**	0.74	0.75	0.36	-0.70
CLI>0.6	-0.43	0.26	-0.28	**0.99**	1.00	**0.98**	0.73	0.77	0.41	-0.59
CLI>0.4	-0.30	0.32	-0.19	**0.95**	**0.98**	1.00	0.80	0.75	0.33	-0.50
PGEMS2	-0.06	0.23	-0.17	0.74	0.73	0.80	1.00	0.52	-0.22	-0.54
BMSLib2	-0.63	0.42	-0.72	0.75	0.77	0.75	0.52	1.00	0.44	-0.60
BMSS2	-0.25	0.56	-0.21	0.36	0.41	0.33	-0.22	0.44	1.00	0.05
PGEM:BMS	0.80	0.23	0.73	-0.70	-0.59	-0.50	-0.54	-0.60	0.05	1.00

p.t.o.

Table 6.5 continued *Correlation matrix of selected mineralogical and chemical parameters against R_f, R_s, 100-U, k_f and ks. Marked correlations (boldface) are significant at $p<0.05$.*

B. Samples C1, C2, C3, C4 and C5 (Millerite-bearing UG2 ore)													
n=5	R_f	R_s	*100-U*	k_f	k_s	*PGEMLib1*	*NSul*	*PGEMS1*	*BMSLib1*	*BMSS1*	*pn*	*pn:mil*	*ChrS*
R_f	1.00	**-0.97**	**-0.97**	**0.96**	0.56	0.72	-0.42	-0.59	-0.49	-0.14	-0.16	-0.05	-0.64
R_s	**-0.97**	1.00	**0.89**	-1.00	-0.69	-0.61	0.50	0.41	0.27	0.03	0.28	0.18	0.79
100-U	**-0.97**	**0.89**	1.00	-0.88	-0.41	-0.78	0.31	0.72	0.66	0.23	0.03	-0.08	0.46
k_f	**0.96**	-1.00	-0.88	1.00	0.67	0.56	-0.47	-0.36	-0.24	0.02	-0.28	-0.23	-0.81
k_s	0.56	-0.69	-0.41	0.67	1.00	0.43	-0.92	-0.13	0.20	-0.32	-0.71	-0.32	-0.60
PGEMLib1	0.72	-0.61	-0.78	0.56	0.43	1.00	-0.41	**-0.94**	-0.78	-0.53	0.10	0.54	-0.12
NSul	-0.42	0.50	0.31	-0.47	**-0.92**	-0.41	1.00	0.18	-0.16	0.62	0.84	0.36	0.28
PGEMS1	-0.59	0.41	0.72	-0.36	-0.13	**-0.94**	0.18	1.00	**0.93**	0.56	-0.28	-0.65	-0.14
BMSLib1	-0.49	0.27	0.66	-0.24	0.20	-0.78	-0.16	0.93	1.00	0.37	-0.51	-0.68	-0.24
BMSS1	-0.14	0.03	0.23	0.02	-0.32	-0.53	0.62	0.56	0.37	1.00	0.43	-0.10	-0.49
pn	-0.16	0.28	0.03	-0.28	-0.71	0.10	0.84	-0.28	-0.51	0.43	1.00	0.78	0.23
pn:mil	-0.05	0.18	-0.08	-0.23	-0.32	0.54	0.36	-0.65	-0.68	-0.10	0.78	1.00	0.36
ChrS	-0.64	0.79	0.46	-0.81	-0.60	-0.12	0.28	-0.14	-0.24	-0.49	0.23	0.36	1.00
Cu_{as}	**-0.96**	**0.97**	**0.90**	**-0.96**	-0.59	-0.69	0.36	0.52	0.40	-0.05	0.05	-0.05	0.77
Ni_{as}	0.32	-0.36	-0.26	0.41	-0.21	-0.21	0.52	0.23	0.03	0.86	0.39	-0.14	-0.65
ΣPGE	-0.17	0.36	-0.02	-0.40	-0.54	0.44	0.45	-0.65	-0.75	-0.25	0.76	0.93	0.64
CLI>0.8	0.44	-0.33	-0.51	0.31	0.39	0.51	-0.65	-0.52	-0.39	**-0.89**	-0.56	-0.20	0.22
CLI>0.6	0.41	-0.29	-0.51	0.26	0.33	0.56	-0.59	-0.60	-0.47	**-0.91**	-0.47	-0.09	0.30
CLI>0.4	-0.04	0.21	-0.12	-0.23	-0.10	0.29	-0.26	-0.46	-0.44	**-0.89**	-0.24	0.07	0.73
PGEMS2	0.28	-0.34	-0.21	0.38	0.30	-0.29	-0.38	0.35	0.36	-0.10	-0.75	-0.93	-0.29
BMSLib2	-0.06	-0.01	0.12	0.07	-0.41	-0.53	0.68	0.51	0.27	**0.97**	0.43	-0.18	-0.46
BMSS2	-0.76	0.80	0.67	-0.76	-0.87	-0.79	0.75	0.55	0.26	0.34	0.32	-0.11	0.56
PGEM:BMS	**0.92**	-0.83	**-0.95**	0.83	0.44	0.66	-0.44	-0.61	-0.55	-0.38	-0.28	-0.17	-0.37

p.t.o.

Table 6.5 continued *Correlation matrix of selected mineralogical and chemical parameters against R_f, R_s, 100-U, k_f and ks. Marked correlations (boldface) are significant at $p<0.05$.*

F. Samples C1, C2, C3, C4 and C5 (Millerite-bearing UG2 ore)										
n=5	*Cu_{as}*	*Ni_{as}*	*ΣPGE*	*CLI>0.8*	*CLI>0.6*	*CLI>0.4*	*PGEMS2*	*BMSLib2*	*BMSS2*	*PGEM:BMS*
R_f	**-0.96**	0.32	-0.17	0.44	0.41	-0.04	0.28	-0.06	-0.76	**0.92**
R_s	**0.97**	-0.36	0.36	-0.33	-0.29	0.21	-0.34	-0.01	0.80	-0.83
100-U	**0.90**	-0.26	-0.02	-0.51	-0.51	-0.12	-0.21	0.12	0.67	**-0.95**
k_f	**-0.96**	0.41	-0.40	0.31	0.26	-0.23	0.38	0.07	-0.76	0.83
k_s	-0.59	-0.21	-0.54	0.39	0.33	-0.10	0.30	-0.41	-0.87	0.44
PGEMLib1	-0.69	-0.21	0.44	0.51	0.56	0.29	-0.29	-0.53	-0.79	0.66
NSul	0.36	0.52	0.45	-0.65	-0.59	-0.26	-0.38	0.68	0.75	-0.44
PGEMS1	0.52	0.23	-0.65	-0.52	-0.60	-0.46	0.35	0.51	0.55	-0.61
BMSLib1	0.40	0.03	-0.75	-0.39	-0.47	-0.44	0.36	0.27	0.26	-0.55
BMSS1	-0.05	0.86	-0.25	**-0.89**	**-0.91**	**-0.89**	-0.10	0.97	0.34	-0.38
pn	0.05	0.39	0.76	-0.56	-0.47	-0.24	-0.75	0.43	0.32	-0.28
pn:mil	-0.05	-0.14	**0.93**	-0.20	-0.09	0.07	-0.93	-0.18	-0.11	-0.17
ChrS	0.77	-0.65	0.64	0.22	0.30	0.73	-0.29	-0.46	0.56	-0.37
Cu_{as}	1.00	-0.43	0.16	-0.20	-0.18	0.29	-0.11	-0.07	0.81	-0.77
Ni_{as}	-0.43	1.00	-0.25	-0.57	-0.59	-0.73	0.12	**0.93**	0.13	0.13
ΣPGE	0.16	-0.25	1.00	-0.02	0.09	0.36	-0.79	-0.26	0.13	-0.14
CLI>0.8	-0.20	-0.57	-0.02	1.00	**0.99**	0.83	0.47	-0.77	-0.38	0.71
CLI>0.6	-0.18	-0.59	0.09	**0.99**	1.00	0.87	0.38	-0.79	-0.36	0.69
CLI>0.4	0.29	-0.73	0.36	0.83	0.87	1.00	0.17	-0.77	0.07	0.31
PGEMS2	-0.11	0.12	-0.79	0.47	0.38	0.17	1.00	0.05	0.03	0.47
BMSLib2	-0.07	0.93	-0.26	-0.77	-0.79	-0.77	0.05	1.00	0.42	-0.23
BMSS2	0.81	0.13	0.13	-0.38	-0.36	0.07	0.03	0.42	1.00	-0.58
PGEM:BMS	-0.77	0.13	-0.14	0.71	0.69	0.31	0.47	-0.23	-0.58	1.00

p.t.o.

Table 6.5 continued *Correlation matrix of selected mineralogical and chemical parameters against R_f, R_s, 100-U, k_f and ks. Marked correlations (boldface) are significant at $p<0.05$.*

KEY

R_f = fast-floating fraction
R_s= slow-floating fraction
100-U = non-floating fraction
k_f = rate of recovery of fast-floating fraction
k_s = rate of recovery of slow-floating fraction
PGEMLib1 = Predicted PGE mineral liberation
NSul = % non-sulphide PGE mineral
PGEMS1 = PGE mineral median grain diameter prior to milling, i.t.o. number of grains
BMSLib1 = Predicted base-metal sulphide liberation
BMSS1 = base-metal sulphide median grain diameter prior to milling
pn = pentlandite content
pn:mil = pentlandite/(pentlandite+millerite) ratio
ChrS = chromite median grain diameter
Ni_{as}, Cu_{as} = acid soluble nickel and copper contents
ΣPGE = Σ(Pt,Pd,Rh,Au) content
CLI>0.8 = % PGE mineral-bearing particles with cumulative liberation index >0.8
CLI>0.6 = % PGE mineral-bearing particles with cumulative liberation index >0.6
CLI>0.6 = % PGE mineral-bearing particles with cumulative liberation index >0.6
PGEMS2 = PGE mineral median grain diameter after milling, i.t.o. number of grains
BMSLib2 = Base-metal sulphide apparent degree of liberation
BMSS2 = base-metal sulphide median grain diameter after milling
PGEM:BMS = (liberated PGE mineral)/(liberated PGE mineral+BMS) for PGE mineral bearing particles with CLI>0.8

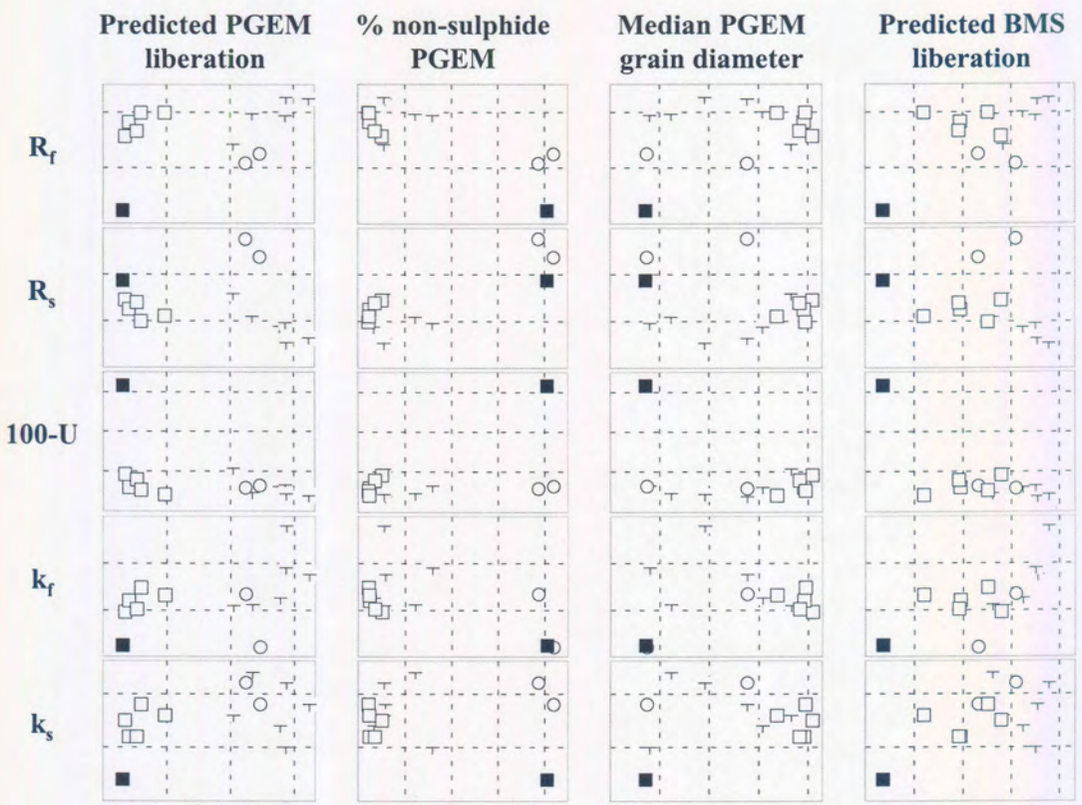

Figure 111 *Relationship between mineralogical, chemical and flotation parameters + = samples A1, A2, A3, B1, B2, and B3. □ = samples C1, C2, C3, C4 and C5. o = samples A4 and B4. ■ = sample A5.*

p.t.o.

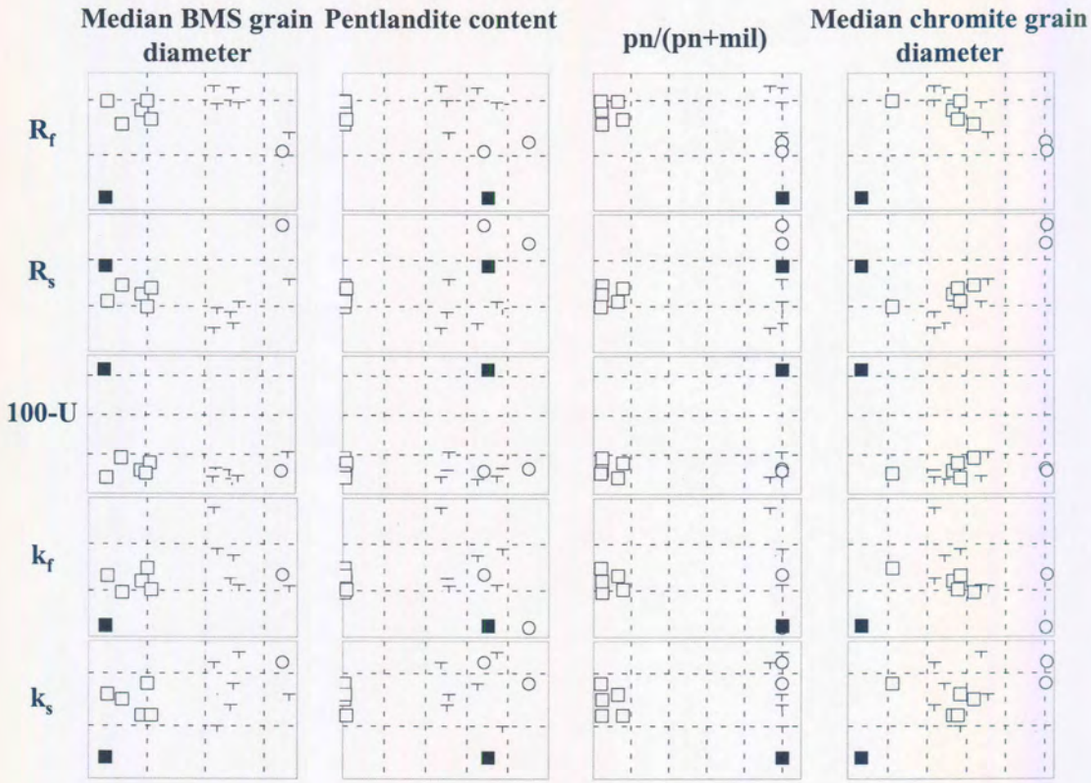

Figure 111 continued *Relationship between mineralogical, chemical and flotation parameters + = samples A1, A2, A3, B1, B2, and B3. □ = samples C1, C2, C3, C4 and C5. o = samples A4 and B4. ■ = sample A5.*

p.t.o.

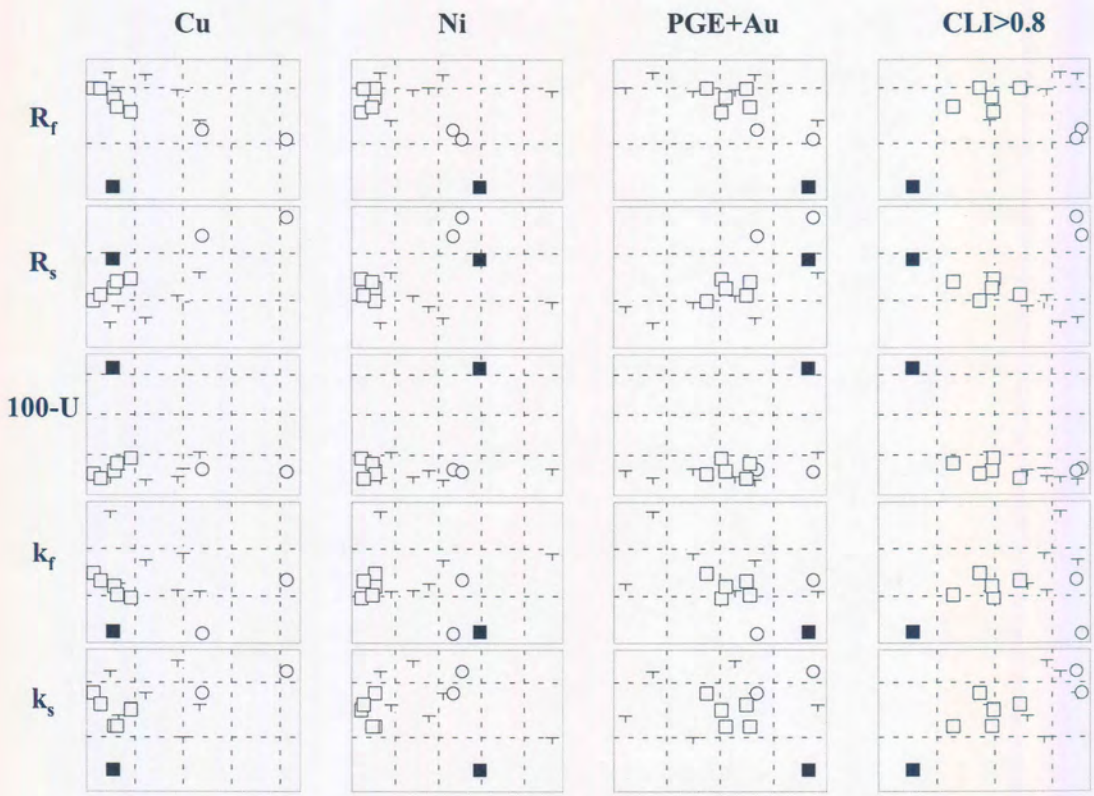

Figure 111 continued *Relationship between mineralogical, chemical and flotation parameters + = samples A1, A2, A3, B1, B2, and B3. □ = samples C1, C2, C3, C4 and C5. o = samples A4 and B4. ■ = sample A5.*

p.t.o.

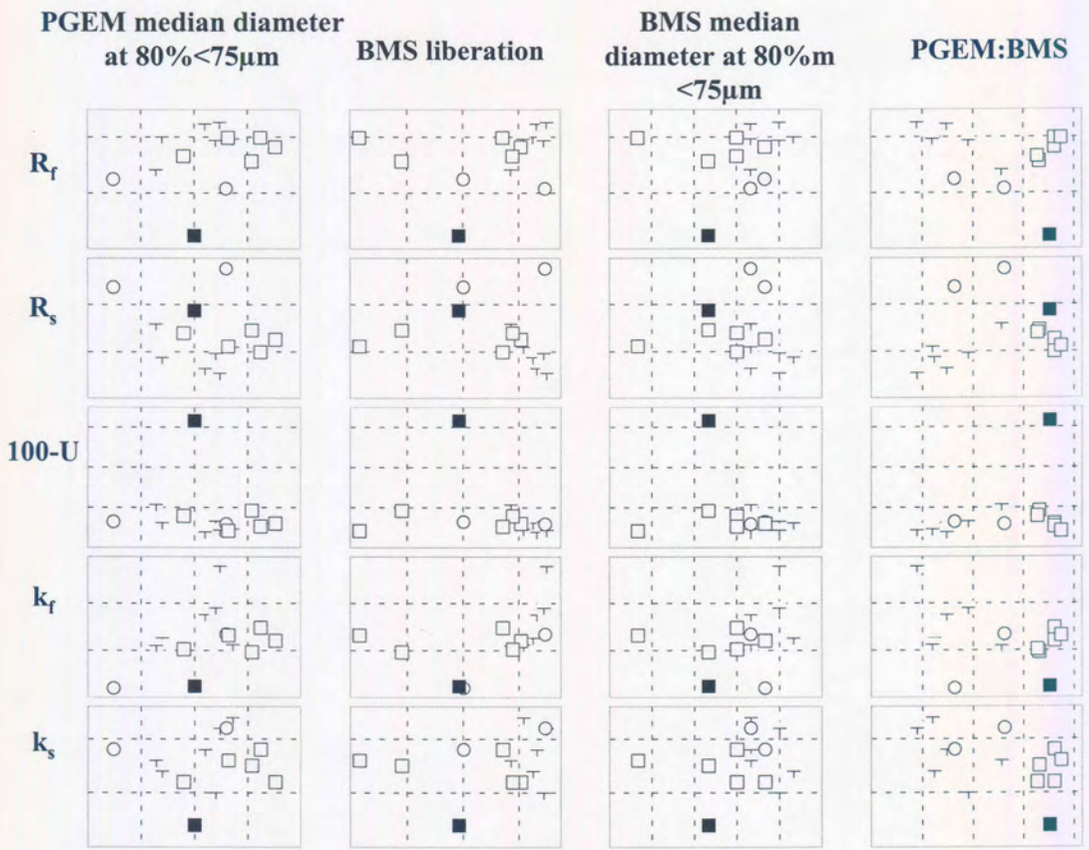

Figure 111 continued *Relationship between mineralogical, chemical and flotation parameters + = samples A1, A2, A3, B1, B2, and B3. □ = samples C1, C2, C3, C4 and C5. o = samples A4 and B4. ■ = sample A5.*

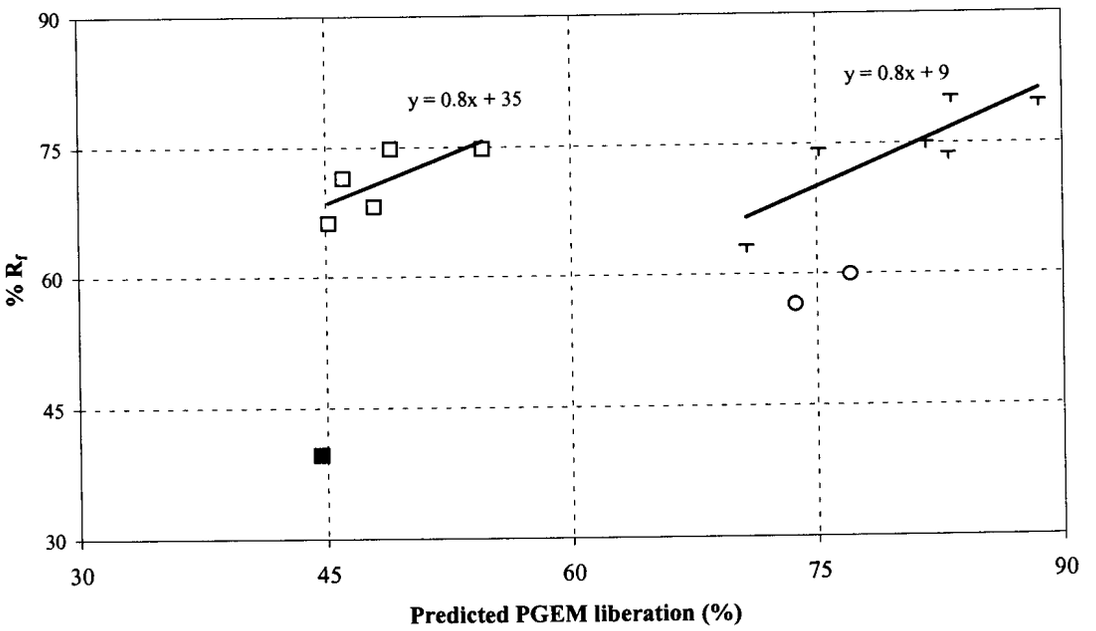

Figure 112 *Relationship between predicted PGE mineral liberation in flotation feed and % R_f. + = samples A1, A2, A3, B1, B2, and B3. □ = samples C1, C2, C3, C4 and C5. o = samples A4 and B4. ■ = sample A5.*

the large amount of PGE minerals at silicate-silicate grain boundaries, a difficult parameter to quantify. Such grains may be liberated quite easily. In addition, the presence of higher concentrations of secondary silicates in these samples, in particular talc, as well as the absence of slow-floating pyrrhotite, may lead to better recovery of composite particles compared to the relatively unaltered samples.

Values of R_f for the sintered samples A4 and B4, are low, presumably because of the large proportion of liberated, but slow-floating, non-sulphide PGE mineral grains in these samples.

For R_s the inverse relationship holds, with a Pearson correlation coefficient of r=-0.89 and –0.61, for the relatively unaltered samples and the millerite-bearing samples, respectively (Figure 113). The amount of slow-floating PGE+Au in sintered samples A4 and B4 is high, due to the contribution of liberated, but slow-floating PGE minerals in these samples.

Similarly, the non-floatable PGE+Au fraction, correlates negatively with predicted PGEM liberation. Sintered samples A4 and B4 falls on the regression line for

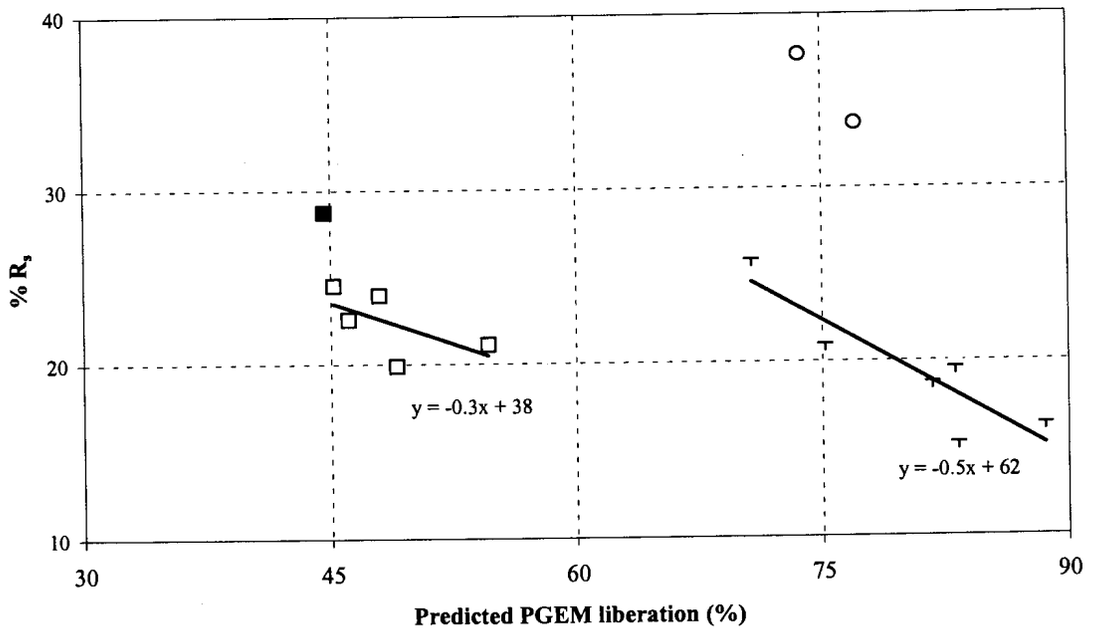

Figure 113 *Relationship between predicted PGE mineral liberation in flotation feed and R_s. + = samples A1, A2, A3, B1, B2, and B3. □ = samples C1, C2, C3, C4 and C5. o = samples A4 and B4. ■ = sample A5.*

relatively unaltered ore (Figure 114). This confirms mineralogical observations that the non-sulphide PGE minerals, given sufficient time, will report to the flotation concentrates.

The relationship between predicted PGE mineral liberation and k_f is similar to that with R_f, but a lot more scattering of the data points is present (Figure 111). No systematic relationship could be discerned between predicted PGE mineral liberation and k_s.

Type of PGE mineral (NSul)

Samples with a high non-sulphide PGE mineral content (A4, B4 and A5) are characterised by relatively low values for R_f, and high values for R_s, due to the slow-floating nature of these minerals. However, due to the big difference in non-sulphide PGE mineral content between these samples and the rest of the samples, the existence of a linear relationship could not be confirmed, and the data essentially falls into two groups (Figure 111). The amount of non-floatable PGE+Au is similar in samples A4 and B4 to the rest of the samples. The reason for the high amount of non-floatable

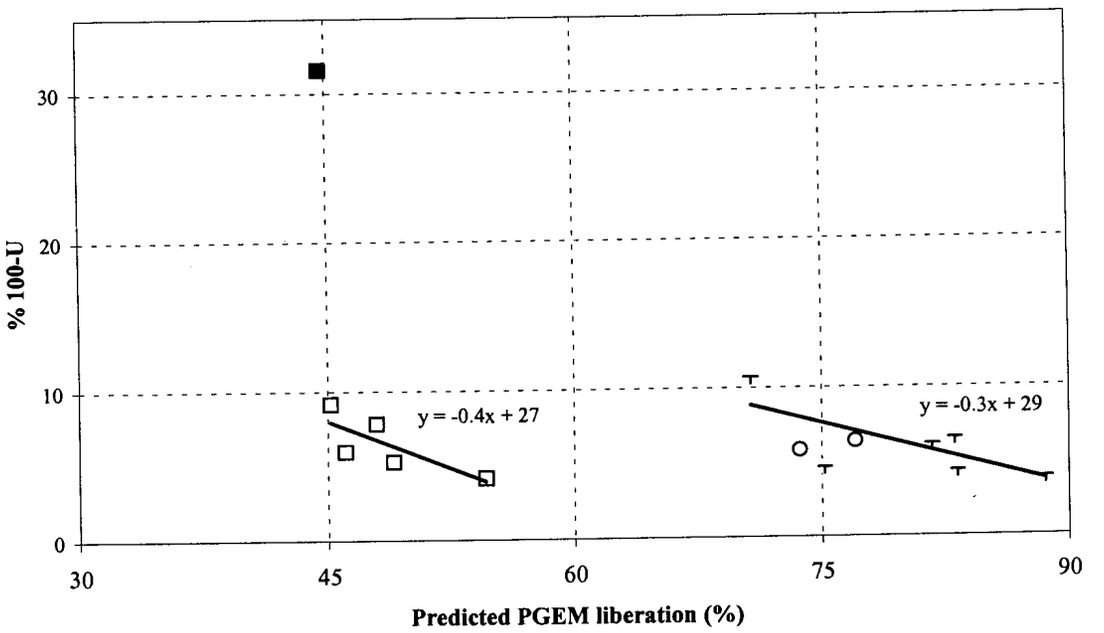

Figure 114 *Relationship between predicted PGE mineral liberation in flotation feed and R_s. + = samples A1, A2, A3, B1, B2, and B3. □ = samples C1, C2, C3, C4 and C5. o = samples A4 and B4. ■ = sample A5.*

PGE+Au in sample A5 is probably related to poor liberation, rather than type of PGE mineral.

PGE mineral grain diameter at <2mm (PGEMS1)

No clear relationship can be seen between any of the flotation parameters and PGE mineral grain diameter prior to milling (Figure 111).

Predicted base-metal sulphide liberation (BMSLib1)

In general, the relationships between the flotation characteristics and predicted base-metal sulphide liberation is similar to that with predicted PGE mineral liberation, but with more scattering of the data points (Figure 111). This is to be expected as the predicted degree of PGE mineral liberation also takes into account the degree of liberation of base-metal sulphide grains associated with PGE minerals.

Base-metal sulphide grain size prior to milling (BMSS1)

No meaningful relationship were found between the base-metal sulphide grain size prior to milling and any of the flotation parameters.

Pentlandite content (pn) and pentlandite/(pentlandite+millerite) ratio (pn:mil)

Pentlandite content and pentlandite/(pentlandite+millerite) ratio essentially divides the data into two groups, those from areas A and B as opposed to the millerite-bearing ores from area C, with no linear relationship discernible (Figure 111).

Chromite grain size (ChrS)

A strong negative linear relationship (Pearson correlation coefficient r = -0.83, for all samples excluding cataclastic UG2 chromitite, sample A5) exists between median chromite grain diameter in the crushed ore and R_f (Table 6.5 and Figure 111). There is a strong positive correlation between median chromite diameter and R_s (r=0.87). Chromite grain size in itself is not a factor affecting recovery, but is, to a certain extent, a reflection of the increase in slow-floating non-sulphide PGE mineral in sintered UG2 chromitite ore. The Pearson correlation coefficient between chromite grain diameter and % non-sulphide PGE mineral in all samples except A5, is 0.84. No correlations were found between median chromite grain diameter and 100-U, k_f or k_s.

Acid soluble copper, nickel and total PGE+Au

In general, there is a negative correlation between copper and total PGE+Au with R_f and k_f, and a positive correlation between copper and total PGE+Au and R_s and U-100. No correlation could be found between copper or total PGE+Au with k_s. There doesn't appear to be a systematic relationship between nickel and any of the flotation parameters.

6.6.2 Predicting flotation parameters from crushed UG2 ore

Fast-floating fraction (R_f)

Using multiple linear regression analysis* it was determined that R_f can be predicted from the mineralogical characteristics of the crushed feed using the non-sulphide PGE

---

* Statistica package.

R – correlation coefficient, the degree to which two or more x variables are related to y

mineral content, predicted PGE mineral liberation, pentlandite/(pentlandite+millerite) ratio and PGE mineral grain size, as independent parameters (R^2=0.98) (Table 6.6 and Figure 115). The relationship appears to be stable, with the relationship not unduly affected by systematic exclusion of any one of the samples from the analysis (Tables 1a and b, Appendix K).

Based on the results already discussed, it was expected that the predicted PGE mineral liberation and the amount of non-sulphide PGE mineral would be significant independent variables. The pentlandite/(pentlandite+millerite) ratio serves to distinguish between the samples from area C and the rest, and compensates for the faster than expected flotation of composite particles in these samples.

The role of the PGE median mineral grain diameter prior to milling, is more difficult to understand. Mineralogical analysis of flotation product samples indicated that coarser PGE mineral grains are faster floating. There is, however, no correlation between PGE mineral grain diameter before and after milling. In addition, it can be seen from Table 6.6 that the median PGE mineral grain diameter correlates negatively with recovery. It is postulated that the median PGE mineral grain diameter serves a function similar to that of the pentlandite/(pentlandite+millerite) ratio, reflecting a difference between groups of samples not satisfactorily explained by any of the other

---

R^2- measures the reduction in the total variation of the dependent variable due to the multiple independent variables

Adjusted R^2 – R^2 is adjusted by dividing the error sums of squares and total sums of squares by their respective degrees of freedom

The F-value and resulting p-value is an overall F-test of the relationship between the dependent variable and the set of independent variables

Standard error of estimate – This statistic measures the dispersion of the observed values about the regression line

B – regression coefficients for a linear model equation

St. Err. of B – standard error of B

t – the t-value associated with the statistics for the respective variable

p – the statistical significance of the t-value

Partial correlation – correlation of x-variable with y, after controlling for all other independent variable

Semipartial correlation – correlation of unadjusted x-variable with y

independent parameters, rather than directly affecting the rate of flotation. The possibility that this is the result of a spurious correlation can also not be excluded.

The median PGE mineral grain diameter is the least significant of the four independent parameters. Exclusion of this parameter still yields a satisfactory model with a R^2 value of 0.95 (Table 6.7 and Figure 116), although exclusion of some of the samples leads to a less reliable result (Tables 2a and b, Appendix K). If samples from area C are excluded from the analysis, the pentlandite/(pentlandite+millerite) ratio becomes superfluous (Table 6.8 and Figure 117).

Slow-floating fraction (R_s)

Table 6.9 summarises the multiple regression results for R_s (Figure 118). In addition to the amount of non-sulphide PGE mineral, predicted degree of PGE mineral liberation, pentlandite/(pentlandite+millerite) ratio, and PGE mineral grain size, chromite grain diameter is also required as a independent variable. Omission of any one of these parameters leads to unsatisfactory results. The regression is not very stable and depends largely on sample A5 (Tables 3a and b, Appendix K).

However, if sample A5 is excluded from the analysis, a more satisfactory result is obtained with the amount of non-sulphide PGE mineral, predicted degree of PGE mineral liberation, pentlandite/(pentlandite+millerite) ratio and PGE mineral grain size as independent parameters (Table 6.10, Figure 119). Omitting PGE mineral grain size as a parameter still gives a reasonably acceptable result (Figure 120 and Table 6.11), although the regression does seem to rely on sample A3 to a large extent (Tables 4a and b, Appendix K).

Non-floating fraction (100-U)

Regression analysis with 100-U as dependent variable yielded unsatisfactory results. Because of the large difference in the amount of non-floating PGE+Au between sample A5 and the remainder of the samples, the regression depended largely on sample A5 (Table 6.12 and Figure 121). If sample A5 is excluded, no statistically significant regression line could be fitted through the points, using the mineralogical parameters examined (Table 5, Appendix K).

Table 6.6 *Regression summary for dependent variable R_f with four independent variables. Fourteen samples.*

$R = .99$ $R^2 = .98$ Adjusted $R^2 = .97$ $F(4,9) = 102.05$ $p < .00000$ Standard Error of estimate: 1.92						
	B	*St. Err. of B*	*t(10)*	*p-level*	*Partial Correlation*	*Semipartial Correlation*
Intercept	61.65	6.69	9.21	0.00		
Predicted PGEM liberation	0.68	0.06	10.64	0.00	0.96	0.52
% non-sulphide PGEM	-0.22	0.03	-7.60	0.00	-0.93	-0.37
pn/(pn+mil)	-22.30	2.89	-7.72	0.00	-0.93	-0.38
PGEM median diameter <2mm	-7.17	1.97	-3.64	0.01	-0.77	-0.18
Independent variables not in equation						
Predicted BMS liberation				0.95	0.02	0.00
BMS median diameter <2mm				0.96	-0.02	0.00
pentlandite content				0.95	0.02	0.00
Median chromite diameter				0.48	-0.25	-0.04
Cu content				0.85	-0.07	-0.01
Ni content				0.34	-0.33	-0.05
PGE+Au content				0.75	-0.12	-0.02

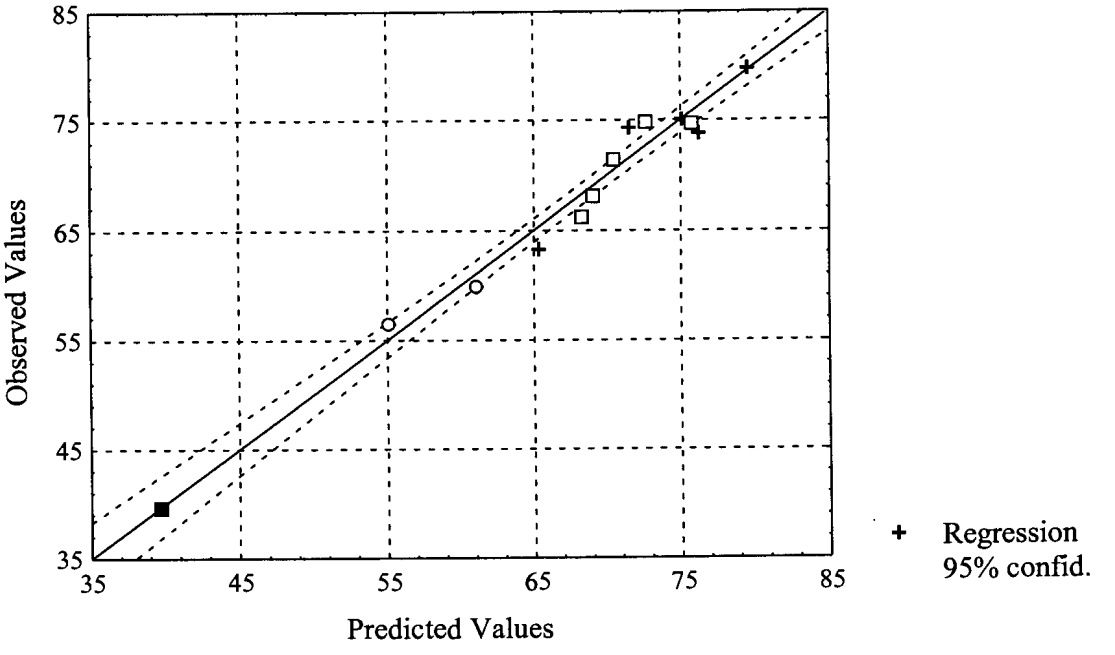

Figure 115 *Comparison of observed and predicted values of R_f based on predicted PGE mineral liberation, pentlandite/(pentlandite+millerite) ratio, amount of non-sulphide PGE mineral and PGE mineral grain diameter prior to milling. + = samples A1, A2, A3, B1, B2, and B3. □ = samples C1, C2, C3, C4 and C5. o = samples A4 and B4. ■ = sample A5.*

Table 6.7 *Regression summary for dependent variable R_f with three independent variables. Fourteen samples.*

$R = .97$ $R^2 = .95$ Adjusted $R^2 = .93$ $F(3,10) = 59.144$ $p < .00000$ Standard Error of estimate: 2.87						
	B	*St. Err. of B*	*t(10)*	*p-level*	*Partial Correlation*	*Semipartial Correlation*
Intercept	40.14	4.69	8.56	0.00		
Predicted PGEM liberation	0.69	0.10	7.27	0.00	0.92	0.53
% non-sulphide PGEM	-0.17	0.04	-4.48	0.00	-0.82	-0.33
pn/(pn+mil)	-19.17	4.12	-4.66	0.00	-0.83	-0.34
Independent variables not in equation						
PGEM median diameter <2mm				0.00	-0.77	-0.18
Predicted BMS liberation				0.42	-0.27	-0.06
BMS median diameter <2mm				0.21	-0.41	-0.09
pentlandite content				0.11	0.51	0.12
Median chromite diameter				0.12	-0.49	-0.11
Cu content				0.13	-0.49	-0.11
Ni content				0.81	0.08	0.02
PGE+Au content				0.19	-0.43	-0.10

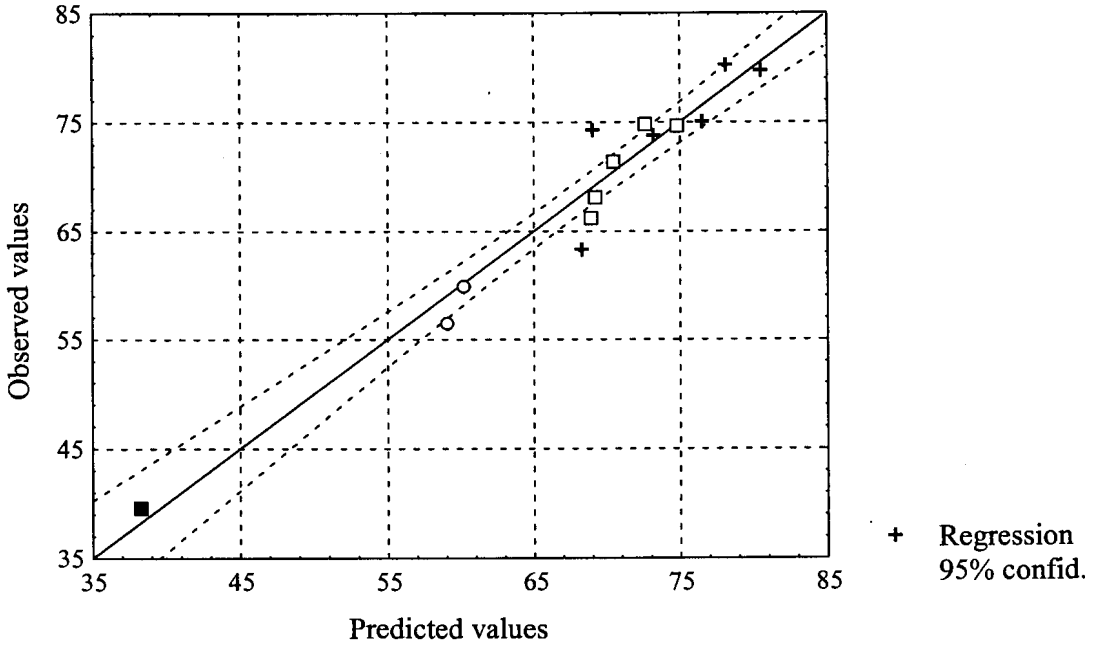

Figure 116 *Comparison of observed and predicted values of R_f based on predicted PGE mineral liberation, pentlandite/(pentlandite+millerite) ratio and amount of non-sulphide PGE mineral. + = samples A1, A2, A3, B1, B2, and B3. □ = samples C1, C2, C3, C4 and C5. o = samples A4 and B4. ■ = sample A5.*

Table 6.8 *Regression summary for dependent variable R_f with two independent variables. Samples from area C excluded.*

$R = .97$ $R^2 = .95$ Adjusted $R^2 = .93$ $F(3,10) = 59.144$ $p < .00000$ Standard Error of estimate: 2.87						
	B	*St. Err. of B*	*t(6)*	*p-level*	*Partial Correlation*	*Semipartial Correlation*
Intercept	22.37	10.26	2.18	0.07		
% non-sulphide PGEM	-0.18	0.05	-3.79	0.01	-0.84	-0.35
Predicted PGEM liberation	0.68	0.12	5.65	0.00	0.92	0.53
Independent variables not in equation						
PGEM median diameter <2mm				0.02	-0.81	-0.19
pn/(pn+mil)				0.35	-0.41	-0.09

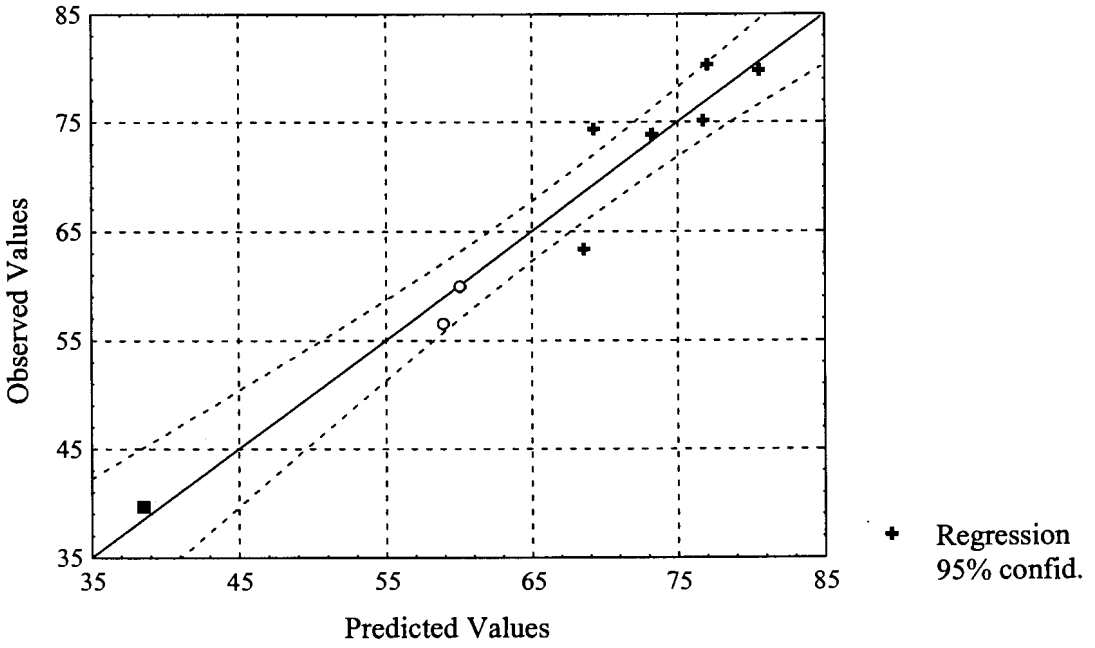

Figure 117 *Comparison of observed and predicted values of R_f for samples from areas A and B based on predicted PGE mineral liberation, and amount of non-sulphide PGE mineral. + = samples A1, A2, A3, B1, B2, and B3. o = samples A4 and B4. ■ = sample A5.*

Table 6.9 *Regression summary for dependent variable R_s*

R= .99 R^2= .99 Adjusted R^2= .98						
F(5,8)=54.12 p<.00000 Standard Error of estimate: 0.83						
	B	*St. Err. of B*	*t(8)*	*p-level*	*Partial Cor.*	*Semipart Cor.*
Intercept	-5.76	2.89	-2.00	0.08		
Predicted PGEM liberation	-0.20	0.04	-5.40	0.00	-0.89	-0.20
% non-sulphide PGEM	0.17	0.02	10.17	0.00	0.96	0.37
pn/(pn+mil)	5.03	1.40	3.59	0.01	0.79	0.13
PGEM median diameter <2mm	6.12	0.95	6.43	0.00	0.92	0.23
Chromite median diameter	0.11	0.01	8.29	0.00	0.95	0.30
Independent variables not in equation						
Predicted BMS liberation				0.82	-0.09	-0.01
BMS median diameter <2mm				0.27	0.41	0.04
pentlandite				0.88	-0.06	-0.01
Cu				0.46	0.28	0.03
Ni				0.39	0.33	0.03
PGE+Au				0.69	-0.16	-0.02

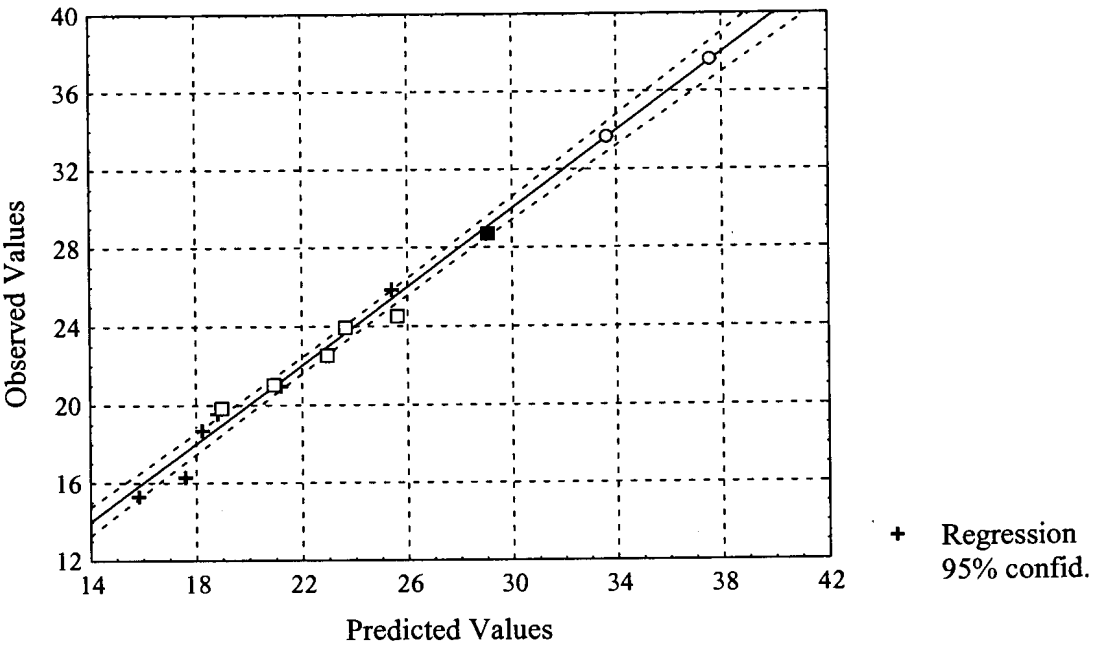

Figure 118 *Comparison of observed and predicted values of R_s based on predicted PGE mineral liberation, pentlandite/(pentlandite+millerite) ratio, amount of non-sulphide PGE mineral, PGEM grain diameter prior to milling, and chromite grain diameter prior to milling. + = samples A1, A2, A3, B1, B2, and B3. □ = samples C1, C2, C3, C4 and C5. o = samples A4 and B4. ■ = sample A5.*

Table 6.10 *Regression summary for dependent variable R_s for four independent variables and excluding sample A5.*

$R= .99$ $R^2= .99$ Adjusted $R^2= .98$ $F(4,8)=130.39$ $p<.00000$ Standard Error of estimate: 0.96						
	B	*St. Err. of B*	*t(9)*	*p-level*	*Partial Correlation*	*Semipartial Correlation*
Intercept	21.94	5.31	4.13	0.00		
Predicted PGEM liberation	-0.40	0.07	-6.07	0.00	-0.91	-0.26
% non-sulphide PGEM	0.23	0.02	15.54	0.00	0.98	0.68
pn/(pn+mil)	12.07	2.29	5.28	0.00	0.88	0.23
PGEM median diameter <2mm	6.10	1.11	5.48	0.00	0.89	0.24

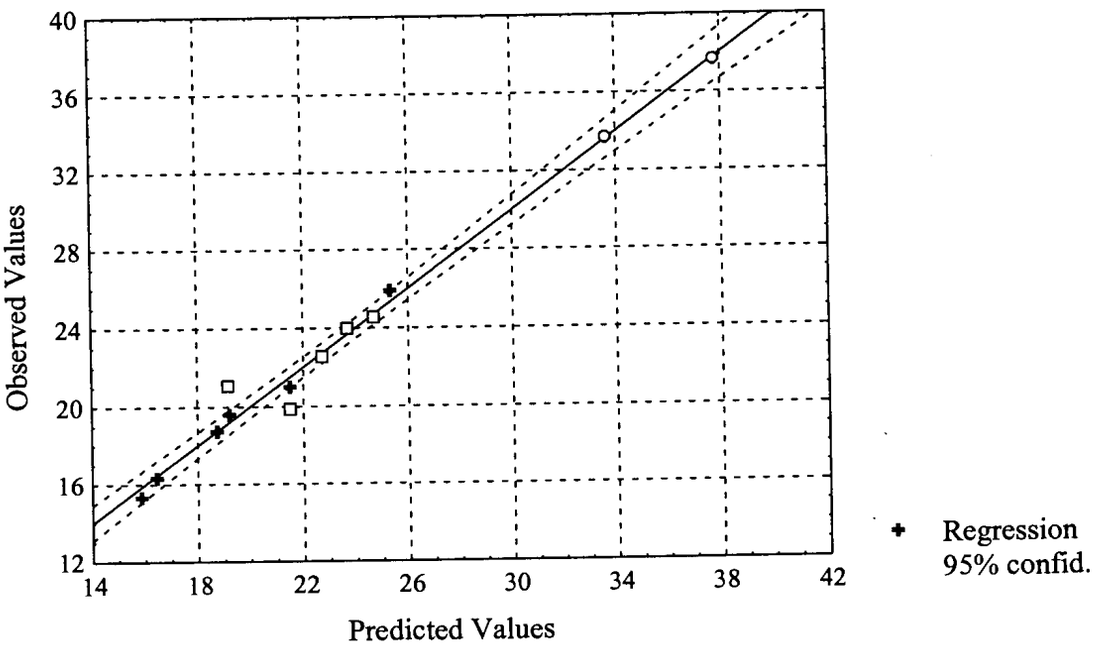

Figure 119 *Comparison of observed and predicted values of R_s based on predicted PGE mineral liberation, pentlandite/(pentlandite+millerite) ratio, amount of non-sulphide PGE mineral and PGEM grain diameter prior to milling. + = samples A1, A2, A3, B1, B2, and B3. □ = samples C1, C2, C3, C4 and C5. o = samples A4 and B4.*

Table 6.11 *Regression summary for dependent variable R_s for three independent variables and excluding sample A5.*

$R = .96$ $R^2 = .93$ Adjusted $R^2 = .90$ $F(3,9) = 38.77$ $p < .00000$ Standard Error of estimate: 1.98						
	B	*St. Err. of B*	*t(9)*	*p-level*	*Partial Correlation*	*Semipartial Correlation*
Intercept	46.74	5.72	8.17	0.00		
Predicted PGEM liberation	-0.55	0.12	-4.51	0.00	-0.83	-0.40
% non-sulphide PGEM	0.19	0.03	7.24	0.00	0.92	0.65
pn/(pn+mil)	14.44	4.62	3.13	0.01	0.72	0.28

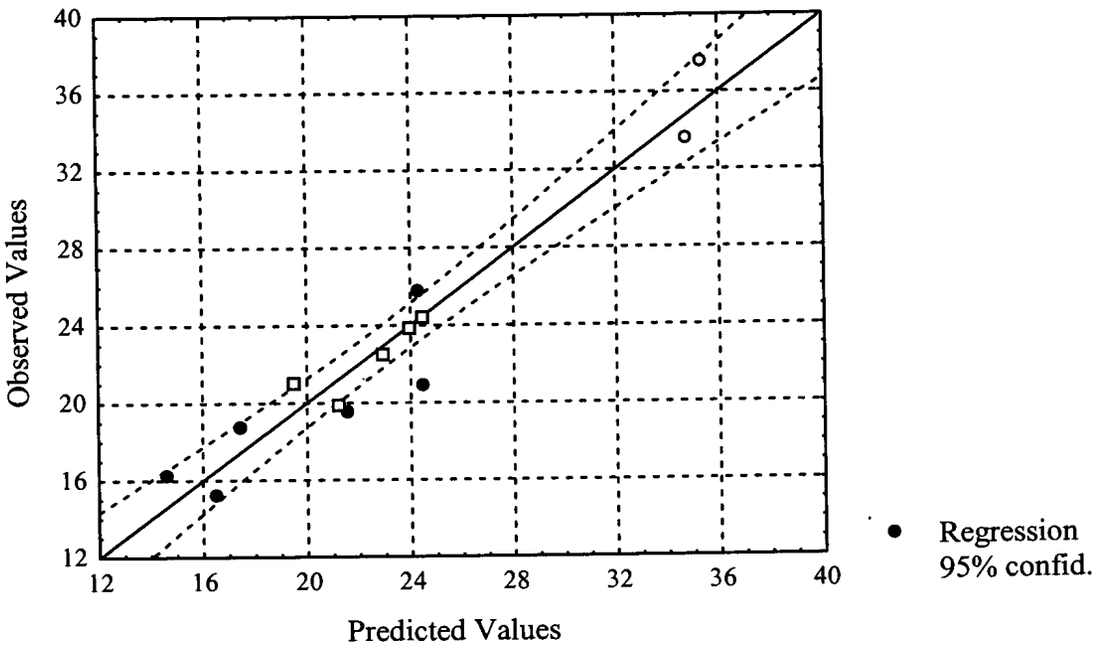

Figure 120 *Comparison of observed and predicted values of R_s based on predicted PGE mineral liberation, pentlandite/(pentlandite+millerite) ratio and amount of non-sulphide PGE mineral. ● = samples A1, A2, A3, B1, B2, and B3. □ = samples C1, C2, C3, C4 and C5. o = samples A4 and B4.*

Table 6.12 *Regression summary for dependent variable 100-U*

R= .97 R^2= .94 Adjusted R^2= .92						
F(3,10)=50.59 p<.00000 Standard Error of estimate: 2.00						
	B	*St. Err. of B*	*t(11)*	*p-level*	*Partial Cor.*	*Semipart Cor.*
Intercept	37.18	2.74	13.58	0.00		
Predicted PGEM liberation	-0.54	0.06	-8.79	0.00	-0.94	-0.69
pn/(pn+mil)	22.80	2.06	11.06	0.00	0.96	0.87
BMS median ECD <2mm	-0.31	0.10	-3.02	0.01	-0.69	-0.24
Independent variables not in equation						
% non-sulphide PGEM				0.94	0.02	0.01
PGEM median ECD <2mm				0.90	0.04	0.01
pentlandite				0.99	0.00	0.00
Predicted BMS liberation				0.76	0.11	0.03
Chromite median ECD <2mm				0.23	-0.39	-0.10
Cu				0.20	0.19	0.05
Ni				0.57	-0.42	-0.10
PGE+Au				0.83	-0.07	-0.02

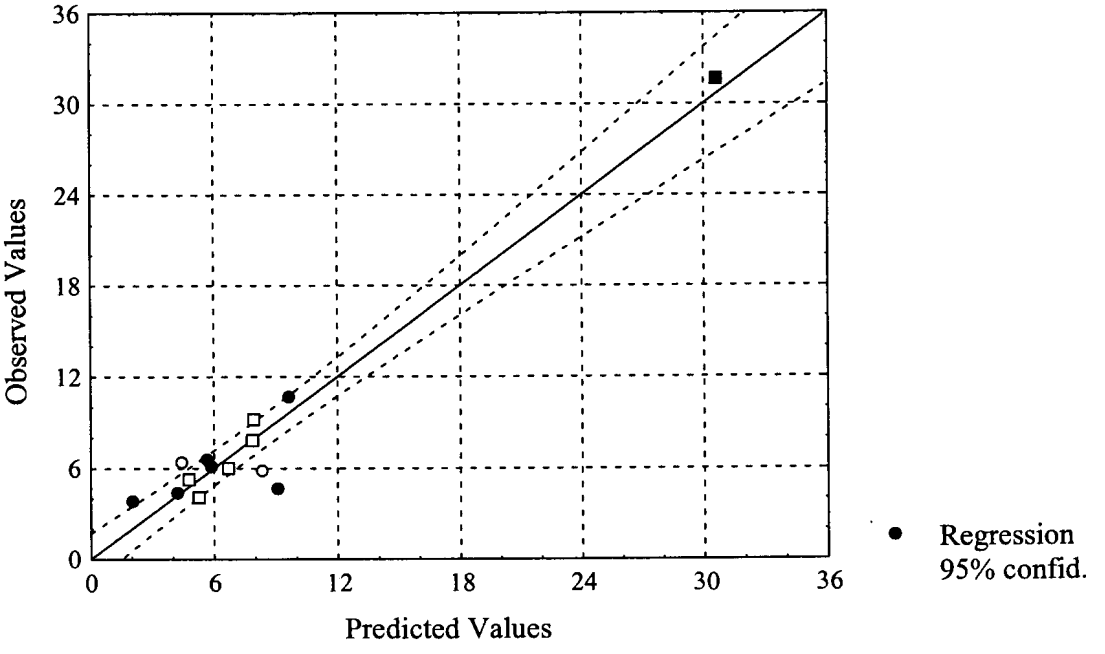

Figure 121 *Comparison of observed and predicted values of 100-U based on predicted PGE mineral liberation, pentlandite/(pentlandite+millerite) ratio, base-metal sulphide grain size prior to milling. ● = samples A1, A2, A3, B1, B2, and B3. □ = samples C1, C2, C3, C4 and C5. o = samples A4 and B4. ■ = sample A5.*

Flotation rate of fast- and slow-floating fractions (k_f and k_s)

No satisfactory model could be found for the prediction of k_f or k_s (Tables 6 and 7, Appendix K).

6.6.3 Relationship between flotation characteristics and selected mineralogical parameters in milled ore.

The mineralogical characteristics of the milled ore can be summarised by the following parameters:

- combined liberation index of PGE mineral-bearing particles
- amount of non-sulphide PGE mineral
- PGE mineral grain diameter expressed as median diameter based on per cent number of grains
- base-metal sulphide degree of liberation
- base-metal sulphide grain size expressed as median diameter
- ratio PGEM/(PGEM+BMS) in particles with a combined liberation index of >0.8
- amount of pentlandite
- pentlandite/(pentlandite+millerite) ratio

PGE mineral liberation (CLI>0.8, CLI>0.6 and CLI>0.4)

The relationships between the degree of PGE mineral liberation and the different flotation parameters are similar to those between the predicted degree of PGE mineral liberation and the flotation parameters. As expected from the examination of mineral particles in the flotation products, the higher the degree of PGE mineral liberation (CLI>0.8), the higher the value for R_f. The regression coefficient for these two parameters for the relatively unaltered UG2 ores (samples A2, B2, A3, B3, A1 and B1) is 0.94 (Table 6.5 and Figure 122). The millerite-bearing samples from area C plot slightly above the regression line for the relatively unaltered ores, due to the better than expected flotation of composite particles from these ores. For the sintered ores (A4 and B4), the actual values for R_f are much lower than expected, as a result of

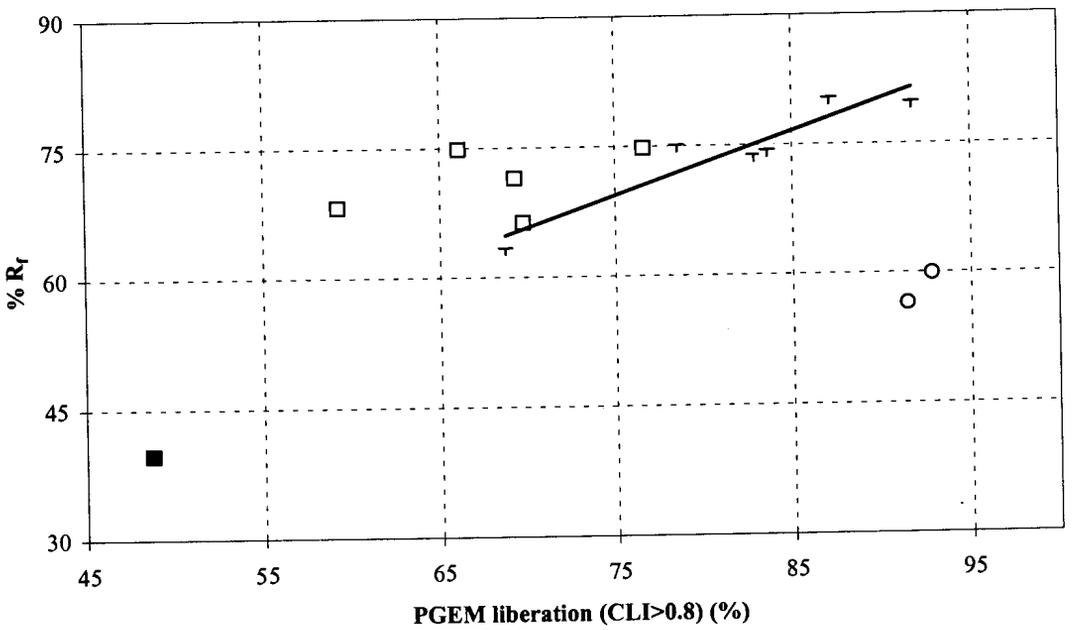

Figure 122 *Relationship between PGE mineral liberation in the milled flotation feed and % R_f. + = samples A1, A2, A3, B1, B2 and B3. □ = samples C1, C2, C3, C4 and C5. o = samples A4 and B4. ■ = sample A5. Regression line calculated for relatively unaltered samples A1, A2, A3, B1, B2 and B3.*

the presence of significant amounts of liberated, but slow-floating, non-sulphide PGE minerals in these two samples.

For R_s the inverse relationship holds – the higher the degree of liberation of PGE minerals and the sulphides associated with them, the lower the proportion of slow-floating PGE minerals (Figure 123) (Pearson correlation coefficient for the relatively unaltered UG2 samples is –0.89 (Table 6.5)). The R_s values for the millerite-bearing samples from area C plot close to, but slightly lower than the regression line. As expected, the R_s values for sintered samples A4 and B4, are relatively high. Cataclastic sample A5 appears to follow the same trend as the millerite-bearing samples. The situation is very similar for the non-floatable PGE+Au (Table 6.5, Figure 124).

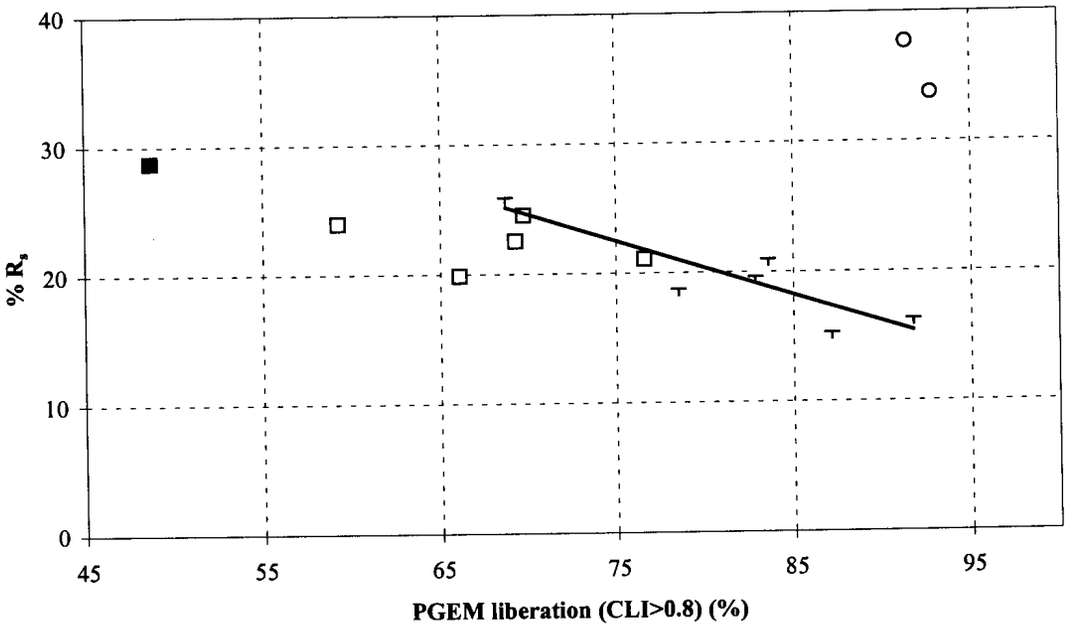

Figure 123 *Relationship between PGE mineral liberation in milled flotation feed and R_s. + = samples A1, A2, A3, B1, B2 and B3. □ = samples C1, C2, C3, C4 and C5. o = samples A4 and B4. ■ = sample A5. Regression line calculated for relatively unaltered samples, A1, A2, A3, B1, B2 and B3.*

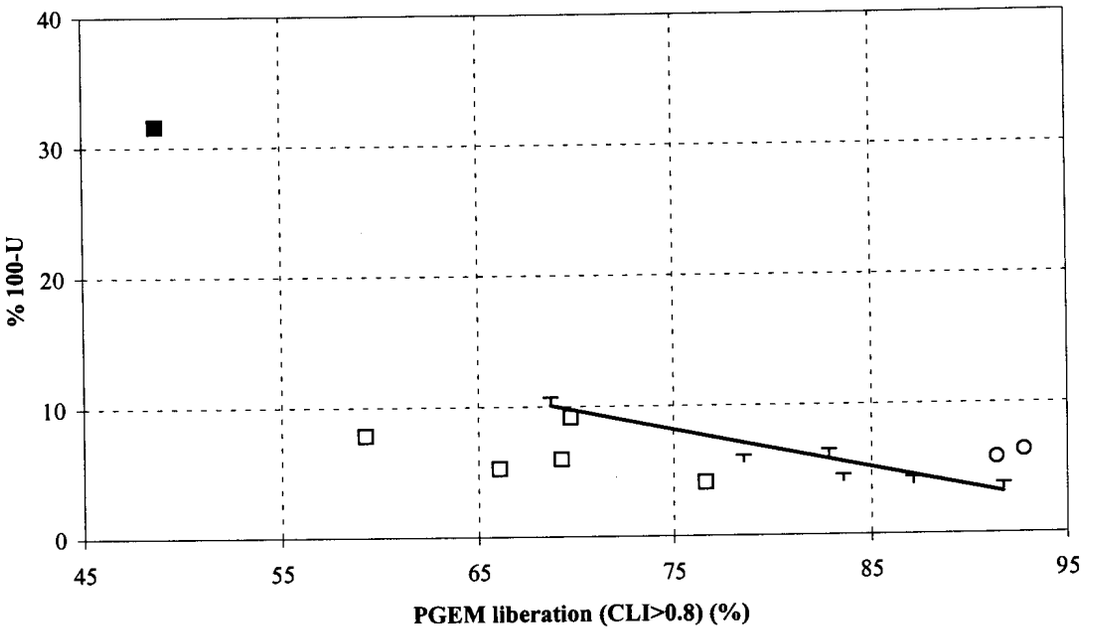

Figure 124 *Relationship between PGE mineral liberation in flotation feed and % non-floatable fraction. + = samples A1, A2, A3, B1, B2 and B3. □ = samples C1, C2, C3, C4 and C5. o = samples A4 and B4. ■ = sample A5. Regression line calculated for relatively unaltered samples, A1, A2, A3, B1, B2 and B3.*

The nature of the relationships between the degree of PGE mineral liberation and k_s and k_f, is unclear (Figure 111).

Since it is known that a very small floatable component can, under the right circumstances, induce flotation of a composite particle (Trahar, 1991; Sutherland, 1989), the relationships between the amount of PGE mineral-bearing particles with CLI>0.6 and CLI>0.4 were also investigated. The general trends were found to be the same as for CLI>0.8, but the regression coefficients are lower (Table 6.5). Consequently, CLI>0.8 was selected as the independent variable during regression analysis.

PGE mineral grain diameter at 80%<75µm (PGEMS2)

The relationship between PGE mineral size after milling, and all five flotation parameters appear to be random (Figure 111). Even though the mineralogical examination of the flotation products have indicated better recovery of coarser PGE mineral grains, the difference in PGE mineral grain size between the different samples may not be large enough to affect flotation results.

Base-metal sulphide degree of liberation (BMSLib2)

For relatively unaltered UG2 samples, a linear relationship exists between base-metal sulphide liberation and R_f (0.83) and R_s (-0.89) (Table 6.5). To a large extent this is a reflection of the correlation between the degree of liberation between PGE minerals and base-metal sulphide. The relationship does not hold for the remainder of the samples.

Base-metal sulphide grain diameter at 80%<75µm (BMSS2)

The relationships between base-metal sulphide grain diameter after milling and all five flotation parameters appear to be random (Figure 111).

Amount of liberated PGE mineral as a ratio of all particles with a combined liberation index of >0.8 (PGEM:BMS)

It has been shown that the higher the base-metal sulphide component in PGE mineral-bearing particles, the faster-floating the particle. In other words, liberated PGE

mineral particles generally float slower than particles consisting of liberated base-metal sulphide grains. For the relatively unaltered samples (A1, A2, A3, B1, B2 and B3) there is a strong negative correlation between R_f and (PGEM:BMS)(r=-0.86 in Table 6.5), with the inverse relationship holding for R_s and 100-U. (Figure 125). For the millerite-bearing samples from area C, the relationships appear to be reversed (Table 6.5). This may be related to differences in the nature of the base-metal sulphide and PGE minerals from the different areas, but more data is required before any conclusions can be drawn.

6.6.4 Predicting flotation parameters from milled UG2 ore

Fast-floating fraction (R_f)

For most samples, R_f largely depends on the degree of liberation of the PGE minerals, with lower than expected values for samples with a significant proportion of slow-floating, non-sulphide PGE mineral contents. Multiple regression analysis confirmed that the amount of fast-floating PGE+Au can be predicted from the PGE mineral liberation and the amount of non-sulphide PGE mineral, but the relationship is not very stable and depends to a large extent on cataclastic sample A5 (Table 6.13 and Figure 125 and Tables 8a and b, Appendix K).

The prediction can be improved by the inclusion of the PGE mineral grain size prior to milling, the degree of base-metal sulphide liberation and the pentlandite/(pentlandite+millerite) ratio (Table 6.14 and Figure 126, Tables 9a and 9b, Appendix K), partly due to the better than expected recovery of composite particles in millerite-bearing samples from area C.

Slow-floating fraction (R_s)

The amount of slow-floating PGE+Au can be predicted using the degree of PGE mineral liberation, the amount of non-sulphide PGE mineral, and the PGE mineral and chromite grain diameters in the crushed ore as independent variables (Table 6.15 and Figure 127 and Tables 10a and b, Appendix K). With increasing retention time, a significant proportion of particles reports to flotation concentrates as a result of other processes, such as entrainment, rather than true flotation. Consequently the recovery process becomes more unpredictable and it is therefore difficult to predict R_s. In

addition, the behaviour of composite grains, many of which report to the slower-floating concentrates, is still poorly understood.

Non-floating fraction (100-U)

No satisfactory model could be generated for the prediction of 100-U (Table 11, Appendix K). Examination of flotation tailings indicated that most of the PGE mineral grains in the flotation tailings are present in composite grains with only a small floatable component. The unpredictable behaviour of such particles has already been discussed. In addition, the presence of occasional liberated PGE mineral grains in some of the tailings samples were difficult to explain. While composition and grain size may have played a role, not enough grains were examined to reach any conclusion in this regard. It is possible that some of these grains may have become trapped between silicate grains and thus prevented from floating, especially where a lot of fine silicates were present.

Table 6.13 *Regression summary for R_f with PGE mineral degree of liberation and amount of non-sulphide PGE mineral as independent parameters.*

R= .96 R^2= .92 Adjusted R^2= .91 F(2,11)=67.23 p<.00000 Standard Error of estimate: 3.26						
	B	*St. Err. of B*	*t(11)*	*p-level*	*Partial Cor.*	*Semipart Cor.*
Intercept	40.80	5.29	7.72	0.00		
PGEM with CLI>0.8	0.47	0.07	6.79	0.00	0.90	0.56
% non-sulphide PGEM	-0.31	0.03	-10.24	0.00	-0.95	-0.85
Independent variables not in equation						
PGEM median diameter <75µm				0.66	0.14	0.04
BMS median diameter <75µm				0.54	0.20	0.05
pentlandite				0.75	0.10	0.03
pn/(pn+mil)				0.82	-0.07	-0.02
Cu				0.05	-0.58	-0.16
Ni				0.29	0.33	0.09
PGE+Au				0.05	-0.58	-0.16
PGEM/PGEM+BMS)				0.51	-0.21	-0.06

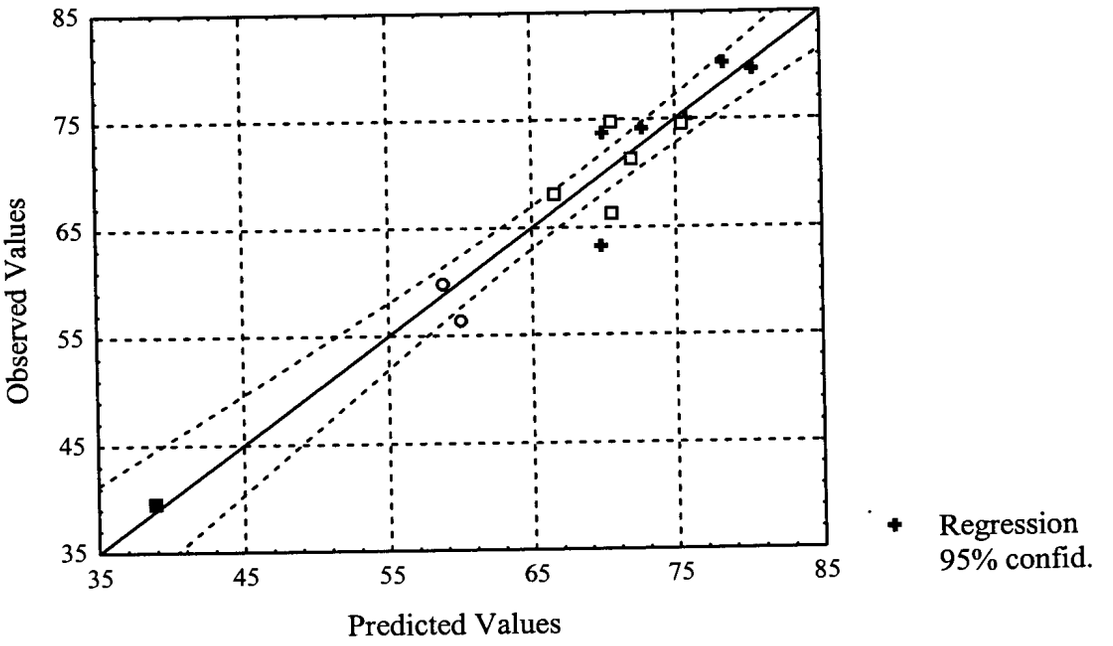

Figure 125 *Comparison of observed and predicted values of R_f based on PGE mineral liberation and amount of non-sulphide PGE mineral. + = samples A1, A2, A3, B1, B2, and B3. □ = samples C1, C2, C3, C4 and C5. o = samples A4 and B4. ■ = sample A5.*

Rate of flotation of fast- and slow-floating fractions (k_f and k_s)

No satisfactory model could be generated to predict the non-floatable fraction, k_f or k_s (Tables 12 and 13, Appendix K). These parameters are probably affected by very small differences between particles. Differences in k_f and k_s may conceivably occur in response to enviromental factors such as humidity or the time lapsed between milling of the ore and flotation, which can affect the surface characteristics of particles.

6.6.5 Factors affecting the recovery of individual PGEs

Although this aspect wasn't investigated in detail, some interesting observations were made. For example, palladium appeared to be slower-floating in samples of sintered UG2 chromitite. The reasons for this could not be established. Palladium levels in

Table 6.14 *Regression summary for R_f with PGE mineral degree of liberation, % non-sulphide PGE mineral, PGE mineral grain diameter before crushing, base-metal sulphide degree of liberation and pentlandite/(pentlandite+millerite) ratio as independent variables.*

$R = .99$ $R^2 = .98$ Adjusted $R^2 = .97$ $F(5,8) = 89.485$ $p < .00000$ Std.Error of estimate: 1.84						
	B	*St. Err. of B*	*t(8)*	*p-level*	*Partial*	*Semipart*
Intercept	62.08	6.39	9.72	0.00		
PGEM with CLI>0.8	0.47	0.04	10.75	0.00	-0.32	-0.04
% non-sulphide PGEM	-0.34	0.02	-14.39	0.00	-0.14	-0.02
PGEM grain diameter <2mm	-9.15	1.91	-4.80	0.00	-0.09	-0.01
BMS degree of liberation	0.08	0.03	2.54	0.03	0.06	0.01
pn/(pn+mil)	-7.56	2.06	-3.67	0.01	-0.33	-0.04
Independent variables not in equation						
PGEM grain diameter <75µm				0.40	-0.53	-0.07
pentlandite content				0.71	-0.55	-0.07
PGEM/PGEM+BMS)				0.82		
Nickel content				0.87		
PGE+Au				0.38		
Cu content				0.13		
Chromite grain diameter				0.12		

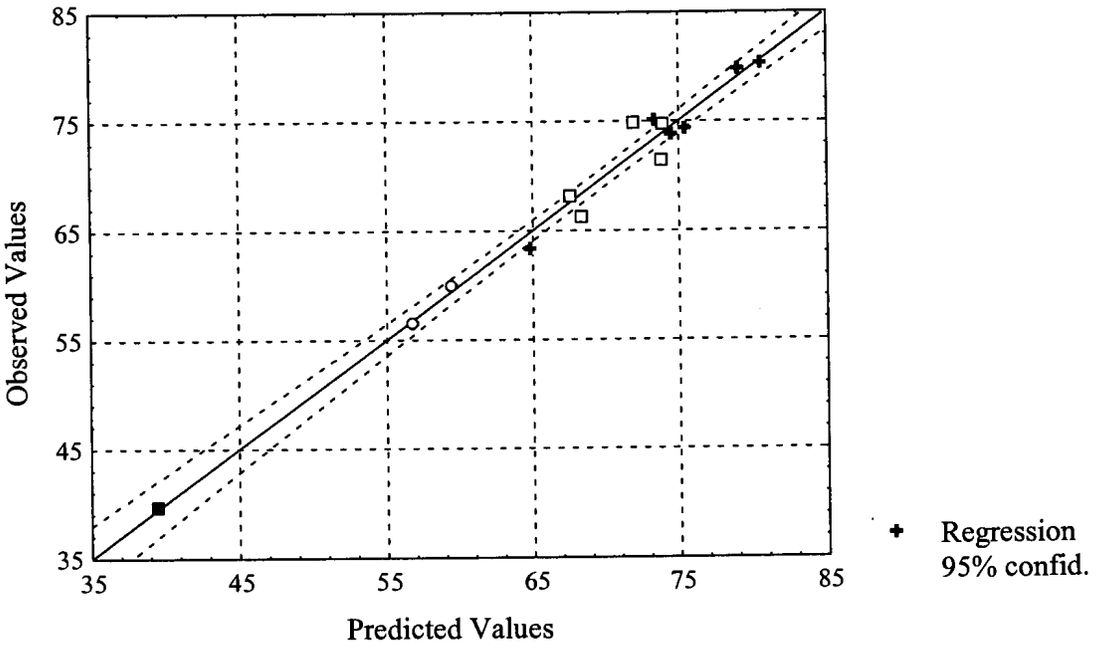

Figure 126 *Comparison of observed and predicted values of R_f based on PGE mineral liberation , amount of non-sulphide PGE mineral, base-metal sulphide liberation, pentlandite/(pentlandite+millerite) ratio, and median PGE mineral grain diameter before crushing. + = samples A1, A2, A3, B1, B2, and B3. □ = samples C1, C2, C3, C4 and C5. o = samples A4 and B4. ■ = sample A5.*

Table 6.15 *Regression summary for R_s based on PGE mineral liberation, amount of non-sulphide PGE mineral and PGE mineral and chromite grain diameter prior to milling.*

$R= .996$ $R^2= .99$ Adjusted $R^2= .99$ $F(4,9)= 317.04$ $p<.00000$ Standard Error of estimate: 0.64						
	B	*St. Err. of B*	*t(10)*	*p-level*	*Partial Cor.*	*Semipart Cor.*
Intercept	-6.04	2.05	-2.94	0.02		
PGEM with CLI>0.8	-0.16	0.02	-7.68	0.00	-0.93	-0.22
% non-sulphide PGEM	0.20	0.01	20.88	0.00	0.99	0.58
PGEM ECD <2mm	6.02	0.66	9.15	0.00	0.95	0.26
Chromite ECD <2mm	0.12	0.01	10.94	0.00	0.96	0.31
Independent variables not in equation						
PGEM ECD 80%<75µm					0.25	0.02
pentlandite					0.02	0.00
PGEM ass. w. BMS					0.15	0.01
BMS liberation					0.02	0.00
BMS ECD 80%<75µm					-0.68	-0.06
pn/(pn+mil)					0.06	0.00

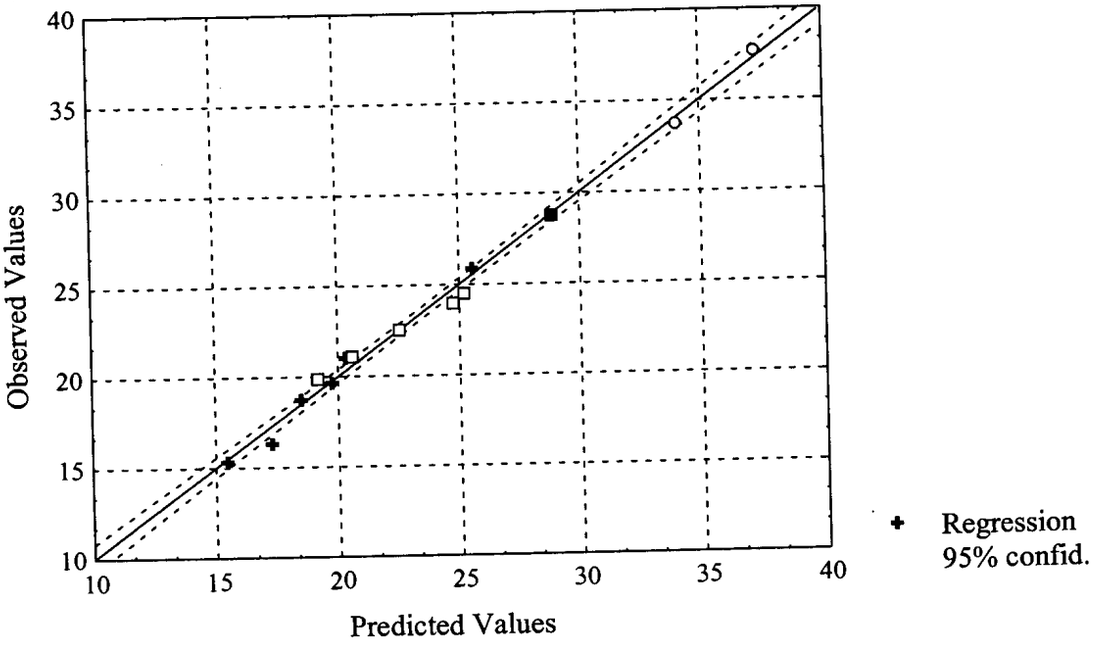

Figure 127 *Comparison of observed and predicted values of R_s based on PGE mineral liberation, amount of non-sulphide PGE mineral and PGE mineral and chromite grain diameter prior to milling. + = samples A1, A2, A3, B1, B2, and B3. □ = samples C1, C2, C3, C4 and C5. o = samples A4 and B4. ■ = sample A5.*

pentlandite appeared to be similar in relatively unaltered and sintered chromitite, and both platinum and palladium tend to occur in non-sulphide PGE minerals.

Another interesting observation relates to the comparison of platinum and palladium rate of flotation in samples of relatively unaltered UG2 with that in millerite-bearing samples from area C. In relatively unaltered UG2 a proportion of the palladium occurs sub-microscopically in pentlandite. Pentlandite is scarce in millerite-bearing samples from area C. The apparent absence of any differences in the flotation behaviour of palladium compared to platinum in the two sets of samples, suggests that the presence of submicroscopic palladium in pentlandite did not have any significant affect on palladium recovery.

7. DISCUSSION

As a result of this study it was possible to identify different types of UG2 chromitite and the major factors affecting the recovery of the PGEs using mineralogical characteristics quantified by image analysis. Although several shortcomings have been identified in this approach, many of these can only be addressed once further technological advances have been made.

7.1 Characterisation of PGE-mineral bearing particles

7.1.1 PGE minerals

Fully automated quantification of grains as small and complex, and present at such low concentration levels as the PGE minerals in the UG2 chromitite, unfortunately remains beyond reach. The semi-automated process proposed here is labour intensive and expensive, but still much faster and more objective than manual searching techniques. For practical reasons, a sample of 200 PGE mineral grains was accepted as being representative of a given sample. This is a relatively small sample, and the errors associated with it are large. In the low-grade tailings samples the problem is even worse, as collection of data on more than approximately fifty PGE mineral grains during routine analysis is impractical. However, in the day-to-day investigations undertaken by most mineral processing laboratories, a limited amount of data on a relatively small number of grains is often all that is required to solve the problem in hand.

7.1.2 Associated minerals

The characterisation of the associated minerals is as important as that of the PGE minerals themselves, as it determines the flotation behaviour of composite particles, as well as the nature of the gangue in flotation concentrates. In the case of the base-metal sulphides, backscattered-electron intensities are sometimes so close together, e.g. for pentlandite and chalcopyrite, that grey level is an unreliable method of discriminating between different phases. Variability in sulphide composition, especially in the case of pentlandite, compounds the problem. The relative proportions of the individual base-metal sulphides was obtained using EDS analysis on a coarse grid pattern. Obtaining textural information on individual sulphides (grain size, mode

of occurrence and liberation) is more problematic as it would require characterisation of each pixel belonging to sulphide by EDS analysis, a process which could take an hour or longer for each particle. As a result, the base-metal sulphide mineralogy was quantified in terms of mode of occurrence and size of total base-metal sulphide, rather than for the individual sulphides. This is a drawback, as the different sulphide minerals do not behave in the same way during processing of the ore. Pyrrhotite for instance, is slow-floating compared to the other base-metal sulphides. In addition, pentlandite appears to be the only sulphide mineral containing appreciable amounts of PGEs in its structure.

For similar reasons, the individual minerals in the silicate component could not be recognised during analysis. Consequently, all silicate minerals were classed together as silicate gangue. As talc is naturally floatable, and most other silicates are not, this is a shortcoming, and certainly one of the reasons for the apparent unpredictability of the flotation behaviour of composite particles.

With newer technology it is already possible to achieve faster analysis and processing times, and the resolution and stability of backscattered-electron detectors are improving. Consequently, accurate characterisation of PGE-bearing particles should become less of a problem in the future.

7.2 In situ trace-element analysis

7.2.1 Base-metal sulphide

Electron-microprobe analysis has indicated that pentlandite hosts significant amounts of submicroscopic palladium and rhodium. In most samples, pentlandite is also the most abundant base-metal sulphide mineral. If the other base-metal sulphide minerals do accommodate submicroscopic PGEs, it is generally at concentration levels below the detection limits of the routine electron-microprobe technique, and probably represents a relatively small proportion of the total PGEs. From a mineral processing point of view, it is more important to obtain a good average value for the PGE concentration in pentlandite. The relatively high detection limits associated with the electron-microprobe technique is therefore not the biggest concern.

Obtaining suitable standards for the in situ trace-element analysis is a bigger problem, and should be addressed before further analyses are attempted. Once this has been achieved, the next challenge is to obtain accurate pentlandite compositions to determine a reliable average for UG2 chromitite, and establishing whether this can be related to different types of UG2 chromitite. Considering the small grain sizes and low, but variable, concentration levels, this is no easy task.

7.2.2 Chromite

Considering the high chromite content of the UG2 ore, any submicroscopic PGEs, even at the ppb level, might represent a significant proportion of the total PGE. For instance, at 67 per cent chromite, an average concentration level of 150 ppb PGE in chromite represents a total of 0.1 ppm. This fraction of PGEs would be impossible to recover using the current technology. The possibility that chromite can accommodate PGEs in its crystal structure deserves to be further investigated.

7.3 Effect of geological environment on mineralogy

As a result of the small number of samples studied, limited information was obtained on the effect of geological environment on the mineralogy of UG2 chromitite. For instance, a much larger number of samples would need to be studied to determine the effect, if any, of pothole structures on the mineralogy. This should ideally involve the collection of samples at different distances from the centre of potholes.

7.4 Relating mineralogical characteristics to recovery

Information obtained from the mineralogical examination of different flotation products indicated that the rate of recovery of PGE+Au depends largely on the degree of liberation of the PGE minerals and base-metal sulphides, and the amount of slow-floating non-sulphide PGE minerals. This premise was confirmed using multiple regression analysis. A number of factors contribute to scattering of data points about the regression line:

- Relatively large statistical errors during data collection is an inevitable consequence of the low concentration levels at which the PGEs are present in the UG2 chromitite.

- Because of the low concentration levels of PGEs, a huge effort is required to collect data on a relatively small number of grains. As a result, only a few samples was analysed, leading to further uncertainties.

- More information on silicate distribution and flotation behaviour is necessary to accurately predict the behaviour of composite particles.

- Although the bulk composition, liberation, and size of a particle are key factors affecting its response to flotation, surface composition and topography control surface reactivity, and therefore also play a major role. Such effects were not taken into account during the current study. Time-of-flight secondary ion mass spectrometry (TOF-SIMS) makes it possible to characterise the surface composition of mineral particles (Stowe *et al.*, 1995). This type of information may further contribute to the understanding of the flotation behaviour of base-metal sulphide and PGE minerals.

7.5 Concentrate grade

Concentrate grade is an important flotation parameter. For the purpose of the current project, the flotation procedure was limited to rougher flotation with no cleaning stages. As a result, the concentrate grades were very low, to a large extent obscuring any trends with regard to grade. Most of the silicate and chromite particles in the flotation concentrates do not have any PGE or base-metal sulphide minerals attached to them. Some of these particles report to the flotation concentrates because of the natural floatability of talc, many more do so as a result of entrainment, which is facilitated by small particle sizes. Understanding all the factors affecting concentrate grade would require a much more detailed study of the behaviour of gangue minerals during flotation.

8. SUMMARY AND CONCLUSIONS

8.1 Characterisation of UG2 ore and mineral processing products

Using the current technology, it is not possible to characterise all aspects of the mineralogy of the UG2 ore and its mineral processing products using fully automated image analysis. However, the data generated using semi-automated image analysis techniques was sufficient to quantify mineralogical differences between the different samples. These mineralogical differences could be related to different geological environments. Characterisation of the mineralogy of different flotation products allowed for the identification of fast-, slow- and non-floating particles, thereby explaining differences in the flotation response of different types of UG2 chromitite.

8.2 Relating variations in mineralogy to geological environment

Large variations in mineralogy, in terms of the modal proportions and compositions of minerals, as well as their textural settings, were observed in the UG2 chromitite layer over a relatively short distance (~50 km). These mineralogical variations can often be related to local geological disturbances such as the presence of iron-rich ultrabasic replacement pegmatoid or faulting, but in some cases appear to result from larger scale hydrothermal activity.

- Relatively unaltered UG2 chromitite (represented by samples A1, A2, A3, B1, B2 and B3) consists of rounded chromite grains in a primary silicate matrix, comprising predominantly plagioclase and orthopyroxene, with minor phlogopite, clinopyroxene, and secondary silicates such as talc and chlorite. Minor sintering of chromite grains may be present. Base-metal sulphides, mostly pentlandite, pyrrhotite, chalcopyrite and minor pyrite, occur at concentration levels of <0.1 volume per cent, frequently as composite grains (median equivalent circle diameter ~30 μm), usually at chromite/silicate grain boundaries.

  PGEs occur both as discrete PGE minerals and sub-microscopically (in solid solution?) in base-metal sulphides. The PGE mineral assemblage consists predominantly of platinum and/or palladium-sulphide (cooperite, braggite and vysotskite), platinum-rhodium-copper-nickel-sulphide (nickeloan malanite) and laurite ($(Ru,Os,Ir)S_2$). The PGE mineral grains are small (median equivalent

circle diameter ~6.5 μm), and are generally associated with base-metal sulphides, predominantly pentlandite, often situated at grain boundaries. Small amounts of palladium and rhodium are hosted submicroscopically in pentlandite.

Although, this group of samples includes UG2 chromitite with anorthosite, norite and pegmatoid footwall, as well as samples collected from the edges of pothole structures, the mineralogical and chemical characteristics are very similar.

- The local interaction of UG2 chromitite with late stage, Fe-and Ti-rich hydrothermal fluids led to the formation of iron-rich ultrabasic replacement pegmatoid footwall, and in the UG2 itself caused the enlargement of chromite grains through sintering. This gave rise to the sintered samples, A4 and B4. The silicate mineralogy is characterised by the formation of minor clinopyroxene and amphibole as a result of the interaction with fluids. PGE mineral assemblages are dominated by laurite, Pt-Rh-Fe and Pt-Pd-Fe alloys, and other non-sulphide PGE minerals. In the samples examined, the base-metal sulphide assemblage does not appear to have been affected, apart from an increase in grain size.

- A more prominent, and regionally important group, is the millerite-bearing UG2 chromitite, represented by samples C1 to C5. Interaction of magmatic base-metal sulphides with low temperature hydrothermal fluids lead to the corrosion of sulphides and the precipitation of sulphide-rich, low temperature chalcopyrite-millerite-pyrite±siegenite assemblages. The size reduction of base-metal sulphide grains resulted in the isolation of PGE minerals from base-metal sulphides, with PGE minerals occurring in the vicinity of, but not necessarily in direct contact with, the base-metal sulphides. PGE mineral assemblages from these areas are characterised by a decrease in the relative amount of cooperite, and an increase in braggite and nickeloan malanite, compared to relatively unaltered UG2. Primary silicate assemblages in UG2 chromitite have to varying extents been replaced by albite, quartz, pumpellyite, epidote, prehnite, chlorite, sphene and talc.

- Faulting can cause local cataclasis of chromitite, and in this study A5 represents such a case. Fractures act as conduits for fluids, leading to the cementation of fractured chromite grains by low-temperature hydrous silicates, quartz and calcite.

These conditions lead to the formation of non-sulphide PGE minerals, often enclosed in silicate.

8.3 Factors affecting the flotation response of PGE mineral-bearing particles

A large proportion of the PGE minerals in the milled feed samples are present as liberated particles (between 48 and 79 per cent). Milling of the ore caused an even further reduction in the grain size of the already small PGE mineral grains, resulting in a median measured PGE mineral diameter of ~5 μm in the milled product. In samples of relatively unaltered (A1, A2, A3, B1, B2 and B3) and sintered UG2 chromitite (A4 and B4), the remainder of the PGE minerals are mostly associated with liberated base-metal sulphide grains. In samples characterised by the association of PGE minerals and base-metal sulphide with secondary silicates, such as the millerite-bearing (C1 to C5) and cataclastic UG2 chromitite (A5), a large proportion of the PGE minerals in the milled product occurs in particles with a significant gangue component. A small proportion of the total PGEs is present submicroscopically in pentlandite, most of which is present as liberated particles, or as part of liberated base-metal sulphide particles. Poor liberation accounts for most of the PGE minerals in the tailings samples.

Examination of the different flotation products indicates that most of the PGE minerals reporting to the flotation concentrates are liberated PGE minerals. The rate of flotation of PGE minerals is determined by grain size and type of mineral, with the coarsest grains recovered to the faster-floating concentrates. Flotation rates for the different PGE minerals, in decreasing order, are braggite > cooperite > malanite ≈ Pt-Fe alloy and other non-sulphide PGE minerals. PGE minerals associated with liberated base-metal sulphides also report to flotation concentrates, and are generally faster-floating than liberated PGE minerals. Some of the PGEs, especially palladium and rhodium, are recovered with the base-metal sulphides, predominantly pentlandite, as a result of their presence in submicroscopic form. The rate of recovery for the individual sulphides appears to be pyrite > chalcopyrite ≥ millerite ≥ pentlandite >> pyrrhotite.

The flotation behaviour of composite particles is largely governed by the amount of exposed surface area of PGE mineral and base-metal sulphide in the particle. PGE

minerals report to the tailings predominantly in the form of inclusions in silicate, predominantly silicate. The recovery of composite particles also depends on particle size, with finer particles reporting to the faster-floating concentrates. Some samples are characterised by a faster than expected rate of recovery of composite particles. This has been attributed, at least partly, to the presence of naturally floatable talc.

8.4 Relating ore type to variations in flotation response

The flotation behaviour of the ores is described in terms of the amount of fast-floating PGE+Au recovered in the first one to two minutes of flotation (R_f), the amount of slow-floating PGE+Au (R_s), and the amount of non-floating PGE+Au (100-U), that fraction which would not be recovered even if flotation continued indefinitely. The rates of recovery for the fast-and slow-floating fractions (k_f and k_s) were also calculated.

Some of these flotation parameters could be related to mineralogical variations in the UG2 chromitite. Samples of sintered UG2 chromitite are characterised by a large amount of slow-floating PGE+Au, compared to relatively unaltered UG2. The non-floatable PGE+Au fraction, however, is similar in relatively unaltered and sintered UG2 chromitite. This is attributed to the presence of slow-floating non-sulphide PGE minerals in the sintered UG2 chromitite. It also seems that palladium, and possibly rhodium, tend to be slow-floating relative to platinum in these samples.

Cataclastic UG2 chromitite contains a large portion of non-floating PGE+Au, as a result of the association of PGE minerals and base-metal sulphides with secondary silicates in this ore. This results in poor liberation characteristics of the PGE minerals and base-metal sulphides, and consequently a large non-floating fraction in this type of ore.

Examination of the relationships between the flotation parameters and various mineralogical parameters indicates that PGE+Au recovery can be correlated with the mode of occurrence of the PGE minerals and base-metal sulphides, the amount of non-sulphide PGE minerals in the samples, the (pentlandite/pentlandite+millerite) ratio and chromite grain size. Using multiple regression analysis with these characteristics as independent parameters, variations in the R_f and R_s can be predicted fairly accurately.

8.5 Relating the characteristics of PGE mineral-bearing particles to flotation parameters

The flotation behaviour of PGE mineral-bearing particles seems to be determined largely by the degree of liberation and type of PGE and base-metal sulphide mineral. Although differences were observed in the median grain diameters of PGE minerals and base-metal sulphides in the different flotation products, differences between the samples are probably too small to have much of an effect. The apparently smaller sizes of the non-sulphide PGE minerals may however contribute to their slower-floating nature.

Multiple linear regression confirmed that R_f can to a large extent be predicted by the type and degree of liberation of the PGE minerals in the milled flotation feed. Much scattering of data-points about the regression line is present. Although this can be explained, at least partly, by the unpredictable behaviour of composite particles, other factors such as the small number of samples analysed and large statistical errors as a result of the low concentration levels of PGEs and base-metal sulphides also contributed. R_s and the non-floating fraction are even more difficult to accurately predict as, with long flotation times, recovery processes become complicated by the contribution of other processes such as entrainment. In the case of k_f and k_s more subtle differences, such as changes in surface composition, probably also affect these values.

8.6 Concluding remarks

While laboratory flotation tests can be performed relatively cheaply, and in a fraction of the time required for mineralogical analysis, these tests can not supply the reasons for variations in recovery. The approach developed and reported here has definite application to the study of PGE+Au recovery from the UG2 chromitite ores.

It has been demonstrated that reasonable estimates of the recovery of PGE+Au from UG2 chromitite can be made from chemical and mineralogical analysis of representative ore samples crushed to <2mm and/or 80%<75μm. When the results of laboratory flotation tests are combined with chemical and mineralogical characterization of samples ore from proposed mining areas, it becomes a powerful tool, making it possible to recognize different types of ore, and, more importantly,

potential problems during processing, allowing for provision for appropriate adjustments to metallurgical flowsheets.